Optimal energy management for solar-powered cars

Peter Pudney M.App.Sc, B.App.Sc

University of South Australia

August 2000

Contents

Summary

Solar powered cars may never be practical. Nevertheless, in the 1996 World Solar Challenge the Honda *Dream* carried two people 3000km across Australia at an average speed of 90km/h, powered only by sunlight. You clearly don't need a 2500kg machine powered by polluting fuels to get you to work and back each day.

The Australian Aurora 101 solar powered car requires less than 2000W of power to travel at 100km/h. To achieve such high performance the car has high aerodynamic efficiency, motor efficiency greater than 98%, low rolling resistance tyres, and weighs less than 280kg with the driver in it. The energy used to propel the car is generated by high-efficiency photovoltaic cells

Another key to achieving high performance is efficient energy management. The car has a small battery that can store enough energy to drive the car about 250km at 100km/h. Energy stored in the battery can be used when extra power is required for climbing hills or for driving under clouds. More importantly, energy stored while the car is not racing can be used to increase the average speed of the car.

How should the battery be used? The motivation for this problem was to develop an energy management strategy for the Aurora solar racing team to use in the World Solar Challenge, a triennial race across Australia from Darwin to Adelaide. The real problem—with weather prediction, detailed models of the car and numerous race constraints—is intractable. But by studying several simplified problems it is possible to discover simple rules for an efficient energy management strategy.

The simplest problem is to find a strategy that minimises the energy required to drive a car with a perfectly efficient battery and a constant drive efficiency. The optimal strategy is to drive at a constant speed. This is just the beginning of the solar car problem, however.

More general problems, with more general models for the battery, drive system and solar power, can be formulated as optimal control problems, where the control is (usually) the flow of power from or to the battery. By forming a Hamiltonian function we can use Pontryagin's Maximum Principle to derive necessary conditions for an optimal strategy. We then use these conditions to construct an optimal strategy. The strategies for the various simplified problems are similar:

- On a level road, with solar power a known function of time, and with a perfectly efficient drive system and battery, the optimal strategy has three driving modes: maximum power, speed holding, and maximum regenerative braking.

- If the perfectly efficient battery is replaced by a battery with constant energy efficiency then the single holding speed is replaced by two critical speeds. The lower speed is held when solar power is low, and the upper speed is held when solar power is high. The battery discharges at the lower speed and charges at the higher speed. The difference between the upper and lower critical speeds is about 10km/h. There are precise conditions for switching from one mode to another, but small switching errors do not have a significant effect on the journey.

- If we now change from a level road to an undulating road, the optimal strategy still has two critical speeds. With hills, however, the conditions for switching between driving modes are more complex. Steep gradients must be anticipated. For steep inclines the control should be switched to power before the incline so that speed increases before the incline and drops while the car is on the incline. Similarly, for steep declines the speed of the car should be allowed to drop before the decline and increase on the decline.

- With more realistic battery models the optimal control is continuous rather than discrete. The optimal strategy is found by following an optimal trajectory in the phase space of the state and adjoint equations. This optimal trajectory is very close to a critical point of the phase space for most of the journey. Speed increases slightly with solar power. As before, the optimal speed lies within a narrow range for most of the journey.

- Power losses in the drive system affect the initial power phase, the final regenerative braking phase, and the speed profile over hills. The optimal speed still lies within a narrow range for most of the journey.

- With spatial variations in solar power it is possible to vary the speed of the car in such a way that the extra energy collected more than compensates for the extra energy used. Speed should be increased under clouds, and decreased in bright sunlight. The benefits of 'sun-chasing' are small, however.
- Solar power is not known in advance. By modelling solar power as a Markov process we can use dynamic programming to determine the target distance for each remaining day of the race. Alternatively, we can calculate the probability of completing the race at any given speed.

These principles of efficient control have been used successfully since 1993 to develop practical strategy calculations for the Aurora solar racing team, winner of the 1999 World Solar Challenge.

Declaration

I declare that this thesis does not incorporate without acknowledgment any material previously submitted for a degree or diploma in any university; and that to the best of knowledge it does not contain any materials previously published or written by another person except where due reference is made in the text.

Acknowledgements

I was introduced to solar cars in 1993, about six months before the World Solar Challenge. The Aurora team had decided to use non-rechargeable lithium batteries for half of their battery pack, but was not sure when to use them. Aurora approached the CSIRO Division of Mathematics and Statistics for help. Phil Howlett and I were drawn into the group because of our previous work on optimal train control. Together we solved the battery problem, and, supported by a CSIRO–University of South Australia Research Grant, went on to develop a driving strategy for the race. In October 1993 I raced across Australia with Aurora; we were the first Australian team to finish, and fifth overall.

In 1994 Aurora started building a new car, the Aurora 101. The aim was to win the 1996 World Solar Challenge. Many people and organisations contributed to the campaign. I worked on refining the driving strategy, supported by an ARC Collaborative Research Grant. Sadly, the race ended for us when we crashed just 32km south of Darwin.

Several people at the University of South Australia have helped and inspired me: Phil Howlett, my supervisor and co-author of many papers; Basil Benjamin, my associate supervisor; John Boland, who helped develop solar irradiation models; and Peter Murphy—I gained a much better appreciation of the technology when I helped design and build Ned 26 with the South Australian Solar Car Consortium.

Finally, I would like to thank Aurora, who introduced me to solar cars and have taught me so much about design and engineering; the team members that designed, built and raced the Aurora Q1, the team that designed, built and almost raced the Aurora 101, and the 1999 race team who improved and rebuilt the 101, and who didn't say a thing when other teams passed us.

PART ONE

Introduction

1 Motivation

In November 1996 the Honda *Dream* transported two people 3000km across Australia in four days, at an average speed of 90km/h. It used about 50kWh of electrical energy for the trip from Darwin to Adelaide. From the electricity grid this energy would have cost about $6; the *Dream* generated its own electricity from sunlight. For the same trip, the support cars and vans travelling with the team would each have used fuel costing $200–$450.

The following table compares the Honda *Dream* (Roche et al 1997) to a popular 4WD.

	solar car	4WD
mass (kg)	167	2400
peak power (kW)	6	160
size (m)	6 × 2 × 1.1	4.8 × 1.9 × 1.9
occupants	2	'enough space for a family outing or a meeting on the fly'... but usually just one or two people
power required to drive at 80km/h (kW)	1	~18
Darwin to Adelaide fuel cost ($)	$6 worth of electricity—no cost	$430 of petrol

Table 1-1: The Honda Dream compared to a popular 4WD.

Solar cars may not be practical, but do we really need 2.4 tonnes of machinery to take us to work each day?

2 Solar cars and the World Solar Challenge

Every three years teams from all over the world come to Australia to race solar powered cars across the continent from Darwin to Adelaide—a distance of over 3000km. The solar cars use panels of photovoltaic cells to convert sunlight into electrical power that drives an electric motor connected to the wheels. The race rules specify maximum dimensions for the car and for the solar panel. Up to 5kWh of electrical energy may be stored in batteries. The cars start the race with full batteries—enough energy to travel about 300km at cruising speed. The energy required to complete the race must be obtained from the sun. To be competitive, the cars must use the available energy as efficiently as possible.

2.1 Solar cars

A solar car is a special type of electric car, with photovoltaic cells on the upper surface of the car to generate the energy required for long trips.

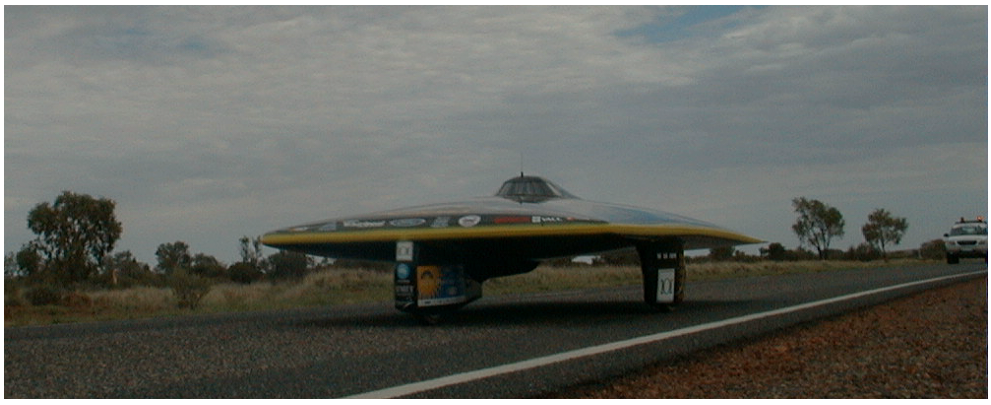

Figure 2-1: The Aurora 101, winner of the 1999 World Solar Challenge.

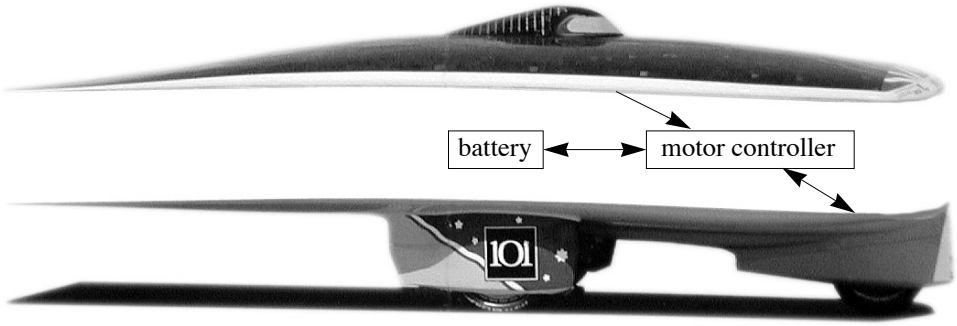

Figure 2-2: Electrical power generated by photovoltaic cells on the upper surface of the car is used to drive an ultra-efficient electric motor built into the front wheel. Energy can also be stored in batteries, in this case silver-zinc batteries.

The main components and power flows in a solar car are indicated in Figure 2-2.

Solar panel

The solar panel is made from hundreds or even thousands of photovoltaic cells. Each cell converts sunlight to electrical power. The efficiency of the conversion process ranges from 15% up to 24% for the best cells. On a clear day, with the sun directly overhead, the sunlight falling on the earth's surface has a power of about 1000 W/m^{-2}. A typical commercial cell is 100 mm square with an efficiency of 15% and generates a current of 3 amperes at 0.5 volts, giving 1.5 W of power.

The photovoltaic cells are connected in series and parallel to form an array. A panel with an area of 8 m^2 will generate around 1200 W—enough power to run a toaster.

The cells on the Aurora 101 were made by the Photovoltaics Special Research Centre at the University of New South Wales, and are over 20% efficient. The encapsulation has deteriorated since 1996, when the panel was built; for the 1999 World Solar Challenge the panel generated about 1300W.

Motor

The car is propelled by an ultra-efficient electric motor. Motor efficiency for the fastest cars is in the range 95-98%, compared to around 50% for the motors commonly found in household appliances. Solar car motors are usually brushless DC motors with rare-earth permanent magnets. An electronic controller switches the current from one motor winding to the next. The combined efficiency of the motor and controller can be as high as 96%.

Since 1993, motors that connect directly to a wheel have become popular. Some are even built into wheels. The advantage of a wheel motor is that it does not require a transmission. Drive systems with a belt or chain transmission suffer transmission power losses of about 5%.

The Aurora 101 uses a wheel motor developed by the CSIRO and the University of Technology Sydney, with a peak efficiency of 98%

Battery

A solar car could operate without a battery; the power from the solar panel would be applied directly to the wheels. But a battery offers important advantages. First, it allows energy to be collected when the car is not being driven. With a large enough battery, energy can be collected for up to 14 hours each day. The energy collected during this extended period can be expended during a shorter time interval when the car is being driven, increasing the average power available while driving. A second important advantage of having a battery is that excess solar power can be stored in the battery then used later when extra power is required for climbing hills or for driving under clouds.

Without a battery there is only one sensible energy management strategy—use all the available power whenever possible. A battery allows other driving strategies to be used. The problem addressed in this thesis is to find the best strategy.

In the 1996 World Solar Challenge the top cars used silver-zinc batteries. In 1999, most of the top cars used lithium ion batteries.

Mechanical efficiency and aerodynamics

To make the best use of the energy collected by the solar panel, the car must be as efficient as possible. At 100km/h, over 75% of the power applied at the road will be used to overcome aerodynamic drag. The rest is used to overcome rolling resistance in the tyres and bearings.

Aerodynamic drag is minimised by careful design of the car shape and the smoothness of the surfaces. Roche et al (1997) give nine rules for minimising drag:

1. flow should be attached over every surface of the car;
2. wetted area should be minimised (without detaching the flow);
3. laminar flow should cover as much of the car as possible;
4. all surfaces should be as smooth as possible;

5. the car should produce zero lift;
6. wing tip drag should be minimised by thinning and rounding the edges of the car;
7. frontal area should be minimised;
8. interference drag should be minimised by, for example, fairing the joints between wheel spat and the main body; and
9. ventilation drag, caused by air flowing through the car, should be minimised.

(Flow is attached if air moving close to the surface of the car stays close to the car until it leaves at the tail. Flow is laminar if the flow is in smooth layers, as opposed to turbulent flow. The wetted area is the surface area of the car that is in contact with the surrounding air flows. A wheel spat is an aerodynamic cover surrounding a wheel.)

The Aurora car has been tested in a full-size wind tunnel at speeds up to 140km/h. It has attached flow over every surface, and the flow is laminar along the edges of the top for over 3m (Watkins et al 1998).

Tyre and bearing resistance are minimised by careful design and by minimising the mass of the car. Solar car bodies are usually built from light-weight materials such as honeycomb or foam sandwiched between layers of carbon fibre cloth. With an 80kg driver and 40kg of batteries, the Aurora 101 has a mass of about 300kg.

The Aurora 101 requires about 1900W of power to drive at 100km/h. The solar panel can generate about 12kWh of energy during a day. Allowing for energy losses in the battery, the car could drive about 600km at 100km/h each day.

Driving a solar car

Driving a solar car is easier than driving a conventional car. In most solar cars the driver uses a rotary knob to set the desired speed, and the motor controller automatically adjusts the power applied to the motor to keep the car at that speed. The electrical circuit is such that if more power is required than is available from the solar panel, it is drawn from the battery. Similarly, any excess power from the panel is stored in the battery. Driving at a constant speed is very efficient, and so the default control system for most solar cars is also the best possible.

2.2 The World Solar Challenge

In 1982 Hans Tholstrup and Larry Perkins drove the 'Quiet Achiever' solar car 4000 km across Australia, from Perth to Sydney. The journey took 20 days. At the end of the journey, several people were quick to point out deficiencies in their car. Hans threw the challenge back at them, and organised the first World Solar Challenge for October 1997. The race has been run every three years since.

A book by Tuckey (1989) describes the development of the General Motors *Sunraycer*, winner of the first World Solar Challenge in 1987. Kyle (1991), Storey et al (1994) and Roche et al (1997) have each prepared excellent reports on the 1990, 1993 and 1996 races.

The main rules for the World Solar Challenge are outlined below.

Vehicle specifications

- Apart from the initial battery charge, solar irradiance is the only power source that may be used to power the car.
- The car must fit inside a rectangular box 6 m long, 2 m wide and 1.6 m high. The driver's eyes must be at least 0.7 m above the road.
- The cars must pass a safety inspection before the race; this safety inspection includes a stability test and a brake test.
- A single-seater car must carry a driver with a mass no less than 80 kg; a two-seater car must carry two people with a combined mass no less than 160 kg. Bags of lead shot are used to ballast each occupant to 80 kg.

Solar collectors

- Solar collectors may be constructed in any way. For a single seater car the solar collector must fit in a 4.4 m × 2 m × 1.6 m rectangular box, and must fit within an 8 m^2 rectangle. For a two-seater car solar power may be obtained from the entire surface of the car.
- When stationary, the height of the solar collector must not exceed 2.5 m.

Battery

- Fuel cells, which convert liquid or gaseous fuels directly to electricity, are not allowed.
- The batteries must be rechargeable.

- Batteries may be charged from the solar collector between sunrise to sunset, and by regenerative braking while the car is moving.
- A flywheel is considered to be a battery.
- The car must travel the entire route with the same batteries.
- The maximum allowable battery mass depends on the type of battery. The battery masses correspond to a nominal energy content of 5kWh:
    - silver-zinc and experimental batteries: 40kg
    - lead-acid: 125kg
    - nickel-zinc: 75kg
    - nickel-cadmium and nickel-iron: 100kg.

The race

- The race is over a 3000km course from Darwin to Adelaide. The cars start together on the first day. The first car to Adelaide is the overall winner.
- Cars may be driven only between 8.00am and 5.00pm each day. A ten minute grace period after 5.00p.m. allows teams to find a suitable place to stop. The next day, the start is delayed by the extra time used.
- The car must stop at eight specified locations for thirty minutes each. These stops are for media publicity, race control, and to allow participants to refuel their conventional cars.
- An observer travels with each team.

2.3 Previous race results

The following table shows the average speeds of the fastest five cars in each of the races up to 1999. The speed of the fastest car has increased from 66.9km/h, achieved by the GM *SunRaycer* in 1987, to 89.8km/h achieved by the Honda *Dream* in 1996.

Place	1987	1990	1993	1996	1999
1	66.9	65.2	85.0	89.8	73.0
2	44.5	54.7	78.3	86.0	72.1
3	42.9	52.5	70.8	80.7	71.9
4	36.9	52.4	70.4	66.7	71.3
5	31.5	51.4	70.1	64.9	67.9
Mean:	44.5	55.2	74.9	77.6	71.2

Table 2-1: Speeds of the fastest five cars, in km/h, for each of the races up to 1999. The 1999 race had three days of heavy cloud.

2.4 Aurora Vehicles

The research work described in this thesis was done in collaboration with the Aurora Vehicles Association. Aurora was formed by a group of enthusiasts, many of them engineers at Ford Australia, who had previously built and raced cars in the Shell Mileage Marathon; during the 1980's they held the world record three times. Since 1987 the team has concentrated on racing solar cars, and has continued to excel:

- in 1987, as the Ford *Sunchaser* team, Aurora came second overall and first amongst the Australian teams;
- in 1990, as the AERL team, Aurora came sixth overall and first amongst the Australian teams;
- in 1993, with the Aurora *Q1* car, the team came fifth overall and was once again first amongst the Australian teams;
- in 1994, the team drove the *Q1* from Perth to Sydney in 8 days, breaking the previous record of 20 days set by Hans Tholstrup and Larry Perkins in 1982;
- in 1996, with the Aurora 101, the team had to withdraw from the race after only 32km when a brake failure caused the car to crash;
- in 1999, the Aurora 101 was the winner of the 1999 World Solar Challenge;
- in 2000, the Aurora 101 was driven 870km from Sydney to Melbourne in a day.

The driving strategies described in this thesis were first used by Aurora for the 1993 World Solar Challenge, and have been developed and adapted for subsequent events.

2.5 Electric and hybrid cars

Solar cars may never be practical, but electric cars will be. By removing most of the solar cells from solar cars and connecting them to the electricity grid it is possible to make smaller, more aerodynamic cars, and at the same time make better use of energy generated by flatter panels pointed more directly at the sun. Energy is fed into the electricity grid by the photovoltaic panels, and drawn from the grid to recharge the electric car.

Electric cars are already practical. Based on their experience in the 1987 World Solar Challenge, General Motors have developed the Impact electric car. Other major car manufacturers are also building and selling electric cars.

One of the main problems with electric cars is their limited range compared to petrol cars. Petrol burned in a conventional engine has a net specific energy of about 2800 Wh/kg; that is, each kilogram of fuel burned produces about 2800Wh of useful energy. Lead acid batteries have a specific energy of just 35Wh/kg. More advanced, experimental batteries such as lithium ion batteries have specific energies of 125 Wh/kg. Zinc-air batteries have a specific energy of 225 Wh/kg, but must be returned to a factory to be recharged. Fuel cells that convert fuel directly into electrical energy may eventually overcome the energy storage problems.

An alternative to the pure electric car is the hybrid car, where a small combustion engine and generator supplement the batteries. Without a direct connection to the wheels, the engine can be operated much more efficiently than in a conventional car. In late 1997 Toyota launched the Prius, a hybrid car that uses half the fuel of a similar car with a conventional drive system.

Since 1991 the Rocky Mountain Institute (http://www.rmi.org/) has been developing the concept of a ‘hypercar’ — an aerodynamic car made from lightweight composite materials and with a hybrid electric drive system. They argue that such a car could have 4 to 8 times the efficiency of a conventional car. The combustion engine and batteries could eventually be replaced by fuel cells. Commercial car makers have now started implementing these ideas.

2.6 Using energy wisely

The aim of the work described in this thesis was to develop efficient energy management strategies for a solar car. The same techniques can be used to develop energy management strategies for a wide range of systems. In fact, the techniques described here were developed from earlier work on efficient driving strategies for suburban and long-haul trains (Howlett & Pudney 1995).

Until an abundant, lightweight, clean source of energy is found, efficient energy management will play an important part in reducing the dangerous pollutants we generate by burning fossil fuels.

3 The research problem

How should energy be managed to maximise the performance of a solar-powered car? How should the car be driven? How should the power flow between the solar panel, energy storage system and drive system, and within the energy storage system?

Figure 3-1 shows the power system for a hypothetical solar car. Unlike the solar car described in the last chapter, it has more than one energy storage device and it has an energy management controller for controlling power flows.

In 1993 Aurora Vehicles reasoned that only half of the allowable battery capacity would be recharged, so they replaced half of their lead-acid battery pack with much lighter, non-rechargeable lithium cells. The World Solar Challenge rules were subsequently changed to allow only rechargeable batteries. Nevertheless, by mixing storage devices with different characteristics it may be possible, with the right energy management strategy, to achieve better energy storage efficiency than with a single storage device. For example, supercapacitors are relatively heavy but very efficient. For journeys where the power cycles in and out of the storage system, a supercapacitor can be used to reduce power losses in a less efficient battery.

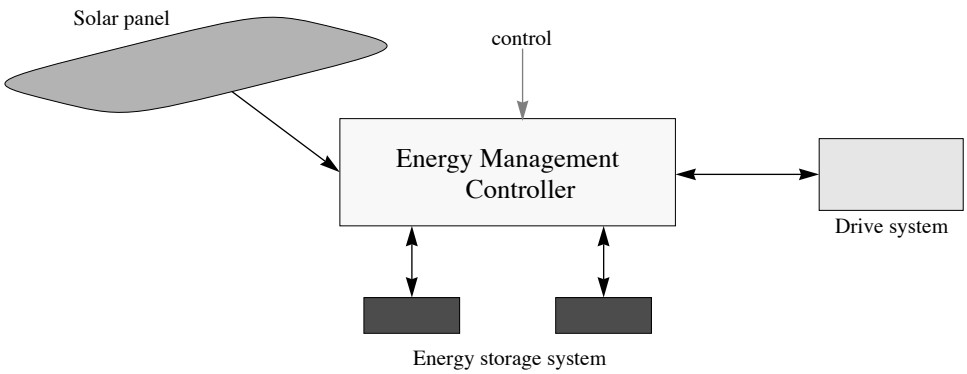

Figure 3-1: The power system for a solar car. The dark arrows represent possible current flows. For convenience, we can consider the power associated with these current flows as 'power flows'.

For a conventional solar car with a single energy storage system, a single control is required—either the power to the motor, or the power from the battery. Usually, the driver controls the power to the motor, and the battery makes up the difference between the motor power and the power from the solar panel.

For a car with two energy storage systems, two controls are required. The controls can be either both storage powers, or the motor power and one storage power. In a practical system the driver would control the motor power and the energy management controller would automatically control the power mix from the two storage devices. For calculating the optimal strategy, however, it is often more convenient to consider the two storage powers as the controls.

Under certain conditions it may be prudent to transfer energy from one battery to another. For example, consider a car with two batteries; battery A can deliver high power but for short durations only, while battery B can only deliver low power, but for longer durations. Following a period of high power use the controller can slowly recharge battery A from battery B.

In the remainder of this thesis I formulate and solve problems associated with finding the best way of operating a solar powered car. The aim is to develop practical control strategies that can be applied not only to solar cars, but also to lightweight electric cars and to other renewable energy systems. The problems are formulated as mathematical control problems, and solutions found by applying the standard techniques of optimal control. By starting with simple versions of the control problem and gradually refining the models used to formulate the problem we get valuable insight into the problems and the solutions.

PART TWO

Modelling the problem

4 Solar power

Irradiance is a measure of the power per unit area received from the sun, and is measured in Watts per square metre (Wm^{-2}). The irradiance at the surface of the earth depends on many factors, including the relative positions of the sun and earth and the trasmissivity of the atmosphere. In this chapter we develop a practical scheme for calculating solar irradiance profiles.

We also show that to maximise the energy collected by a World Solar Challenge car, the car should have a box-shaped panel that fills the allowable volume for the car. Of course, the increased aerodynamic drag on such a car would completely overwhelm the increased power. Clearly there is a compromise shape that will maximise the performance of the car; finding it is beyond the scope of this work.

4.1 Solar irradiance

The clear-sky irradiance falling on an inclined plane is usually modelled as having three components: beam irradiance that travels in a straight line from the sun, diffuse irradiance from a uniformly bright sky, and irradiance reflected from the ground. The geometry is illustrated in Figure 4-1.

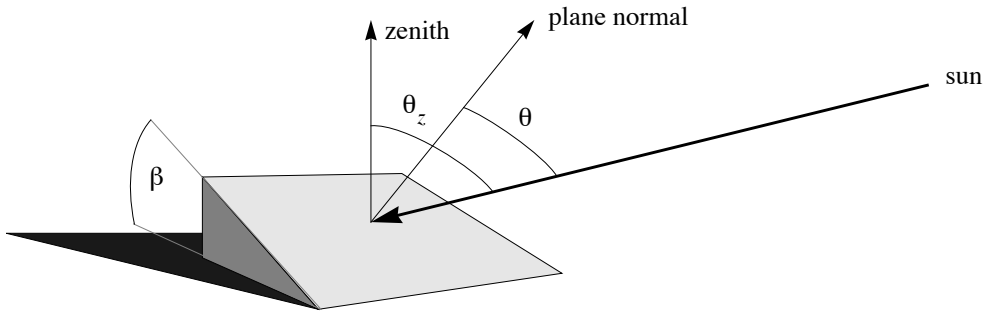

Figure 4-1: Geometry for calculating the total irradiance on an inclined plane.

Total irradiance on the plane is given by

$$I = [I_b \cos\theta]_+ + I_d\left[\frac{1+\cos\beta}{2}\right] + [I_b + I_d]\,\rho\left[\frac{1-\cos\beta}{2}\right] \qquad (4.1)$$

where I_b is beam irradiance normal to the beam, θ is the angle of incidence of the beam, I_d is diffuse irradiance on a horizontal plane, β is the inclination of the plane, and ρ is ground reflectance (Duffie & Beckman 1980; Frick et al 1988). The subscript '+' on the first term indicates the positive part of the term; that is, the term is included only if it is positive.

Clear-sky beam irradiance is given by

$$I_{bc} = I_0 \tau_b$$

where I_0 is extra-terrestrial irradiance and τ_b is beam transmittance. Diffuse irradiance is assumed to be distributed uniformly over the sky, and for a horizontal plane is given by

$$I_{dc} = I_0 \tau_d \cos\theta_z$$

where τ_d is diffuse transmittance and θ_z is the angle between the sun and the zenith. Duffie & Beckman (1980) give empirical formulas for calculating τ_b and τ_d based on time of year, latitude, climate and elevation.

The sky is not usually clear. A more convenient model, used by the Aurora team, uses

$$I_b = BI_{bc} \qquad (4.2)$$

$$I_d = BI_{dc}$$

where B is an estimated 'brightness factor'. The instantaneous brightness factor can be calculated by dividing the measured irradiance by the calculated clear-sky irradiance.

Frick et al (1988) has historical irradiance data for five locations on or near the Stuart Highway: Darwin, Alice Springs, Oodnadatta, Woomera and Adelaide. The mean irradiance on a horizontal plane during October–November is shown in Figure 4-2.

Daily irradiation for each site can be found by integrating irradiance with respect to time. We can then find the historical brightness factor for each location by dividing the calculated clear-sky daily irradiation by the historical daily irradiation. In Chapter 18 I describe a scheme for predicting brightness based on observed daily irradiation. Irradiation observations are available each evening from airport meteorological offices in Darwin, Alice Springs and Adelaide, or from an irradiation map based on satellite observations.

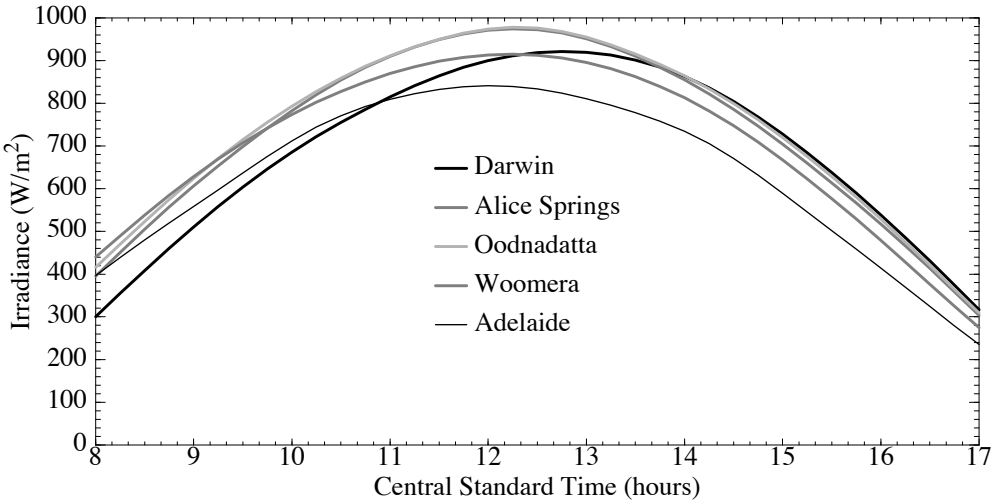

Figure 4-2: Historical mean solar irradiance on a horizontal plane for October–November at five locations along the Stuart Highway.

4.2 Photovoltaic cells

A solar panel uses photovoltaic cells to convert solar irradiance to electrical power. The power generated by the panel depends on several factors, including the temperature of the cells and the current drawn from the panel.

Temperature

The efficiency of the panel decreases as the panel temperature rises, and can be modelled by

$$\eta = \eta_0 [1 - \alpha (T_P - T_0)]$$

where T_P is the temperature of the panel in degrees Celsius, α is a temperature coefficient, and η_0 is the efficiency of the panel at temperature T_0. The efficiency of a cell might drop from 17% at 25°C to 16% at 45°C. The temperature of the panel is modelled by the equation

$$T_P = T_A + \theta_I (1 + \theta_{T_A} T_A) (1 - \theta_w w) I$$

where T_A is the ambient temperature in degrees Celsius, w is the apparent wind speed and I is solar irradiance, and where $\theta_I = 0.0138$, $\theta_{T_A} = 0.031$ and $\theta_w = 0.042$ are constants obtained from experiments. The power from the panel is

$$P_P = A_P \eta I$$

where A_P is the area of the solar panel.

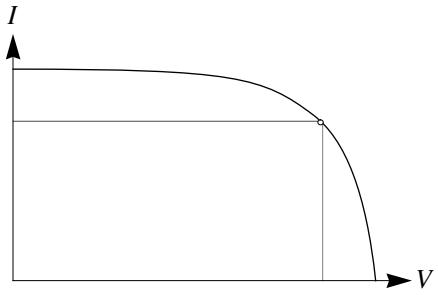

Figure 4-3: The relationship between current I and voltage V for a solar cell. The dotted lines indicate the voltage and current corresponding to maximum power, which is given by the area of the rectangle.

Current

As the current drawn from a photovoltaic cell increases the cell voltage decreases, as shown in Figure 4-3. With no current being drawn, the panel voltage is V_{oc}. As the current increases to I_{sc} the voltage drops to zero. At some point on the current–voltage curve the power is maximised.

Solar cells are connected in series strings to give a more convenient voltage. The string current will be the minimum of the individual cell currents; the string voltage will be the sum of the individual cell voltages. The relationship between voltage and current for a string is similar to that for an individual cell.

Solar cars are usually equipped with a maximum power point tracker for each string. These devices are DC-DC power converters that match the optimal string voltage to the voltage required by the load. A good tracker will have an efficiency greater than 98%.

4.3 Panel shape

What shape should a solar panel be to maximise the energy collected in a day?

Consider a simpler problem with the sun moving in a plane and the panel described by a curve in the same plane, extruded one unit perpendicular to the plane as shown in Figure 4-4. This problem is a reasonable approximation to the situation in the World Solar Challenge, where the car travels roughly south as the sun moves overhead across the sky

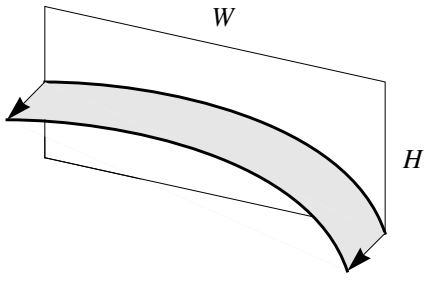

Figure 4-4: A simple extruded panel. The sun moves in the same plane as the rectangle WH.

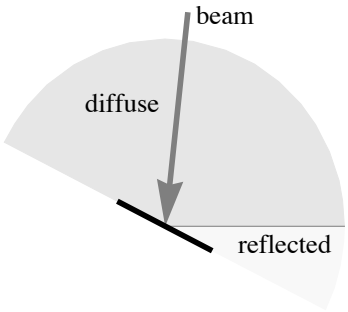

Figure 4-5: The light falling on an element of the panel can be modelled as having three components: beam irradiance that travels directly from the sun, diffuse irradiance from a uniformly bright sky, and reflected irradiance from the ground.

from east to west. We wish to design a panel that maximises the energy collected as the sun moves across the sky. The panel must fit within a rectangular box of width W, height H and unit depth.

Figure 4-5 shows the three types of light falling on an element of the panel. For a concave panel the irradiance at any point on the panel is given by (4.1). If any part of the panel is convex then some of the diffuse and reflected light will be obscured, and calculation of the irradiance on the panel becomes more difficult. Non-concave panels will not be considered.

Consider an element of a concave panel illuminated by a beam with unit width and depth and irradiance I_0, as shown in Figure 4-6. The beam illuminates an element of unit depth and length $l = \cos\theta$, where θ is the angle between the element normal and the beam. The power generated by the element is the area of the element multiplied by the first term of (4.1); that is,

$$p_b = lI_0\cos\theta = I_0.$$

The power collected from a beam is therefore related only to the area and irradiance of the intercepted beam, and not to the shape of the panel. To maximise the energy collected from beam irradiance during a day the panel should be constructed so that the area intercepted is maximised for every angle $\theta_z \in [-\pi/2, \pi/2]$. The required shape that meets the height and width constraints is three sides of a rectangle. For any other concave

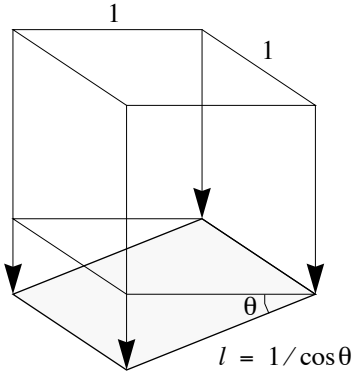

Figure 4-6: Interception of beam with unit width and depth by an element of a concave panel.

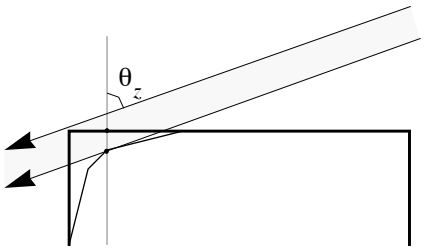

Figure 4-7: The optimal concave panel shape is three sides of a rectangle.For any other concave shape we can find a point where the height is less than the height of the rectangular panel, then construct a tangential beam angle θ_z for which the beam area intercepted is less than the beam area intercepted by the rectangular panel. The shaded area of the diagram shows this difference.

shape we can find an angle θ_z for which the beam area intercepted is less than that for the rectangular panel, as shown in Figure 4-7. By continuity, the beam area intercepted will also be less for surrounding angles, and so the beam energy collected by the lower panel during a day will be less than that collected by the rectangular panel.

To calculate the effect of panel shape on diffuse and reflected energy collection we will describe the concave shape of the panel by a non-decreasing function w such that $w(l)$ is the width of the panel when the length around the perimeter is l, as shown in Figure 4-8. This model has two nice features: it can describe vertical sides, and it has $\cos\beta = w'(l)$.

From (4.1), the diffuse irradiance at any point $l \in [0, L]$ is

$$I_D(l) = I_d\left[\frac{1 + w'(l)}{2}\right]$$

The power collected by the panel from diffuse light is therefore

$$p_d = \int_0^L I_D(l)\,dl$$

$$= \frac{I_d}{2}\left[L + w(L)\right].$$

For a given length of panel, to maximise the diffuse power collected we should maximise the width of the panel. The rectangular panel has maximum width, and therefore maximises the diffuse energy collected in a day.

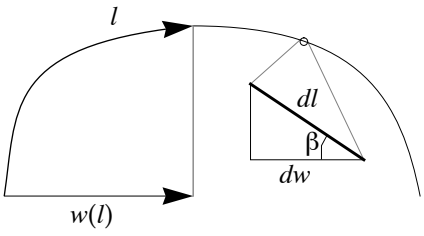

Figure 4-8: The shape of a concave panel can be described by a non-decreasing function w where w(l) is the width of the panel at a given length l around the perimeter.

The power collected by the panel from reflected light is

$$p_r = \int_0^L [I_b + I_d]\,\rho\left[\frac{1 - w'(l)}{2}\right] dl$$

$$= \frac{[I_b + I_d]\,\rho}{2}\,[L - w(L)]\,.$$

For a given length of panel, to maximise the reflected energy collected we should minimise the width of the panel; that is, we should maximise the height. The rectangular panel is as high as is allowed, and so maximises the reflected energy collected in a day.

In three dimensions, the optimal rectangular panel corresponds to a rectangular box with photovoltaic cells on each of the five faces visible from the sky. Of course, the aerodynamic efficiency of a box is dreadful. There is clearly a compromise between aerodynamic efficiency and panel shape, but finding it is beyond the scope of this work.

Examples

In the following examples the solar irradiance parameters are based on empirical data from Duffie & Beckman (1980). They are:

$$I_0 = 1397$$

$$t_b = 0.1522 + 0.7269e^{-0.3682/\cos\theta_z}$$

$$t_d = 0.2710 - 0.2939t_b$$

$$\rho = 0.2$$

Each panel must fit into a rectangular box 2m wide, 4m long and 1.5m high.

Sunrise is at 5.30am (solar time), and sunset at 6.30pm. Power is collected for 9 hours between 7.30am and 4.30pm. These solar times are good approximations to the sunlight and race times for the World Solar Challenge. Note, however, that the results are for clear skies, not average skies. The two panels evaluated are shown in Figure 4-9.

Panel outputs are shown in Figures 4-10 and 4-11. The rectangular panel collects a total of 19.1 kWh—11.6 kWh from the top and 3.7 kWh from each of the sides. The inverted-V collects a total of 14.4 kWh—7.2 kWh from each side. A flat panel would collect the same as the top of the rectangular panel—11.6 kWh.

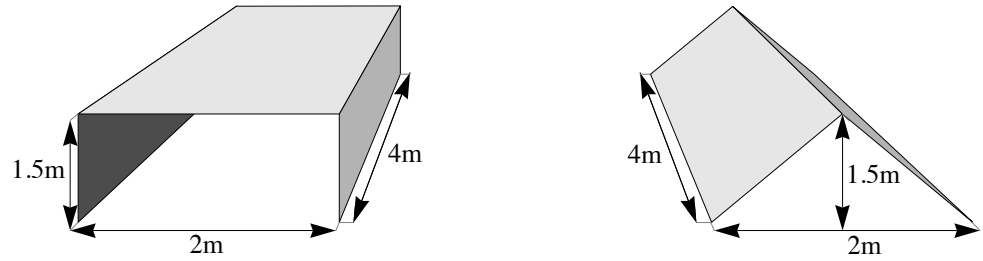

Figure 4-9: The rectangular and inverted-V panel shapes used to compare energy collection.

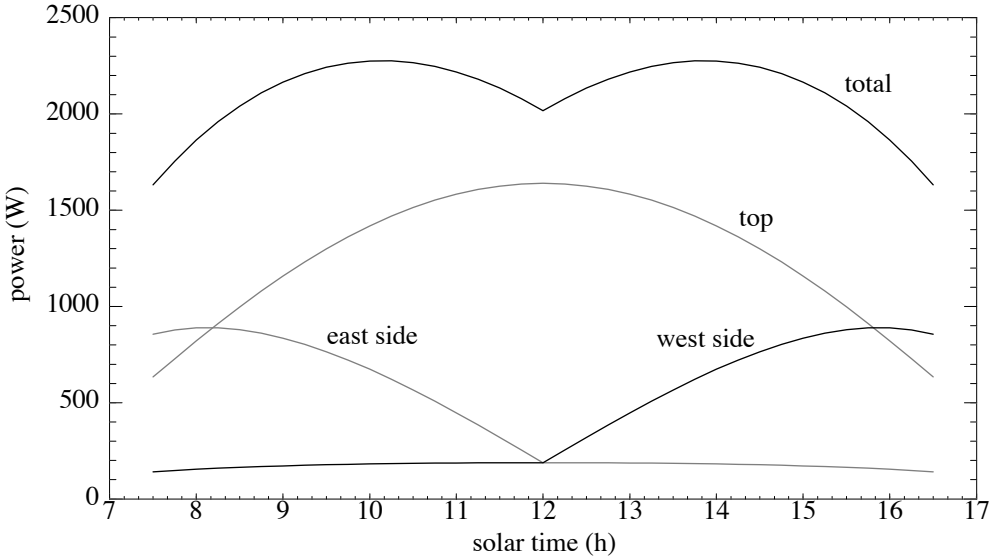

Figure 4-10: Output power for the rectangular panel. Total energy collected is 19.1kWh. A flat panel would collect 11.6kWh.

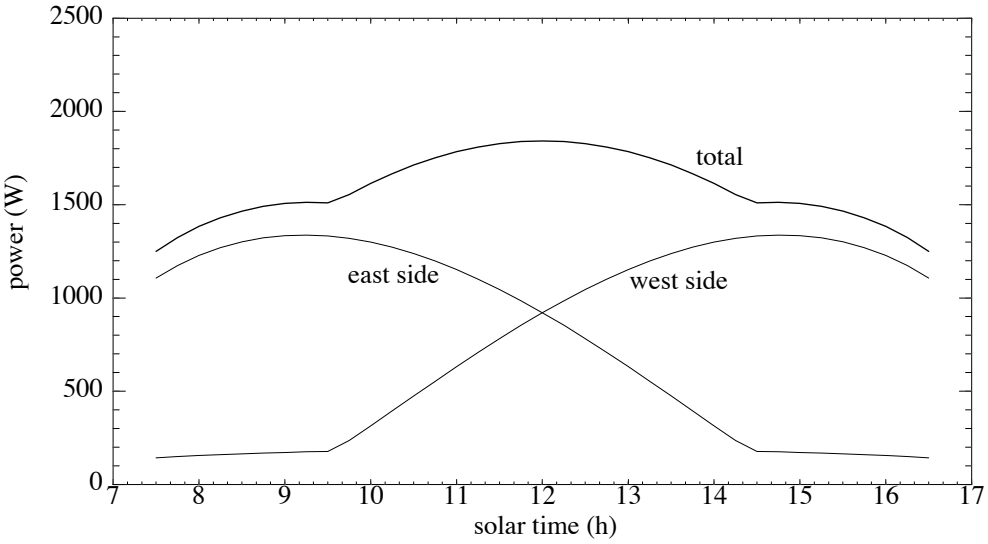

Figure 4-11: Output power for the inverted-V panel. Total energy collected is 14.4kWh. A flat panel would collect 11.6kWh.

5 Energy storage

The most common energy storage device for solar and electric vehicles is a battery. In this chapter we will examine some models of storage batteries, and develop a model for the silver-zinc battery used in the Aurora 101 solar car.

5.1 Electrochemical cells and batteries

An electrochemical cell is a chemical device capable of storing and releasing electrical energy. While discharging, chemical reactions within the battery cause charge to flow from one electrical terminal to the other. During charging the charge flow and chemical reactions are reversed, and electrical energy is converted back to chemical energy.

A battery is a series of one or more electrochemical cells. Each cell consists of a pair of electrodes immersed in an electrolyte. Figure 5-1 is a diagram of a lead-acid battery. Each cell contains a positive electrode containing lead dioxide (PbO_2) and a negative electrode containing spongy lead (Pb). The two electrodes are immersed in an electrolyte of dilute sulphuric acid (H_2SO_4). In solution, the sulphuric acid dissociates into negative sulphate ions (SO_4^{--}) and positive hydrogen ions (H^+).

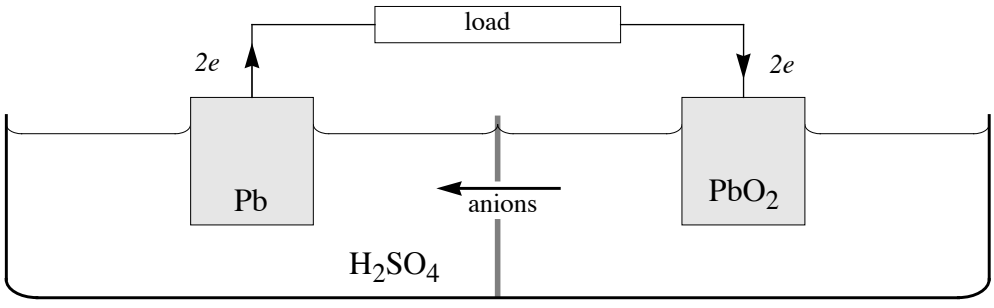

Figure 5-1: An electrochemical cell. The cell is composed of two half-cells at different potentials. Electrons flow through the load from one half-cell to the other, while anions flow through the electrode to maintain the balance of charge in each half-cell.

There is continuous transfer of electrons between each electrode and the electrolyte. At the negative electrode the reaction rates are such that the electrode gains a net negative charge, electrically balanced by excess anions in the electrolyte. This buildup of charge causes the reaction rates to approach equilibrium. The net charge on the electrode determines the electrode potential. A similar process occurs at the positive electrode.

If there is a potential difference between the two electrodes and an external electrical connection between them then electrons will flow through the load. At the same time anions flow through the electrolyte so that each half-cell remains electrically neutral. Current flow causes the half-cell reactions to move away from equilibrium, and the reactions continue.

During discharging, the following reactions occur:

- at the negative electrode, $Pb + SO_4^{--} \longrightarrow PbSO_4 + 2e$
- at the positive electrode, $PbO_2 + H_2SO_4 + 2H^+ + 2e \longrightarrow PbSO_4 + 2H_2O$.

During charging the reverse occurs. The reactions can be summarised as

$$PbO_2 + Pb + 2H_2SO_4 \rightleftharpoons 2PbSO_4 + 2H_2O$$

where the left side corresponds to a fully charged cell and the right side to a fully discharged cell.

Polarisation

As charge flows to or from an electrode the electrode potential changes, causing the cell voltage to change from the equilibrium electromotive force (emf) whenever current flows. The operating voltage of the cell is

$$V = \varepsilon + \eta$$

where ε is the cell emf and η is the polarisation of the cell. Cell voltage increases from the equilibrium emf during charging, and decreases during discharging.

The total polarisation η can be considered as the sum of three separate polarisations: activation polarisation, ohmic polarisation and concentration polarisation. Activation polarisation is caused by rate limiting steps in the reactions or in the charge transfer processes at the electrodes. The response to a change in current is usually an exponential increase or decay. Ohmic polarisation is due to the electrical resistance of the current paths within the battery, and changes instantly with current from one constant level to another.

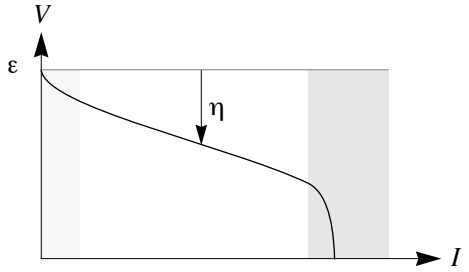

Figure 5-2: A typical discharge polarisation curve. In the first shaded region the polarisation is primarily activation polarisation. In the second (unshaded) region the polarisation is primarily Ohmic. In the final region reactant transport rates cause additional polarisation.

Concentration polarisation is associated with the transport of reactants and products to and from the reaction sites. The response to a change in current is complex, and is usually much slower than the activation polarisation.

A typical discharge polarisation curve is shown in Figure 5-2. The exact shape of the polarisation curve changes with the chemical state of the battery.

Activation rate

The current that can be transferred at an electrode is determined by the rate of the electrode reaction, also known as the activation rate, and by the area of the interface between the electrode and the active electrolyte.

If the concentration of the reactants at the electrode surface does not differ significantly from the bulk concentrations then the current density at an electrode is given by the Butler-Volmer relationship

$$I = I_0 \{ \exp \frac{-\alpha n F \eta_a}{RT} - \exp \frac{(1-\alpha) n F \eta_a}{RT} \} \qquad (5.1)$$

where α is the transfer coefficient, n is the number of electrons transferred in the chemical reaction, F is Faraday's constant, η_a is the activation polarisation, R is the gas constant, T is the absolute temperature and I_0 is the exchange current for the reaction (Kirk-Othmer 1991, Vincent 1984). This relationship can be used to determine the maximum current density for an electrode reaction at a specified polarisation.

When the polarisation is less than about -0.05V the second exponential term becomes negligible, and

$$I \approx I_0 \exp \{ \frac{-\alpha n F \eta_a}{RT} \} .$$

That is,

$$\ln I = \ln I_0 - \frac{\alpha n F \eta}{RT}. \tag{5.2}$$

Equation (5.2) can be rewritten as the well-known Tafel equation for activation polarisation

$$\eta = a - b \log_{10} I$$

where $a = (2.303RT/\alpha nF) \log_{10} I_0$ and $b = 2.303RT/\alpha nF$.

Ohmic polarisation

Ohmic polarisation is caused by the internal resistance of the bulk phases within the cell, and depends on the current paths, cell geometry and characteristics of the electrode surfaces. The ohmic polarisation in a cell with effective internal resistance R_C is given by Ohms law,

$$\eta_o = -IR_C.$$

Mass transport rate

When the local concentration of a reactant differs significantly from its equilibrium concentration the rate of the reaction depends on the transport of that reactant to the reaction site. Transport of reactants and products occurs by diffusion, by migration in a electric potential field, and by convection.

The polarisation resulting from changes in electrolyte reactant concentration is

$$\eta_c = \frac{RT}{nF} \ln (C_e/C)$$

where C_e is the concentration at the electrode surface and C is the average concentration in the bulk of the electrolyte (Kirk-Othmer 1991).

A stationary layer model is often used to model the transport of reactants and products. A thin stationary layer is assumed to extend from the electrode surface into the bulk of the electrolyte. Beyond this layer, the concentration of reactants is uniform. If we assume a linear concentration gradient across the stationary layer, the limiting current density for the diffusion of a reactant is given from Fick's law (Kirk-Othmer 1991, Vincent 1984) by

$$I_l = \frac{DnFC_B}{\delta} \tag{5.3}$$

where D is a diffusion coefficient, C_B is the concentration of the reactant in the bulk of the electrolyte and δ is the thickness of the stationary layer. With electromigration, (5.3) becomes

$$I_l = \frac{DnFC_B}{\delta(1-\tau)}$$

where τ is the transference number of the reactant. The relationship between limiting current density and concentration polarisation is then given by

$$\eta_c = \frac{RT}{nF}\ln\left(1-\frac{I}{I_l}\right)$$

(Kirk-Othmer 1991).

Capacity

The theoretical capacity of a cell is

$$Q_T = xnF$$

where x is the number of moles of reaction associated with a complete discharge, n is the number of electrons transferred in the chemical reaction and F is Faraday's constant (Vincent 1984).

In practice, the rated capacity of a cell is the charge delivered when the cell is discharged under prescribed conditions to a specified cut-off voltage. The capacity of a cell is usually specified for a given C-rate, where a C-rate of ρ indicates that the nominal capacity of the cell, in ampere-hours (Ah), is delivered at a constant rate in $1/\rho$ hours. For example, a 2 Ah cell discharged at C/5 will deliver 0.4 A for 5 hours.

Energy

The energy delivered by a cell is

$$E(t) = \int_0^t V(\tau)I(\tau)d\tau$$

where V is the cell voltage and I is the current drawn.

Power

The current drawn from a cell is determined by the external load. The power delivered is

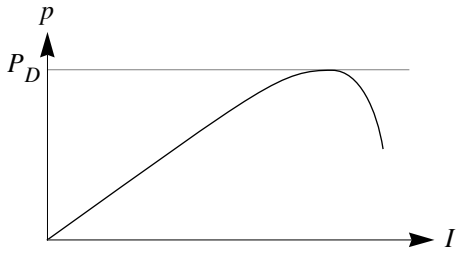

Figure 5-3: A typical power curve. Power p initially increases with current I, but reaches a maximum P_D and then drops as the cell voltage drops due to polarisation effects.

$$P(t) = I(t)V(t)$$

where the cell voltage V depends on polarisation losses. A typical power curve is shown in Figure 5-3. Power initially increases with current, but reaches a maximum and then drops as the cell voltage drops due to polarisation effects.

5.2 Battery models

For the solar car problem we require a battery model that predicts the charge remaining in the battery and battery voltage. We do not need the detail described in the previous sections. In this section we will examine battery models developed by Marr et al (1992), Protogeropolous et al (1994) and Manwell & McGowan (1993).

Marr et al

Marr et al (1992) model the voltage V of an electric traction battery by

$$V = V_0(D) - IR(D)$$

where V_0 is the effective open circuit voltage, I is the discharge current, R is the effective internal resistance of the battery, and D is the depth of discharge. This model is essentially modelling ohmic polarisation in the battery, but has the battery emf V_0 and internal resistance R dependant on the depth of discharge. The functions V_0 and R are obtained by experiment.

Depth of discharge is the fraction of the total capacity that has been used, and is given by

$$D(t) = \frac{1}{C_0}\int_0^t I(\tau)\left[1 + \left(\frac{I(\tau)}{I_0} - 1\right) g\right] d\tau$$

where I_0 is the nominal discharge rate, C_0 is the nominal battery capacity, and g is a constant determined from discharge tests. With a constant discharge current I the discharge time T that gives $D(T) = 1$ is

$$T = \frac{C_0}{I\left[1 + (\frac{I}{I_0} - 1)\, g\right]}.$$

The capacity of the battery with constant discharge rate I is therefore

$$C = IT = \frac{C_0}{\left[1 + g\,(\frac{I}{I_0} - 1)\right]}.$$

Rearranging gives g for known C and I:

$$g = \frac{\frac{C_0}{C} - 1}{\frac{I}{I_0} - 1}.$$

Protogeropoulos et al

Protogeropoulos et al (1994) use a more detailed empirical model, and present an algorithm for predicting battery voltage for piecewise constant charge and discharge currents. Battery voltage V is modelled by

$$V = V_0 + K_e(I)\log\left[1 - \frac{Q}{C(I)}\right] + R_B(I)I \tag{5.4}$$

where

$$Q(t) = \int_0^t |I(\tau)|\, d\tau$$

is the exchanged charge,

$$C(I) = \frac{C_1(I)}{C_2(I)|I|^{C_3(I)} + 1} \tag{5.5}$$

is the battery capacity, and K_e, R_B, C_1, C_2, and C_3 are battery parameters that depend on the sign of the battery current, I. The current flowing through the battery is positive during charge and negative during discharge.

Differentiating (5.4) gives

$$\frac{dV}{dt} = \frac{K_e(I)}{C(I) - Q}\left[I + \frac{C(I)C_2C_3QIC_3 - 1}{C_1}\frac{dI}{dt}\right] + R_B(I)\frac{dI}{dt} \qquad (5.6)$$

When the battery current is constant, $dI/dt = 0$ and (5.6) can be written as

$$\frac{dV}{dt} = \frac{K_e(I)I}{C(I) - Q}.$$

They assume that current is piecewise constant, and that no charge is transferred to or from the battery when the current changes. From (5.4), the change in voltage is

$$\Delta V = \Delta I R_B.$$

Protogeropoulos et al use these equations to predict the battery voltage profile. Battery parameters are obtained by fitting curves to experimental data obtained from constant current charge and discharge tests.

Manwell and McGowan

Manwell and McGowan (1993) use a battery model based on chemical kinetics. They develop their model in terms of an analogous reservoir system, illustrated in Figure 5-4.

The maximum battery charge $q_{\max}$ is represented by the volume of fluid in the two reservoirs. The charge in the battery at any instant is $q = q_1 + q_2$, where q_1 represents charge that is immediately available, and q_2 represents charge that is 'chemically bound'. The conductance k between the two tanks corresponds to the rate of the chemical reaction and diffusion process. The charges q_1 and q_2 are determined by the equations

$$\frac{dq_1}{dt} = -I - k(1 - c)q_1 + kcq_2,$$

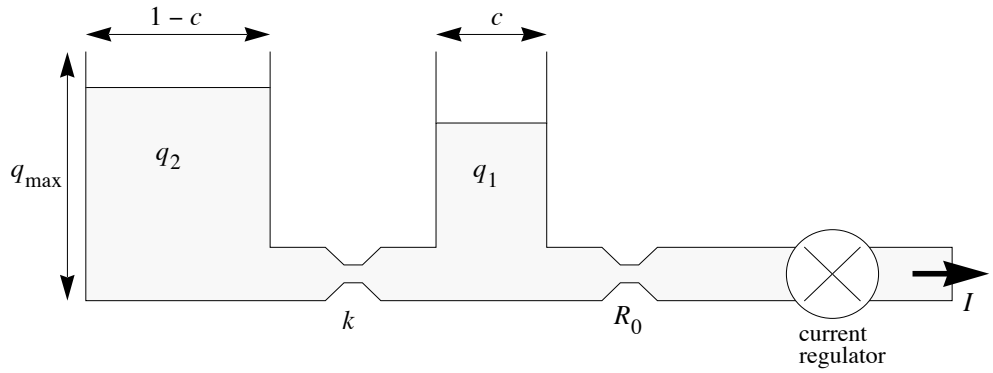

Figure 5-4: Manwell & McGowan's Kinetic Battery Model (KiBaM). The left reservoir represents charge that is bound in the chemistry of the electrolyte, whereas the right reservoir represents charge that is available immediately.

and

$$\frac{dq_2}{dt} = k(1-c)q_1 - kcq_2.$$

The battery voltage is given by

$$V = \varepsilon - IR_0$$

where

$$\varepsilon = v_d + (V_d - v_d)\frac{q_1}{cq_{\max}}$$

during discharge and

$$\varepsilon = v_c + (V_c - v_c)\frac{q_1}{cq_{\max}}$$

during charge, and where v_d and V_d are the minimum and maximum allowable internal discharge voltages, v_c and V_c are the minimum and maximum allowable internal charge voltages, and R_0 is the internal resistance of the battery.

5.3 Ohmic battery model

If the battery is charged and discharged at low rates then the polarisation is primarily due to internal resistance. If we ignore the other forms of polarisation then the battery voltage is given by

$$V = \varepsilon(Q) - IR_B(Q)$$

where ε is the battery emf, Q is the charge remaining in the battery, I is the current drawn and R_B is the internal resistance of the battery. The power corresponding to current I is the quadratic

$$p(I) = [\varepsilon(Q) - IR_B(Q)]I.$$

This equation can be rearranged to give the current drawn at a given power,

$$p(I) = \frac{\varepsilon(Q) - \sqrt{\varepsilon(Q)^2 - 4R_B(Q)p}}{2R_B(Q)}.$$

The capacity efficiency or ampere-hour efficiency of a battery is the ratio

$$\text{capacity efficiency} = \frac{\text{charge out}}{\text{charge in}}$$

for a complete discharge then charge cycle. In practice, the capacity efficiency of a battery is almost perfect. If we assume that the battery has perfect capacity efficiency then the state of charge of the battery is given by

$$Q(t) = Q(0) + \int_0^t I(\tau)d\tau .$$

Aurora used this ohmic model with linear emf ε and constant internal resistance R_B to successfully predict the performance of lead-acid batteries in SunRace 1998, 1999 and 2000. SunRace is a seven-day staged event from Sydney to Melbourne through country New South Wales and Victoria, requiring the solar cars to race 250-300km each day.

5.4 Silver-zinc batteries

Aurora used silver-zinc cells for the 1996 and 1999 World Solar Challenges. To develop a model of a silver-zinc cell, Aurora and the CSIRO tested three different types of silver-zinc cell. The cells were repeatedly subjected to a typical World Solar Challenge discharge profile, as shown and described in Figure 5-5. Cell voltage and current were logged at 20s intervals. The logs were then processed to give voltage, current, power and charge drawn from the battery at 20s intervals. Charge was calculated by integrating the current drawn from the battery.

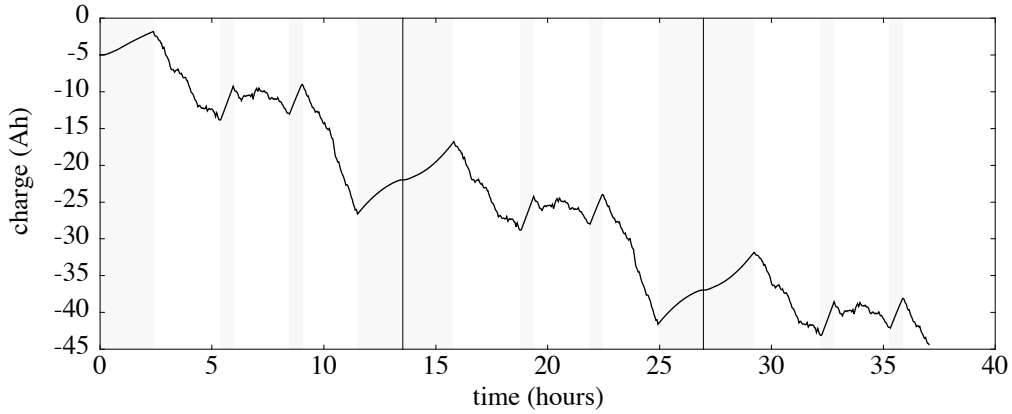

Figure 5-5: Discharge profile for a silver-zinc battery test. The power profile corresponds to almost three days of the World Solar Challenge. The vertical lines indicate the end of each day. The shaded areas indicate periods when the car is stationary. At the beginning and end of each day the solar panel is pointed at the sun.

The capacity efficiency of each cell was determined by measuring the charge required to recharge the cell after each discharge cycle. Each of the three cells tested had a capacity efficiency of about 97%.

To find a relationship between charge, power and current I first looked at scatter graphs of current against power, voltage against current, and voltage against charge. The graph of current against power in Figure 5-6 suggests that there is a clear relationship between power and current that is almost independent of charge and battery voltage.

A simple quadratic model with the form

$$I(b) = b[c_1 + c_2 b]$$

reflects the fact that current will be zero when power is zero. A least-squares fit to the data gave

$$I(b) = b[0.609 + 0.00324b]$$

where I is the current in amperes and b is the power in watts. The fit is shown in Figure 5-6.

This model is for a single cell. If we have n cells in series then the model becomes

$$I(b) = \frac{b}{n}\left[0.609 + \frac{0.00324b}{n}\right].$$

Finally, we can take into account the capacity efficiency of the battery, η_B by modifying the model to

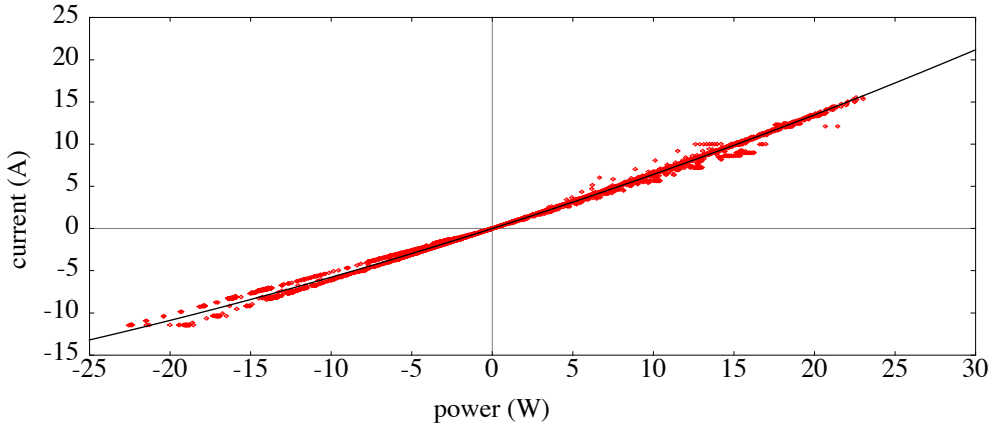

Figure 5-6: Least-squares fit to 6672 points (p, I) from the discharge profile shown in Figure 5-5.

$$I(b) = \begin{cases} \dfrac{b}{n}\left[0.609 + \dfrac{0.00324b}{n}\right] & b \geq 0 \\ \dfrac{\eta_B b}{n}\left[0.609 + \dfrac{0.00324b}{n}\right] & b < 0 \end{cases}.$$

This model was originally developed for the 1996 World Solar Challenge. Unfortunately, Aurora crashed on the outskirts of Darwin, and was unable to complete the race. Instead, in March 1997 the battery was used to drive the car 250km at 100km/h at the Ford Proving Ground, You Yangs, on a day with no sunlight. The distance predicted using the battery model was 253km. This battery model was also used for Aurora's win in the 1999 World Solar Challenge, and for the RACV Energy Challenge in January 2000 when Aurora drove 870km from Sydney to Melbourne in a day.

5.5 Summary

Modelling the detailed behaviour of a battery is difficult and, for our purposes, unnecessary. The simpler ohmic and silver-zinc models described in this chapter are both reasonable models to use with our control problems, and have both been used to successfully to predict the performance of batteries used in the Aurora 101 solar car.

6 The drive system

The drive system for a solar car comprises a motor, control electronics, and a mechanical transmission system.

6.1 Electric motors

An electric motor has two main parts: the stationary part, called the stator, and the rotating part, called the rotor. Current applied to armature windings on either the stator or rotor generates a magnetic field. The current is switched from one set of windings to the next to rotate this field with respect to the armature.

The Aurora 101, uses a permanent magnet, brushless DC motor with an efficiency of 98%. Figure 6-1 illustrates the operation of a simple 3-phase, brushless DC motor. The three armature windings a, b and c are arranged so that current flow a' opposes a, b' opposes b and c' opposes c.The windings are switched in pairs by the motor controller.

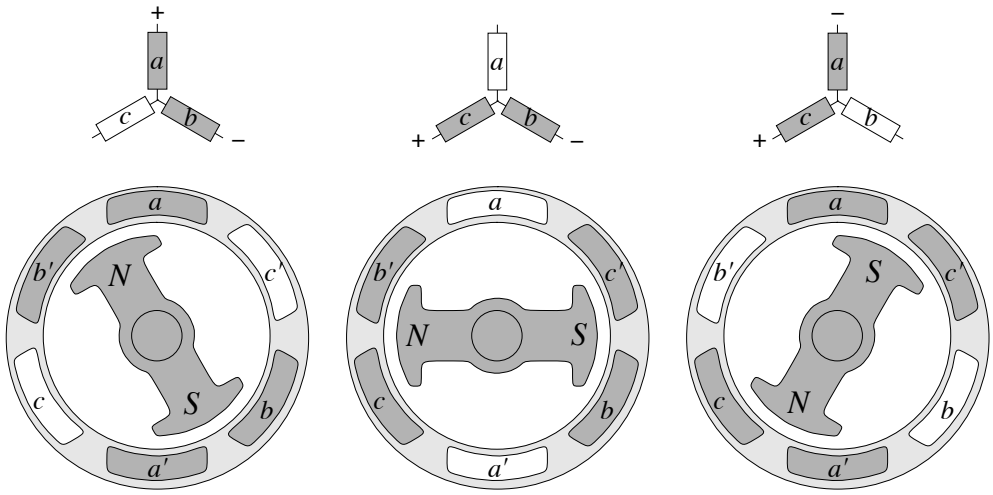

Figure 6-1: Half a cycle of a three-phase brushless DC motor. The three windings are switched in pairs by the motor controller. The magnetic field generated by the energised windings produces a torque on the magnet. For the second half of the cycle the sequence repeats, but with the opposite polarity.

Solar cars have also used wound-field DC, brushed DC, AC induction and switched reluctance motors (Roche et al 1997).

6.2 Motor controller

The motor controller for a brushless DC motor performs two functions. First, it switches current through the windings in the correct sequence; the correct switching times are determined using a position sensor on the rotor. Second, the controller sets the average winding current. Increasing the average current increases the torque produced by the motor.

Winding current is controlled by 'chopping'. That is, the current is switched on and off at a high frequency, and the ratio of on time to off time determines the average current and hence the torque generated by the motor.

Most solar car motor controllers have an automatic speed control mode, where the controller automatically adjusts the motor current to maintain the speed set by the driver.

6.3 Power losses in the motor and controller

The main source of power loss in the motor and controller is due to electrical resistance in the motor.

Motor voltage V is proportional to the angular velocity of the motor, which is in turn proportional to the speed of the car v if the car does not have a variable-speed gearbox. The electrical power to the motor is $p = VI$, where I is the motor current, and so

$$I \propto \frac{p}{v}$$

Resistive losses in a motor are approximately proportional to the square of motor current, and hence

$$L \approx k \left(\frac{p}{v}\right)^2$$

where k is a constant of proportionality.

A more detailed model of power loss in an electric drive system includes electrical resistance in the motor, air drag, bearing friction and losses in the control electronics. The total power loss has the form

$$L(p_{\text{out}}, v) = p_{\text{in}} - p_{\text{out}} = a_0 + a_1 v + a_2 v^2 + a_3 v^3 + k\left(\frac{p_{\text{out}}}{v}\right)^2$$

where P_{out} is the output power of the motor and v is the speed of the car in metres per second (Lovatt 1996, personal communication). The coefficients for the Aurora 101 wheel motor and controller are:

$a_0 = 35$ W

$a_1 = 6.2 \times 10^{-4}$ N

$a_2 = 5.2 \times 10^{-5}$ kg s^{-1}

$a_3 = 4.1 \times 10^{-7}$ kg m^{-1}

$k = 1.1 \times 10^{-2}$ s kg^{-1}.

On a level road, total losses are about 86W at 100km/h.

6.4 Transmission

The top performing solar cars use direct drive between the motor and the driven wheel; in some cases, such as with the Aurora car, the motor is built into the wheel. The main advantage of direct drive is that there are no transmission losses.

Other than direct drive, the most popular form of transmission is a chain or toothed-belt drive. Power losses in such drives are usually 2-5%.

6.5 Summary

Power losses in the Aurora drive system are about 4% at 100km/h on level road. For simplicity, we will assume that the drive system is perfectly efficient for much of our analysis. In Chapter 14, however, we will use the detailed loss model to investigate the effect of the motor losses on optimal driving strategies.

7 Problem model

The main objective of any team in the World Solar Challenge is complete the race as quickly as possible. The race rules impose several important constraints:

- the size of the solar array and the energy storage capacity are limited;
- the cars can be driven on the road only between 8.00 am and 5.00 pm, but can charge their batteries using the solar panel outside this interval; and
- the cars must stop for half an hour at each of seven media stops along the route, but may collect charge during these stops
- the first car to Adelaide wins.

To develop a driving strategy we ignore these constraints, and instead develop driving strategies that minimise the time taken to travel a given distance using various car, route and weather models. The insight gained by solving these simpler problems allows us to develop an effective, practical driving strategy for the World Solar Challenge.

7.1 Power flows

Consider a car with two batteries and regenerative braking. For convenience, we will call the power of a current flow a 'power flow'. The possible power flows for the car are shown in Figure 7-1. They are:

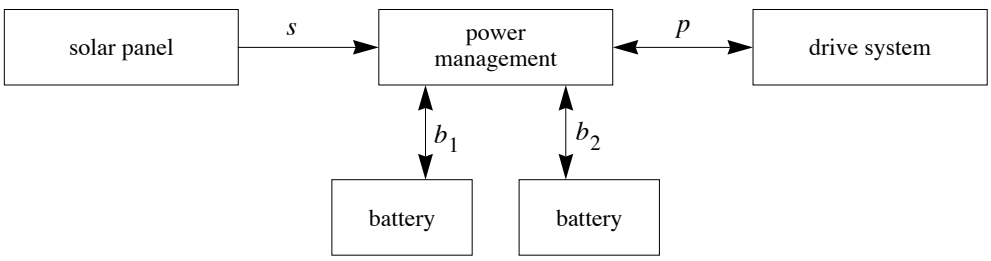

Figure 7-1: Power flows in a solar car with two batteries

s	the power flow from the solar panel, which depends on the time of day and the location of the car,
p	the power flow to the drive system,
b_1	the power flow from the first battery, and
b_2	the power flow from the second battery.

For most of the problems we will consider time to be the independent variable.

The battery flows b_1 and b_2 can be used to control the car. Battery power is positive when current flows from the battery, and negative when current flows to the battery.

The drive power p is positive when the motor is driven, but negative during regenerative braking when current flows from the motor back into the batteries.

The constraints on the power flows are

$$p = s + b_1 + b_2$$

and

$$s > 0 .$$

These constraints allow some unusual driving modes, such as charging one battery while discharging the other. Whether or not these driving modes occur in the optimal strategy will depend on factors such as battery characteristics and the timing of media stops.

7.2 Equations of motion

The drive power p is controlled by the battery power flows b_1 and b_2. The drive force at the wheels is

$$F(b_1, b_2, v) = \frac{\eta_D [b_1 + b_2 + s]}{v}$$

where η_D is the efficiency of the drive system, s is solar power and v is the speed of the car. For most of the problems we will study we will assume that η_D is a constant, but in Chapter 14 we will examine the effects of a more general motor model,

Two forces oppose the motion of the car: resistive force, and gradient force.

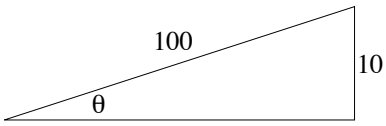

Figure 7-2: Road gradients steeper than 10% are unusual. For a 10% gradient, $\cos\theta \approx 0.995$.

Resistance

Resistance is modelled by the formula

$$R(x, v, w) = mgc_{rr1}\cos\theta(x) + Nc_{rr2}v + \frac{1}{2}\rho C_d A\,[v - w]^2$$

where $g \approx 9.8$ is the acceleration due to gravity, c_{rr1} and c_{rr2} are coefficients of rolling resistance, θ is the angle of slope of the road, N is the number of wheels on the car, $\rho \approx 1.22$ is the density of air, and $c_d A$ is the drag area of the car (Kyle 1991).

Road gradients are usually less than 10%, in which case $\cos\theta$ will lie between 0.995 and 1. It is therefore reasonable to assume $\cos\theta = 1$.

Wind is difficult to predict. For our theoretical analysis we will ignore wind, but will then develop a scheme to cope with the effects of wind when we develop a practical strategy to use during the race.

With no wind and for small gradients, the resistance force on the car is therefore

$$R(v) = mgc_{rr1} + Nc_{rr2}v + \frac{1}{2}\rho C_d A v^2.$$

The coefficients can be found experimentally by measuring the force required to drive the car at various speeds and fitting a least-squares quadratic to the data. For the Aurora 101 the coefficients are:

$$m = 300 \text{ kg}$$

$$c_{rr1} = 0.004$$

$$c_{rr2} = 0.052 \text{ kg s}^{-1}$$

$$C_d A = 0.11 \text{ m}^2.$$

At 100km/h on a level road, about 75% of the resistive force is due to aerodynamic drag.

Gradient

The gradient force acting on the car is

$$G(x) = -mg\sin\theta(x)$$

where θ is the angle of slope of the road at location x. The gradient force is positive when the car is travelling down a hill, and negative when travelling up a hill.

Equations of motion

The equations of motion for our problem are:

$$\frac{dx}{dt} = v \tag{7.1}$$

$$\frac{dv}{dt} = \frac{1}{m}\left[F(b_1, b_2, v) - R(v) + G(x)\right]. \tag{7.2}$$

7.3 Energy storage

The power flow b from a battery depends on the current drawn, as shown in Figure 7-3. Power initially increases with current, but reaches a maximum and then drops as the battery voltage drops due to polarisation effects. The exact shape of the power curve depends on the chemical state of the battery, as discussed in Chapter 5.

The energy efficiency of a battery is highly dependent on the charge and discharge profile. On the other hand, the capacity efficiency of a battery is usually very high, and almost independent of the charge and discharge profile. We therefore use battery charge as a state variable rather than battery energy content. The state equations for the batteries are

$$\frac{dQ_j}{dt} = -I_j(b_j)$$

where $I_j(b)$ is the current required to give power b from battery j. A positive current represents a flow of charge from the battery.

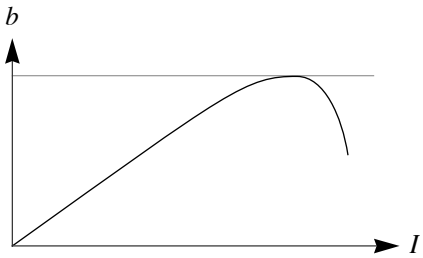

Figure 7-3: Battery power b initially increases with current I, but reaches a maximum P_D and then drops as the cell voltage drops due to polarisation effects.

Battery charge is constrained by

$$0 \le Q_j \le Q_{j\max}$$

for each battery. The initial charge $Q_j(0)$ is usually known.

7.4 Rotational dynamics

For a car without gears all of the rotating masses rotate with the same angular velocity. If we take into account the motion of rotating parts the energy balance equation is

$$\frac{1}{2}mv^2 + \frac{1}{2}I\omega^2 = [F(v) - R(v) + G(x)]\,x \qquad (7.3)$$

where I is the moment of inertia of the rotating masses and ω is the angular velocity of the rotating masses. The angular velocity of the rotating parts is

$$\omega = \frac{v}{r}$$

where r is the radius of the wheels. Substituting this into (7.3) and differentiating with respect to time gives

$$(m + \frac{I}{r^2})\,\frac{dv}{dt} = [F(v) - R(v) + G(x)]\,.$$

If we let $m_R = (m + I/r^2)$ then we have

$$m_R\,\frac{dv}{dt} = F(v) - R(v) + G(x).$$

Comparing this equation with (7.2) we see that m_R is an effective mass of the car that compensates for the effect of rotating parts.

The three wheels of the Aurora 101 have a 250mm rolling radius. The single front wheel contains an in-wheel motor. The mass distribution on the front wheel can be approximated by 5kg at 135mm radius, 1.1kg at 230mm radius, and the remaining 5kg distributed evenly over a disk with radius 210mm. The moment of inertia for the front wheel is

$$I_F = 5 \times 0.135^2 + 1.1 \times 0.230^2 + \frac{5 \times 0.210^2}{2} = 0.260\ \mathrm{kg\,m^2}$$

Each of the two the rear wheels can be modelled as a 2kg disk with radius 210mm, and 1.1kg at 230mm radius. The moment of inertia for each of the rear wheels is

$$I_R = \frac{2 \times 0.210^2}{2} + 1.1 \times 0.230^2 = 0.102 \text{ kg m}^2.$$

The total moment of inertia for the rotating masses is

$$I = I_F + 2I_R = 0.464 \text{ kg m}^2.$$

The rolling radius of the wheels is $r = 0.250$ m. The effective mass of the car is therefore

$$m_R = m + I/r^2 = m + 7.42 \text{ kg}.$$

By using an effective mass of 307kg instead of the actual mass of 300kg we can incorporate the effects of rotational inertial into our equations of motion.

7.5 Summary

The state equations for our simplified solar car model can be written as

$$\frac{dx}{dt} = v$$

$$\frac{dv}{dt} = \frac{1}{m}\left[F(b_1, b_2, v) - R(v) + G(x)\right]$$

$$\frac{dQ_1}{dt} = -I_1(b_1)$$

and

$$\frac{dQ_2}{dt} = -I_2(b_2)$$

where battery power flows b_1 and b_2 are used to control the motion of the car. For most problems, we wish to minimise the time taken to travel a given distance X, subject to the battery constraints $0 \le Q_j \le Q_{j\max}$.

PART THREE

Efficient energy management

8 Minimising energy use

For many vehicles, energy use can be minimised by travelling at a constant speed. In this chapter we will see that a simple vehicle travelling at a constant speed uses less energy than it does for any other strategy with the same average speed. A similar argument was used by Howlett & Pudney (1995) in their book on efficient train control.

Consider a car with constant drive efficiency η_D. When power p is applied to the drive system the force on the road is

$$F(v, p) = \frac{\eta_D p}{v}$$

where v is the speed of the car. If the other forces acting on the vehicle are resistive forces R depending on speed and gradient forces G depending on location then the equation of motion is

$$v\frac{dv}{dx} = \frac{dv}{dt} = \frac{1}{m}\left[F(v, p) - R(v) + G(x)\right]$$

where t is time, x is distance and m is the mass of the car.

Suppose the car is driven at constant speed v^* from the point (t_0, x_0, v^*) to the point (t_1, x_1, v^*), as illustrated in Figure 8-1. We will show that any alternative speed profile with the same average speed uses more energy.

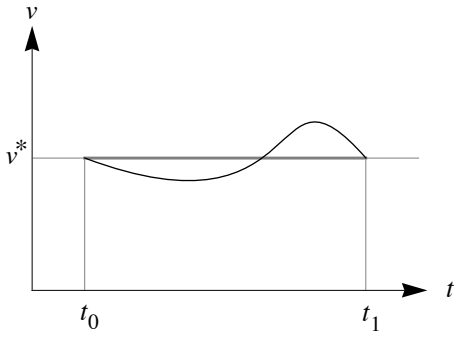

Figure 8-1: Constant and non-constant speed profiles on an interval $[t_0, t_1]$. The distance covered, represented by the area under the curve, is the same for each profile. The curves therefore have the same average speed. The constant speed strategy uses less energy.

The power required to maintain constant speed v^* is

$$p(x) = \frac{v^*}{\eta_D}\left[R(v^*) - G(x)\right].$$

The energy cost of the constant speed strategy is therefore

$$E^* = \int_{x_0}^{x_1} \frac{p(x)}{v^*}\,dx$$

$$= \frac{1}{\eta_D}\int_{x_0}^{x_1}\left[R(v^*) - G(x)\right]dx.$$

Now consider any alternative strategy also starting at (t_0, x_0, v^*) and finishing at (t_1, x_1, v^*). The power required to follow the speed profile v is

$$p(x) = \frac{v(x)}{\eta_D}\left[mv(x)v'(x) + R(v) - G(x)\right].$$

The energy cost of the alternative strategy is

$$E = \int_{x_0}^{x_1} \frac{p(x)}{v(x)}\,dx$$

$$= \frac{1}{\eta_D}\int_{x_0}^{x_1}\left[mv(x)v'(x) + R(v) - G(x)\right]dx.$$

Both speed profiles start and finish at speed v^*, so there is no net change in the kinetic energy of the car. This means that

$$\int_{x_0}^{x_1} mv\frac{dv}{dx}\,dx = \left[\frac{1}{2}mv^2\right]_{x = x_0}^{x_1} = 0.$$

The energy cost of the alternative strategy is therefore

$$E = \frac{1}{\eta_D}\int_{x_0}^{x_1}\left[R(v) - G(x)\right]dx.$$

The energy cost difference between the alternative strategy and the constant speed strategy is

$$E - E^* = \frac{1}{\eta_D} \int_{x_0}^{x_1} [R(v) - R(v^*)]\, dx.$$

If the journeys both take the same time we can rewrite this equation using time as the independent variable to give

$$E - E^* = \frac{1}{\eta_D} \int_{t_0}^{t_1} [vR(v) - v^* R(v^*)]\, dt.$$

The power required to overcome resistive forces at speed v is $p(v) = vR(v)$. This power graph is convex, and so $vR(v) - v^* R(v^*) \geq \lambda [v - v^*]$ for some positive λ, and so

$$E - E^* \geq \frac{\lambda}{\eta_D} \int_{t_0}^{t_1} [v - v^*]\, dt.$$

But the integral in the right is simply the difference in the distance travelled by each of the strategies, which is zero. Thus for any vehicle with constant drive efficiency and convex resistance, travelling at constant speed uses less energy than any other strategy with the same average speed.

Unfortunately, this does not quite solve the solar car problem. If the energy available for a journey is fixed, as is the case for a conventional car with a tank full of petrol, travelling at constant speed will make best use of the available energy. With a solar car, however, the energy used for the journey is collected during the journey. This has three important implications:

1. At the beginning of a journey you do not know how much energy you will have for the journey and so cannot calculate the optimal speed for the journey. This problem is overcome in practice by continually estimating the energy that will be collected over the remainder of the journey and adjusting the speed of the car accordingly.

2. If energy storage is not perfectly efficient then it may be better to vary the speed of the car rather than lose energy in the storage system. For example, during the middle of the day when solar power is greatest it may be better to increase the speed of the car rather than store the excess energy and then later get back less than was stored.
3. If solar power varies with location then the total energy collected will depend on the speed profile; by varying the speed of the car it may be possible to collect enough extra energy to repay the energy cost of the speed variations.

These issues are addressed in the following chapters.

9 Formulation of an optimal control problem

One way to find the optimal driving strategy would be to use a numerical search technique, perhaps based on dynamic programming or genetic algorithms. While such methods may give a solution, they rarely give insight. A more informative approach is to use techniques of optimal control to develop necessary conditions for an optimal strategy, and then use these conditions to construct an optimal strategy.

Consider a car with two types of battery and regenerative braking. Ignore, for now, the morning and evening charge sessions and charging at media stops. We will use this general model of the problem to derive necessary conditions for an optimal strategy. These conditions will be used in subsequent chapters to construct optimal control strategies for various specific battery, motor and irradiance models.

9.1 Problem formulation

The possible power flows for the car are shown in Figure 9-1. They are:

$s \geq 0$	the power flow from the solar panel, which depends on the time of day and the location of the car;
p	the power flow to the drive system;
b_1	the power flow from the first battery; and

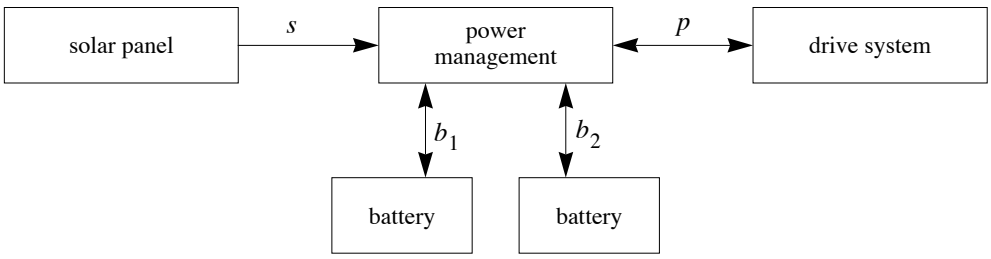

Figure 9-1: Power flows in a solar car with two batteries

b_2 the power flow from the second battery.

The battery power flows b_1 and b_2 are used to control the car. The drive power

$$p = s + b_1 + b_2$$

is positive while driving and negative during regenerative braking. Each battery power b_j is positive while the battery is discharging and negative while the battery is charging. The charge in battery j is Q_j.

We wish to minimise the time taken to drive over a route. If we let $T = [0, t_f]$ be the time interval for the problem then we wish to minimise the finishing time, t_f. This optimisation problem can be formulated as a minimum time Mayer problem (Hestenes 1966; Cesari 1982). The state of the system at time t is

$$\xi(t) = [x(t), v(t), Q_1(t), Q_2(t)] \in \Xi,$$

where x is the position of the car, v is the speed of the car and Q_i is the charge in battery j. The set Ξ is the state space. A function $\xi : T \to \Xi$ will describe the evolution of the state.

The driver controls the power flows b_1 and b_2 to the two batteries. The control at time t can be written as

$$u(t) = [b_1(t), b_2(t)] \in U$$

where U is the set of control values and $\mathcal{U} = \{u \mid u : T \to U\}$ is the space of control functions.

The acceleration of the car depends on the power applied to the drive system and on the resistive and gradient forces acting on the car. In general, the acceleration a will depend on time, location, speed and control.

The current flow I_j from each battery depends on the battery charge and on the power flow from the battery. We will ignore any dependence on time. The general shape of the current curve is shown in Figure 9-2.

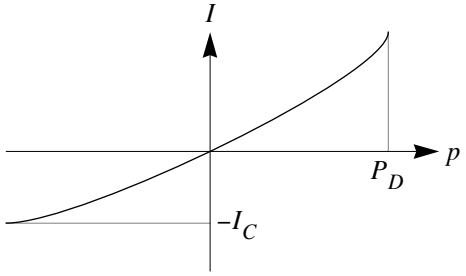

Figure 9-2: Battery current varies with power demand. The exact shape of the curve, the discharge power limit and the charge current limit depend on the battery charge.

Boundary conditions

The car starts the race at rest with full batteries and finishes at a specified location x_f. The boundary conditions can be written as

$$x(0) = 0 \qquad v(0) = 0 \qquad Q_j(0) = Q_{j0} \qquad x(t_f) = x_f$$

or in the form

$$g_i(\beta) = 0 \qquad i = 1, \ldots, 5$$

where $\beta \in B \subseteq (\Xi \times T \times \Xi)$ is defined by

$$b = [x(0), v(0), Q_1(0), Q_2(0), t_f, x(t_f)]$$

and where

$$\begin{aligned} g_1(\beta) &= x(0) \\ g_2(\beta) &= v(0) \\ g_3(\beta) &= Q_1(0) - Q_{1,0} \\ g_4(\beta) &= Q_2(0) - Q_{2,0} \\ g_5(\beta) &= x(t_f) - x_f. \end{aligned}$$

Cost function

We wish to minimise the time t_f required to complete the journey. To do this we minimise the function

$$g_0(\beta) = t_f.$$

Together, the cost function and boundary conditions are described in terms of the function $g : B \rightarrow \Re^6$ defined by $g(t) = [g_0(t), \ldots, g_5(t)]$. $\Re$ denotes the set of real numbers.

State equations

The state equations for the problem are

$$\frac{dx}{dt} = v$$

$$\frac{dv}{dt} = a(t, x, v, p_1, p_2)$$

and

$$\frac{dQ_j}{dt} = -I_j(Q_j, b_j) \qquad j = 1, 2.$$

These can be written more compactly in the form

$$\frac{d\xi}{dt} = f(t, \xi, u)$$

where $f : T \times \Xi \times U \to \Re^4$.

State and control constraints

The state $\xi = [x, v, Q_1, Q_2]$ must satisfy the speed constraint

$$0 \le v(t)$$

and battery charge constraints

$$Q_{j\min} \le Q_j(t) \le Q_{j\max} \qquad j = 1, 2$$

where $Q_{j\min}$ and $Q_{j\max}$ are the lower and upper charge limits for battery j. The control $u = [b_1, b_2]$ must satisfy the drive power constraint

$$-P_R \le s(t, x) + b_1(t) + b_2(t) \le P_T$$

and the battery power constraints

$$-B_{Cj}(Q_j) \le b_j(t) \le B_{Dj}(Q_j)$$

where the power limits are

$P_R > 0$ the maximum power flow from the drive system during regenerative braking;

$P_T > 0$ the maximum power flow to the drive system while driving;

$B_{Cj} > 0$ the maximum power flow to battery j while charging; and

$B_{Dj} > 0$ the maximum power flow from battery j while discharging.

The state and control constraints can be written in the form

$$\varphi_i(t, \xi, u) \le 0 \qquad i = 1, \ldots, 11$$

where

$$\varphi_1(t, \xi, u) = -v(t)$$
$$\varphi_2(t, \xi, u) = Q_{1\min} - Q_1(t)$$
$$\varphi_3(t, \xi, u) = Q_1(t) - Q_{1\max}$$
$$\varphi_4(t, \xi, u) = Q_{2\min} - Q_2(t)$$
$$\varphi_5(t, \xi, u) = Q_2(t) - Q_{2\max}$$
$$\varphi_6(t, \xi, u) = -P_R - [s(t, x(t)) + b_1(t) + b_2(t)]$$
$$\varphi_7(t, \xi, u) = [s(t, x(t)) + b_1(t) + b_2(t)] - P_T$$
$$\varphi_8(t, \xi, u) = -B_{C1}(Q_1(t)) - b_1(t)$$
$$\varphi_9(t, \xi, u) = b_1(t) - B_{D1}(Q_1(t))$$
$$\varphi_{10}(t, \xi, u) = -B_{C2}(Q_2(t)) - b_2(t)$$
$$\varphi_{11}(t, \xi, u) = b_2(t) - B_{D2}(Q_2(t))$$

9.2 Necessary conditions for a solution

Suppose $\hat{u}$ is the optimal control, $\hat{\xi}$ the corresponding state trajectory, and $\hat{\beta}$ the corresponding boundary value. Following Hestenes (1962, Theorem 7-11.1), there exist multipliers

$$\lambda = [\lambda_0, \lambda_1, \lambda_2, \lambda_3, \lambda_4, \lambda_5] \in \Re^6 \text{ with } \lambda_0 \geq 0,$$

$$\pi = [\pi_1, \pi_2, \pi_3, \pi_4] : T \to \Re^4$$

and

$$\mu = [\mu_1, \ldots, \mu_{11}] \in \Re^{11}$$

not vanishing simultaneously, and functions $H : T \times \Xi \times U \times \Re^4 \times \Re^{11} \to \Re$ and $G : B \to \Re$ defined by

$$H(t, \xi, u, \pi, \mu) = \pi \cdot f(t, \xi, u) - \mu \cdot \varphi(t, \xi, u)$$

and

$$G(\beta) = \lambda \cdot g(\beta)$$

such that

1. $\lambda_i \geq 0$ with $\lambda_i = 0$ if $g_i(\hat{\beta}) < 0$.

2. The (Lagrange) multipliers μ_i are piecewise continuous on T and are continuous at each point of continuity of $\hat{u}$. The multipliers also satisfy the (complementary slackness) conditions

$$\mu_i(t)\varphi_i(t, \hat{\xi}(t), \hat{u}(t)) = 0.$$

3. The multipliers π_i are continuous on T and have piecewise continuous derivatives. The functions $\hat{\xi}$, $\hat{u}$, π and μ satisfy the Euler-Lagrange equations

$$\frac{d\xi}{dt} = \frac{\partial H}{\partial \pi}, \frac{d\pi}{dt} = -\frac{\partial H}{\partial \xi}, \frac{\partial H}{\partial u} = 0 \text{ and } \frac{dH}{dt} = \frac{\partial H}{\partial t}$$

on each interval of continuity of $\hat{u}$. The function

$$H(t, \hat{\xi}(t), \hat{u}(t), \pi(t), \mu(t))$$

is continuous on T. The transversality condition

$$dG - H(t_f, \hat{\xi}(t_f), \hat{u}(t_f), \pi(t_f), \mu(t_f))dt_f + \pi_2(t_f)dv(t_f) + \pi_3(t_f)dQ_1(t_f) + \pi_4 dQ_2(t_f) = 0$$

holds on $\hat{\xi}$ for all $d\beta$.

4. The inequality

$$H(t, \hat{\xi}(t), u, \pi(t), 0) \leq H(t, \hat{\xi}(t), \hat{u}(t), \pi(t), 0) \qquad (9.1)$$

holds for all feasible $(t, \hat{\xi}(t), u)$.

The function H is the Hamiltonian for the system. Condition 4 states that at each time t the control $u(t)$ should be chosen so that the value of the Hamiltonian is maximised.

The multipliers π are adjoint variables. The differential equations

$$\frac{d\pi}{dt} = -\frac{\partial H}{\partial \xi}$$

are the adjoint equations.

Hamiltonian

The Hamiltonian for the solar car problem is

$$
\begin{aligned}
&H(t, \xi, u, \pi, \mu) \\
&\quad = \pi_1 v + \pi_2 a(t, x, v, b_1, b_2) - \pi_3 I_1(Q_1, b_1) - \pi_4 I_2(Q_2, b_2) \\
&\qquad - \mu_1 [-v] \\
&\qquad - \mu_2 [Q_{\min 1} - Q_1] - \mu_3 [Q_1 - Q_{\max 1}] \\
&\qquad - \mu_4 [Q_{\min 2} - Q_2] - \mu_5 [Q_2 - Q_{\max 2}] \\
&\qquad - \mu_6 [-P_R - (s(t, x) + b_1 + b_2)] \\
&\qquad - \mu_7 [s(t, x) + b_1 + b_2 - P_T] \\
&\qquad - \mu_8 [-B_{C1}(Q_1) - b_1] - \mu_9 [b_1 - B_{D1}(Q_1)] \\
&\qquad - \mu_{10} [-B_{C2}(Q_2) - b_2] - \mu_{11} [b_2 - B_{D2}(Q_2)] .
\end{aligned}
$$

Adjoint equations

The adjoint equations for the solar car problem are

$$
\begin{aligned}
\frac{d\pi_1}{dt} &= -\pi_2 \frac{\partial a}{\partial x} - (\mu_6 - \mu_7) \frac{\partial s}{\partial x} \\
\frac{d\pi_2}{dt} &= -\pi_1 - \pi_2 \frac{\partial a}{\partial v} + \mu_1 \\
\frac{d\pi_3}{dt} &= \pi_3 \frac{\partial I_1}{\partial Q_1} - (\mu_2 - \mu_3) - \mu_8 \frac{\partial B_{C1}}{\partial Q_1} - \mu_9 \frac{\partial B_{D1}}{\partial Q_1} \\
\frac{d\pi_4}{dt} &= \pi_4 \frac{\partial I_2}{\partial Q_2} - (\mu_4 - \mu_5) - \mu_{10} \frac{\partial B_{C2}}{\partial Q_2} - \mu_{11} \frac{\partial B_{D2}}{\partial Q_2} .
\end{aligned}
$$

Maximising the Hamiltonian

The optimal control $\hat{u}$ maximises the Hamiltonian at each point $[t, \hat{\xi}(t), \pi(t), 0]$. By grouping the terms depending on the control we can rewrite the Hamiltonian as

$$
\begin{aligned}
&H(t, \xi, u, \pi, \mu) \\
&\quad = \pi_2 a(t, x, v, b_1, b_2) - \pi_3 I_1(Q_1, b_1) - \pi_4 I_2(Q_2, b_2) + \ldots
\end{aligned}
$$

The optimal values of b_1 and b_2 depend on the values of the adjoint variables π_2, π_3 and π_4. In the following chapters we use various specific battery, motor and irradiance models to derive key equations for the state and adjoint variables, and then show how these can be used to construct an optimal driving strategy.

9.3 Summary

The solar car problem can be formulated as a minimum time Mayer problem, and necessary conditions for an optimal control found by maximising the Hamiltonian. In subsequent chapters these necessary conditions will be used to find the optimal control for various versions of the problem.

10 Optimal control of a perfectly efficient car on a level road

Rather than try to solve the general solar car problem formulated in the previous chapter, we will gain insight by tackling a sequence of specific problems. Our starting point is to find the optimal control for a solar car with a single, perfectly efficient battery, being driven on a level road. Our assumptions are:

- solar irradiance does not depend on location,
- the driving force on the car does not depend on location,
- there are no losses in the drive system,
- the car has a single battery with perfect energy efficiency, and
- the battery is sufficiently large that battery power and charge constraints are never binding.

This specific problem has an elegant solution—apart from an initial acceleration phase and a final braking phase, the car should be driven at a constant speed.

The proof presented in this chapter that an optimal strategy exists is the basis for the proof used by Howlett & Pudney (1998) for a solar car on an undulating road.

10.1 Problem formulation

We assume that the force generated at the wheels of the car is

$$F = \frac{p}{v}$$

where p is the power applied to the drive system and v is the speed of the car. Drive power p is given by

$$p(t) = s(t) + b(t)$$

where s is the power from the solar panel and b is the power from the battery. If $b < 0$ then power flows to the battery. If the power flow $-b$ to the battery is greater than the solar power s then the net power p to the drive system is negative, and the drive system acts as a regenerative brake.

On a level road the only other significant force acting on the car is a resistive force R that depends only on the speed of the car. We will assume that R is an increasing function of v with strictly increasing derivative. The acceleration of the car is then

$$\frac{dv}{dt} = \frac{1}{m}\left[\frac{p}{v} - R(v)\right].$$

For this model we also assume that the battery has perfect energy efficiency, in which case the current flowing from the battery is

$$I(b) = \frac{b}{\varepsilon}$$

where b is the power flow from the battery and ε is the battery emf.

The problem has state equations

$$\frac{dx}{dt} = v, \tag{10.1}$$

$$\frac{dv}{dt} = \frac{1}{m}\left[\frac{p}{v} - R(v)\right], \tag{10.2}$$

and

$$\frac{dQ}{dt} = -\frac{b}{\varepsilon}. \tag{10.3}$$

As described in the last chapter, the optimal driving strategy can be found by forming a Hamiltonian and then selecting the control to maximise the Hamiltonian. The Hamiltonian for our problem is

$$\begin{aligned} &H(t, \xi, u, \pi, \mu) \\ &\quad = \pi_1 v + \frac{\pi_2}{m}\left[\frac{p}{v} - R(v)\right] - \pi_3 \frac{b}{\varepsilon} \\ &\qquad - \mu_1[-v] - \mu_6[-P_R - (s(t) + b)] - \mu_7[s(t) + b - P_T]. \end{aligned}$$

The multipliers $\mu_2, \ldots, \mu_5$ and $\mu_8, \ldots, \mu_{11}$ are all zero, since we have assumed that battery power and battery charge constraints are never encountered. If they are encountered, the optimal strategy must be modified to follow the boundary constraints.

The adjoint equations for the problem are

$$\frac{d\pi_1}{dt} = 0, \tag{10.4}$$

$$\frac{d\pi_2}{dt} = -\pi_1 + \frac{\pi_2}{m}\left[\frac{p}{v^2} + R'(v)\right] - \mu_1 \tag{10.5}$$

and

$$\frac{d\pi_3}{dt} = 0. \tag{10.6}$$

Equations (10.4) and (10.6) have solutions $\pi_1 = A$ and $\pi_3 = AC\varepsilon$, where A and C are constants. The Hamiltonian and the adjoint and Lagrange multiplier vectors can be normalised by letting

$$H^* = \frac{H}{A}, \pi^* = \frac{\pi}{A} \text{ and } \mu^* = \frac{\mu}{A}.$$

Dropping the (*) notation gives

$$H(t, \xi, u, \pi, 0) = v + \frac{\pi_2}{m}\left[\frac{p}{v} - R(v)\right] - Cb$$

and the adjoint equation

$$\frac{d\pi_2}{dt} = \frac{\pi_2}{m}\left[\frac{p}{v^2} + R'(v)\right] - 1 - \mu_1. \tag{10.7}$$

10.2 Necessary conditions for an optimal strategy

The optimal control $\hat{u}$ maximises the Hamiltonian at each point $[t, \hat{\xi}(t), \pi(t), 0]$. We are only ever interested in the value of the Hamiltonian when $\mu = 0$, and the complementary slackness conditions from the previous chapter give $\mu_i\varphi_i = 0$ anyway, so we can rewrite the Hamiltonian as

$$H = v + \frac{\pi_2}{m}\left[\frac{p}{v} - R(v)\right] - Cb$$

Let

$$\eta = \frac{\pi_2}{mv}$$

and

$$\varphi(v) = vR(v).$$

Setting $p = \varphi(v)$ in the equation of motion (10.2) gives $dv/dt = 0$, and so $\varphi(v)$ is the power that must be applied to the drive system to maintain a constant speed v. Using these definitions of η and φ we can rewrite the Hamiltonian as

$$H = v + \eta\,[p - \varphi(v)] - Cb. \tag{10.8}$$

The variable η evolves according to the differential equation

$$\frac{d\eta}{dt} = \frac{d}{dt}\left[\frac{\pi_2}{mv}\right] = \frac{1}{mv}\,[\eta\varphi'(v) - 1]. \tag{10.9}$$

We now want to find the control that maximises the Hamiltonian. Grouping the terms in (10.8) that depend on the control b, the Hamiltonian can be rewritten as

$$H = [\eta - C]\,b + \ldots$$

where the neglected terms do not depend on the control. At any point on the journey, the optimal control b maximises the Hamiltonian. There are three cases to consider, depending on the value of η:

power	$C < \eta$	$\Rightarrow\ b = P_T - s$
hold	$\eta = C$	$\Rightarrow\ b \in [0, P_T - s]$
regen	$\eta < C$	$\Rightarrow\ b = -P_R - s$

The power and regen cases correspond respectively to maximum power and to maximum regenerative braking.

The (mysteriously named) hold case is singular. It can only be maintained on a non-trivial interval if $d\eta/dt = 0$, in which case (10.9) gives

$$\varphi'(v) = \frac{1}{C}. \tag{10.10}$$

But φ' is a strictly increasing function of v, so (10.10) has a unique solution $v = v^*$. The hold mode corresponds to driving at a constant speed v^*.

10.3 Control transitions in an optimal strategy

Transitions between control modes can occur only when

$$\eta = C = \frac{1}{\varphi'(v^*)}.$$

Transitions may occur between any two of the following control modes:

- power with $p = P_T$ and $\eta > C$;
- hold with $p = \varphi(v^*)$ and $\eta = C$; and
- regen with $p = -P_R$ and $\eta < C$.

Clearly, a transition to or from hold can occur only if $v = v^*$, since speed is continuous. By examining the behaviour of η it is possible to derive more transition conditions.

If p is an analytic function of t in some open interval then the functions v and η are also analytic functions of t in that interval, and it is possible to derive appropriate Taylor series expansions for these functions. The Taylor series expansions in the vicinity of a point $t = t_0$ can be used to derive necessary conditions for a transition at that point.

Let t_0 be the transition time and write $v_0 = v(t_0)$ and $\eta_0 = \eta(t_0)$. Let

$$p_0 = p(t_0) = \lim_{t \to t_0} p(t)$$

and

$$p'_0 = p'(t_0) = \lim_{t \to t_0} p'(t).$$

Because $p(t)$ is not necessarily continuous at $t = t_0$ we use one-sided limits when required. For t near t_0 the Taylor series is

$$\eta(t) = \eta(t_0) + \eta'(t_0)[t - t_0] + \frac{1}{2}\eta''(t_0)[t - t_0]^2 + \frac{1}{6}\eta'''(t_0)[t - t_0]^3 + \ldots.$$

At the transition point we have $\eta(t_0) = C = 1/\varphi'(v^*)$.

The Taylor series is dominated by the first non-zero term. If $v_0 = v^*$ then

$$\eta'(t_0) = \left[\frac{1}{mv_0}\right]\frac{\varphi'(v_0) - \varphi'(v^*)}{\varphi'(v^*)}$$

and the Taylor series is

$$\eta(t) = C + \left[\frac{1}{mv_0}\right]\frac{\varphi'(v_0) - \varphi'(v^*)}{\varphi'(v^*)}[t - t_0] + \ldots.$$

If $v_0 = v^*$ then $n'(t_0) = 0$ and the second term of the Taylor series is zero, so we must look to the third term of the Taylor series. Since $\eta' = 0$ we have

$$\eta'' = \left[\frac{1}{mv}\right]\eta\varphi''(v)v'.$$

Substituting $\eta = 1/\varphi'(v)$ and

$$v' = \frac{p - \varphi(v)}{mv}$$

gives

$$\eta(t) = C + 0 + \frac{1}{2}\left[\frac{1}{mv^*}\right]^2\frac{\varphi''(v^*)}{\varphi'(v^*)}[p_0 - \varphi(v^*)]\,[t - t_0]^2 + \ldots.$$

If $p_0 = \varphi(v^*)$ then $\eta''(t_0) = 0$ and the third term is zero, so we must look to the fourth term of the Taylor series. Since $\eta' = \eta'' = 0$ we have

$$\eta''' = \left[\frac{1}{mv}\right]\eta\varphi''(v)v''.$$

Substituting $\eta = 1/\varphi'(v)$ and

$$v'' = \frac{p'}{mv}$$

gives

$$\eta(t) = C + 0 + 0 + \frac{1}{6}\left[\frac{1}{mv^*}\right]^2\frac{\varphi''(v^*)}{\varphi'(v^*)}p'_0\,[t - t_0]^3 + \ldots.$$

In summary:

- if $v_0 \neq v^*$ then

$$\eta \approx C + \left[\frac{1}{mv_0}\right]\frac{\varphi'(v_0) - \varphi'(v^*)}{\varphi'(v^*)}[t - t_0]$$

- if $v_0 = v^*$ and $p_0 \neq \varphi(v^*)$ then

$$\eta \approx C + \frac{1}{2}\left[\frac{1}{mv^*}\right]^2\frac{\varphi''(v^*)}{\varphi'(v^*)}[p_0 - \varphi(v^*)]\,[t - t_0]^2$$

- if $v_0 = v^*$ and $p_0 = \varphi(v^*)$ then

$$\eta \approx C + \frac{1}{6}\left[\frac{1}{mv^*}\right]^2 \frac{\varphi''(v^*)}{\varphi'(v^*)} p'_0 [t - t_0]^3 .$$

Regenerative braking with $p_0 = -P_R$ will always slow the car, and so a regen phase will always have $p_0 < \varphi(v^*)$. We can also assume that maximum power with $p_0 = P_T$ is always sufficient to increase the speed of the car from any realistic holding speed v^*, and so a power phase will always have $p_0 > \varphi(v^*)$.

Table 10-1 indicates regions near $\eta = C$ where the Taylor series gives a legitimate trajectory for the adjoint variable η.

	regen $\eta < C$		hold $\eta = C$		power $\eta > C$	
	$t < t_0$	$t > t_0$	$t < t_0$	$t > t_0$	$t < t_0$	$t > t_0$
$v_0 > v^*$	✓	×	×	×	×	✓
$v_0 = v^*$	✓	✓	✓	✓	✓	✓
$v_0 < v^*$	×	✓	×	×	✓	×

Table 10-1: Regions near $\eta = C$ where the value of η is valid. Transitions to or from hold V can occur only if $v_0 = v^*$.

The table can be used to determine the possible transitions. For example, a transition from power requires $v_0 \le v^*$ when $t < t_0$, and a transition to regen requires $v_0 \le v^*$ for $t > t_0$, and so a transition from power to regen requires $v_0 \le v^*$. Transitions to and from hold require $v_0 = v^*$. The possible transitions are also indicated in Figure 10-1.

If the car starts from rest there are three possible control sequences for a journey:

- power–regen,
- power–hold, and
- power–hold–regen

These three journey sequences are illustrated in Figure 10-2. The power–regen journey switches from power to regen at speed $v_1 < v^*$, and finishes at location $x_2 = X_1$. The other two journeys switch from power to hold at speed $v_1 = v^*$, and finish at location

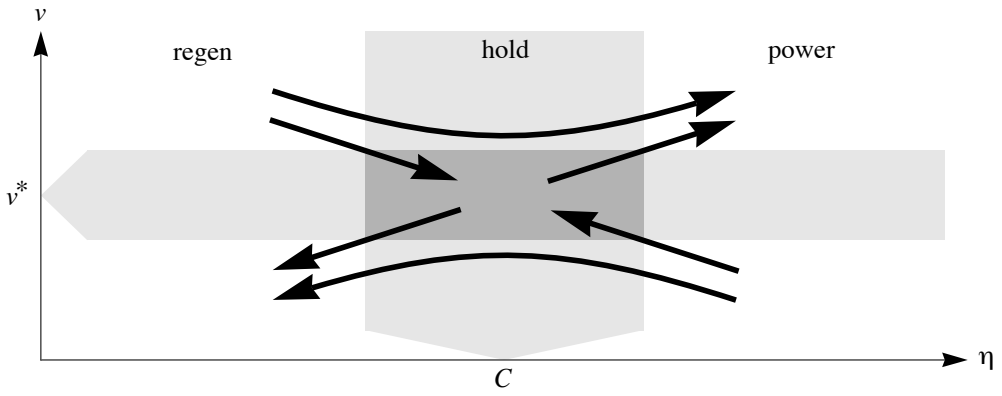

Figure 10-1: Possible control transitions in an optimal strategy.

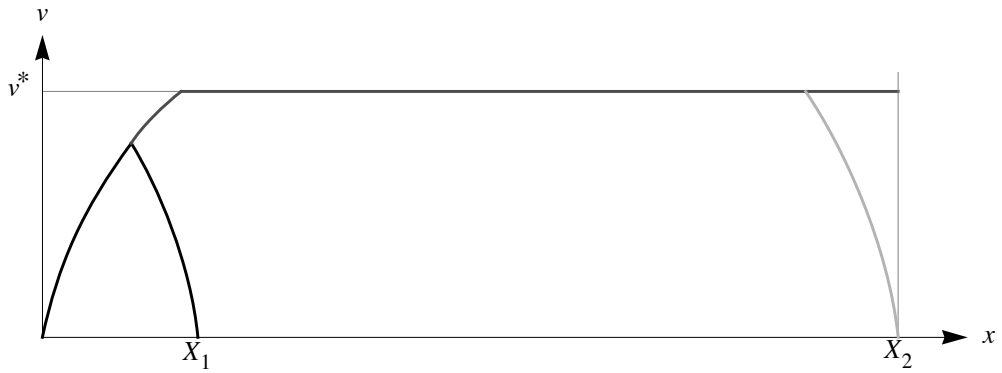

Figure 10-2: Three optimal journeys with holding speed v^* : power–regen, power–hold, and power–hold–regen.

$x_2 = X_2$. The power–hold journey finishes with speed $v_2 = v^*$, and represents a journey where the car crosses the finish line at speed v^*. The power–hold–regen journey finishes with speed $v_2 = 0$.

10.4 Construction of an optimal strategy

Now that we know the form of the optimal strategy, construction of an optimal journey is relatively straightforward. Suppose we wish to drive from $x = 0$ to $x = X$ in minimum time. Suppose also that we start at rest, but will finish at the hold speed v^*.

The time taken for the journey depends on the hold speed v^*. The time taken to power up to speed v^* is

$$t_1(v^*) = \int_0^{v^*} \left[\frac{dt}{dv}\right] dv = \int_0^{v^*} \frac{mv}{P_T - \varphi(v)} dv.$$

The corresponding distance travelled during the power phase is

$$x_1(v^*) = \int_0^{v^*} \left[v\frac{dt}{dv} \right] dv = \int_0^{v^*} \frac{mv^2}{P_T - \varphi(v)} dv.$$

If $x_1(v^*) < X$ then the time taken to complete the journey at constant speed v^* is $[X - x_1(v^*)] / v^*$. The total time for the journey is therefore

$$T(v^*) = \int_0^{v^*} \frac{mv}{P_T - \varphi(v)} dv + \frac{1}{v^*} \left[X - \int_0^{v^*} \frac{mv^2}{P_T - \varphi(v)} dv \right].$$

The solar energy collected during the journey is found by integrating solar power. The energy used is at maximum power P_T on $[0, t_1(v^*)]$ and then at constant power $\varphi(v^*)$ for the remainder of the time. The charge in the battery at the end of the journey is therefore

$$Q_T(v^*) = Q_0 + \frac{1}{\varepsilon} \left\{ \int_0^{T(v^*)} s dt - [P_T t_1(v^*) + \varphi(v^*)(T - t_1(v^*))] \right\}.$$

As v^* increases, $T(v^*)$ and $Q_T(v^*)$ both decrease. To minimise the journey time, v^* should be as large as possible, but with $Q_T(v^*) \geq 0$. Since $Q_T(v^*)$ decreases as v^* increases, the optimal value of v^* will give $Q_T(v^*) = 0$, and the journey will finish with an empty battery.

10.5 A more precise formulation

To prove that an optimal strategy exists it is necessary to formulate the problem more precisely. The existence argument that follows is based on a similar argument for train control (Howlett & Pudney 1995). The argument also appeared in a paper describing the control of a solar car on an undulating road (Howlett & Pudney 1998).

The average speed of a journey can be maximised by either minimising the time taken to travel a given distance, or maximising the distance travelled in a given time. We will maximise the distance travelled,

$$J(v) = \int_0^T v dt,$$

subject to the state equations

$$\frac{dv}{dt} = \frac{1}{m}\left[\frac{p}{v} - R(v)\right] \tag{10.11}$$

$$\frac{dQ}{dt} = -\frac{b}{\varepsilon} \tag{10.12}$$

where battery power b is given by $b = p - s$, and s is solar power.

If the journey starts and finishes at rest then the speed constraints for the journey are $v(0) = v(T) = 0$ and $v(t) \geq 0$. These constraints cause a problem; if $p = P_{\max}$ at $v(0) = 0$ then (10.11) gives

$$mv\frac{dv}{dt} = p - vR(v) \to P_{\max} \quad \text{as} \quad v \downarrow 0$$

$$\Rightarrow \quad \frac{dv}{dt} \uparrow +\infty \quad \text{as} \quad v \downarrow 0.$$

We can avoid this problem by setting $\delta > 0$ and relaxing the speed constraints to $v(0) = v(T) = \delta$ and $v(t) \geq \delta$. We will assume that an optimal solution to the real problem can be found by first finding an optimal solution $v = v_\delta$ to the relaxed problem and then taking the limit of this solution as $\delta \downarrow 0$. The time taken to power from $v = 0$ to $v = \delta$ is

$$t(\delta) = \int_0^\delta \frac{mv}{P_{\max} - vR(v)}\,dv,$$

which decreases to zero as $\delta \downarrow 0$, and so the cost of accelerating from $v = 0$ to $v = \delta$ also decreases to zero as $\delta \downarrow 0$. A similar argument can be made for slowing from $v = \delta$ to $v = 0$ at the end of the journey.

The state equations can now be reformulated as integral equations

$$x(t) = \int_0^T v(\tau)\,d\tau$$

and

$$v(t) = \delta + \frac{1}{m}\int_0^T \left[\frac{p(\tau)}{v(\tau)} - R\left[v(\tau)\right]\right] d\tau$$

with boundary conditions $v(0) = v(T) = \delta$ and constraint $v(t) \geq \delta$. The equation for battery charge becomes

$$Q(t) = Q_0 - \frac{1}{\varepsilon}\int_0^T b(\tau)d\tau .$$

For simplicity we will require that there be no net change in battery charge over the journey, and so $Q(T) = Q_0$.

A driving strategy $\{ (x, v, Q, p) \}$ that satisfies the relaxed state equations will also satisfy the original state equations, except on a set of measure zero. Solutions to the relaxed problem converge to solutions of the original problem as $\delta \downarrow 0$.

10.6 Compactness of the feasible set

We wish to maximise the distance travelled. If x^* is the supremum of distance then there must exist (x_n, v_n) pairs with $x_n > x^* - 1/n$ for each $n = 1, 2, \ldots$. We wish to show that there exists v^* such that $x(v^*) = x^*$. To do this it is necessary to show that if v_n is feasible for all n then there exist subsequences $\{v_{n(i)}\} \subset C$ and $v_\infty \in C$ with $v_{n(i)} \to v_\infty$ in mean square and $Dv_{n(i)} \to Dv_\infty$ weakly.

Let $\mathcal{B}$ be the space of real valued Borel measurable functions on $[0, T]$. We need to consider four subspaces of $\mathcal{B}$.The first space $\mathcal{H}$ is the subspace of square integrable functions. If we define the scalar product

$$(h, k) = \int_0^T h(t)k(t)dt$$

and norm

$$||h||_2 = (h, h)^{1/2}$$

then the space $H = (\mathcal{H}, (\cdot, \cdot)) = L_2([0, T])$ is a Hilbert space.

The second space $\mathcal{K}$ is the subspace of essentially bounded functions, and contains the possible control functions. If we define

$$||p||_\infty = \operatorname*{ess\,sup}_{t \in [0, T]} |p(t)|$$

for each $p \in \mathcal{K}$ then the space $K = (\mathcal{K}, ||\cdot||_\infty) = L_\infty([0, T])$ is a Banach space.

The third space $\mathcal{L}$ is the subspace of essentially Lipschitz functions, and contains speed functions. If we define

$$||v||_{1,\infty} = ||v||_{\infty} + ||Dv||_{\infty}$$

for each $v \in \mathcal{L}$ then the space $L = (\mathcal{L}, ||\cdot||_{1,\infty}) = C^{0,1}([0, T])$ is a Banach space. The notation Dv indicates the generalised derivative of the function v.

The fourth and final space $\mathcal{M}$ is the subspace of functions where the generalised first derivative is essentially Lipschitz, and contains distance functions. If we define

$$||x||_{2,\infty} = ||x||_{\infty} + ||Dx||_{\infty} + ||D^2x||_{\infty}$$

then the space $M = (\mathcal{M}, ||\cdot||_{2,\infty}) = C^{1,1}([0, T])$ is also a Banach space.

The spaces for distance, speed and control satisfy $\mathcal{M} \subseteq \mathcal{L} \subseteq \mathcal{K}$.

The resistance function $R : [0, \infty) \to [0, \infty)$ is positive and strictly increasing. As before, the power required to maintain speed v on a level road is $\varphi(v) = vR(v)$. For a given $\delta > 0$ and $P > 0$ we can define the set of all feasible speed functions as

$$C = C_{\delta, P} \subseteq \mathcal{L}$$

with the conditions

1. $v(0) = v(T) = \delta$,
2. $v(t) \geq \delta$ for all $t \in [0, T]$, and
3. $|mv(t)Dv(t) + \varphi[v(t)]| \leq P$.

When $v \in C$ we have

$$Dv(t) \leq \frac{P}{m\delta}$$

and hence from condition 2 we have

$$\delta \leq v(t) \leq \delta + \frac{P}{m\delta}T = V_{\delta}.$$

It follows from condition 3 that

$$|Dv(t)| \leq \frac{P}{m\delta} + R(V_{\delta}) = A_{\delta},$$

and so

$$||v||_2 \leq T^{1/2} V_\delta$$

and

$$||Dv||_2 \leq T^{1/2} A_\delta .$$

Thus $v \in C$ implies $v \in H$ and $Dv \in H$. The following lemma shows that every sequence in C has a convergent subsequence.

Lemma 10-1 *Let $\{v_n\}$ be a sequence in C. Then $v_n, Dv_n \in H$ and we can find a subsequence $\{v_{n(i)}\}$ and a function $v_\infty \in C$ with $v_\infty, Dv_\infty \in H$ and such that*

$$\left|\left|v_{n(i)} - v_\infty\right|\right|_2 \to 0$$

and

$$(Dv_{n(i)} - Dv_\infty, h) \to 0 \text{ for all } h \in H$$

as $i \to \infty$.

Proof Since $\{v_n\} \subseteq \mathcal{L} \subseteq C([0, T])$ we can use the Arzela-Ascoli theorem (Yosida 1978) to find $v_\infty \in C([0, T])$ and a subsequence $\{v_{n(i)}\}$ with $\left|\left|v_{n(i)} - v_\infty\right|\right|_\infty \to 0$ as $i \to \infty$. But

$$\left|\left|v_{n(i)} - v_\infty\right|\right|_2 \leq T^{1/2} \left|\left|v_{n(i)} - v_\infty\right|\right|_\infty$$

and so $\left|\left|v_{n(i)} - v_\infty\right|\right|_2 \to 0$ as $i \to \infty$.

Since $\left|\left|Dv_n\right|\right|_\infty \leq T^{1/2} A_\delta$ is bounded in the Hilbert space H, the subsequence $\{v_{n(i)}\}$ can be chosen so that $\{Dv_{n(i)}\}$ converges weakly in H to an element $w_\infty \in H$ (Yosida 1978, Theorem 1, p. 126). For each $h \in H$ we have $(Dv_{n(i)} - w_\infty, h) \to 0$ as $i \to 0$. Since $\left|\left|Dv_{n(i)}\right|\right|_\infty \leq A_\delta$ it follows that

$$\left|v_{n(i)}(t) - v_{n(i)}(\tau)\right| \leq A_\delta |t - \tau|$$

for all i and hence that

$$\left|v_\infty(t) - v_\infty(\tau)\right| \leq A_\delta |t - \tau|$$

when $t, \tau \in [0, T]$. Therefore Dv_∞ is well defined with $\left|\left|Dv_\infty\right|\right|_\infty \leq A_\delta$.

We can now show that $Dv_\infty = w_\infty$. Let $\mathcal{S}$ denote the set of all smooth functions $\sigma : [0, T] \to \Re$ with $\text{spt}(\sigma) \subseteq [0, T]$. The set $\text{spt}(\sigma)$ is the support of σ and is the closure of the set of points t where $\sigma(t) \neq 0$. Then

$$\begin{aligned}(Dv_\infty - w_\infty, \sigma) &= \lim_{i \to \infty} (Dv_\infty - Dv_{n(i)}, \sigma) \\ &= (-1)\ (v_\infty - v_{n(i)}, D\sigma) \\ &= 0\end{aligned}$$

for all $\sigma \in \mathcal{S}$. Thus $Dv_\infty = w_\infty$.

It is easy to see that $v_\infty(0) = v_\infty(T) = \delta$ and that $v_\infty(t) \geq \delta$ for all $t \in [0, T]$. To show that v_∞ satisfies the third condition for membership of C we define $x_\infty : [0, T] \to [0, T]$ by

$$x_\infty(t) = \int_0^T v_\infty(\tau) d\tau .$$

For any $k \in K \subseteq H$ with $||k||_\infty \leq 1$ we have $(mv_{n(i)}Dv_{n(i)} + \varphi(v_{n(i)}), k) \leq P$. By taking the limit as $i \to \infty$ it follows from the weak convergence of $Dv_{n(i)}$ to Dv_∞ in H that

$$(mv_\infty Dv_\infty + \varphi(v_\infty), k) \leq P .$$

Since this is true for any k we must have

$$\left| mv_\infty(t)Dv_\infty(t) + \varphi\left[v_\infty(t)\right] \right| \leq P$$

for almost all $t \in [0, T]$ and hence $v_\infty \in C$.

□

10.7 A feasible strategy

Are there any feasible strategies? Let solar power $s : [0, T] \to [0, \infty)$ be a bounded measurable function and let $\mathcal{F}$ denote the set of all journeys $(x, v, Q, p) \in M \times L \times L \times K$ satisfying the state equations, boundary conditions and state constraints.

Clearly it is possible to construct a power–regen strategy with speed v_m satisfying the boundary conditions $v_m(0) = v_m(T) = \delta$, as shown in Figure 10-3. We will assume that this extreme journey uses too much energy, finishing with $Q(T) < Q_0$. If this is the case then it is always possible to construct a journey with $Q(T) = Q_0$. We will show that if $Q(T) < Q_0$ then the set $\mathcal{F}$ is empty.

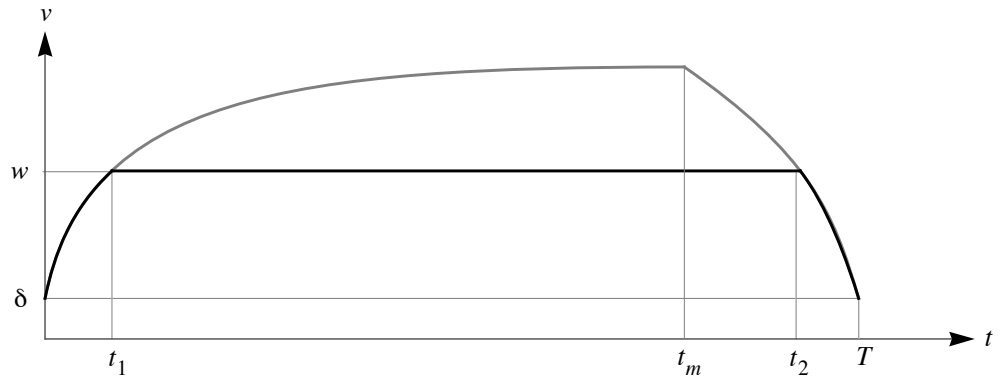

Figure 10-3: A power–hold–regen strategy with speed profile v_w, indicated by the lower curve, will use less energy than the power-regen strategy with speed profile v_m, indicated by the upper dashed curve.

A power–hold–regen strategy with speed $v_w(t) = \min\{v_m(t), w\}$ will use less energy than the power–regen strategy. To show this, we first consider the simplest case with $v(t) = \delta$ and $x(t) = \delta t$. Assume that the solar power $s(t) \geq \varphi(\delta)$ for all $t \in [0, T]$. The net change in battery charge is

$$\Delta Q_\delta = \frac{1}{\varepsilon}\int_0^T [s(t) - \varphi(\delta)]\, dt \geq 0$$

where $s(t) - \varphi(\delta)$ is the excess solar power directed to the battery at time t. The net change in battery charge for the power–regen journey is

$$\Delta Q_m = \frac{1}{\varepsilon}\left\{\int_0^{t_m} [s(t) - P]\, dt + \int_{t_m}^T [s(t) + P]\, dt\right\} \geq 0$$

where t_m is the time at which the control is switched from power to regen. The two integrals are respectively the energy stored during the power phase and the energy stored during the regen phase. The speed at the switching time is $V_m = v_m(t_m)$.

The net change in battery charge for the power–hold–regen journey with hold speed $w \in [\delta, V_m]$ is

$$\Delta Q(w) = \frac{1}{\varepsilon}\left\{\int_0^{t_1}[s(t)-P]\,dt + \int_{t_1}^{t_2}[s(t)-\varphi(w)]\,dt + \int_{t_2}^{T}[s(t)+P]\,dt\right\}.$$

When $w = \delta$ the switching points are $t_1 = 0$ and $t_2 = T$, and $\Delta Q(\delta) \geq 0$. When $w = V_m$ the switching points are $t_1 = t_2 = t_m$, and $\Delta Q(V_m) \leq 0$. Battery change $\Delta Q(w)$ is clearly a continuous function of hold speed w, so we can find a speed w for which $\Delta Q(w) = 0$. This speed gives us a feasible strategy.

10.8 Existence of an optimal strategy

To travel as far as possible in time $[0, T]$ we must maximise

$$J(v) = \int_0^T v(t)dt.$$

That is, we must find a strategy $(x_\infty, v_\infty, Q_\infty, p_\infty) \in \mathcal{F}$ with $J(v_\infty) \geq J(v)$ for all $(x, v, Q, p) \in \mathcal{F}$. Since $\delta \leq v(t) \leq V_m$ it follows that

$$J_{\max} = \sup_{(x, v, Q, p) \in \mathcal{F}} J(v)$$

is well defined and positive. Suppose that $\{(x_n, v_n, Q_n, p_n)\} \subseteq \mathcal{F}$ is a sequence with $J(v_n) \uparrow J_{\max}$ as $n \to \infty$. Since $\{v_n\} \subseteq C$ we can use Lemma 10-1 to find $v_\infty \in C$ and a subsequence $\{v_{n(i)}\}$ with $\|v_{n(i)} - v_\infty\|_2 \to 0$ and $(Dv_{n(i)} - Dv_\infty, h) \to 0$ as $i \to 0$ for all $h \in H$. It is easy to see that

$$J(v_\infty) = J_{\max}.$$

If we define $p_\infty \in \mathcal{K}$ by

$$p_\infty = mv_\infty Dv_\infty + \varphi(v_\infty)$$

then $\|p_\infty\|_\infty \leq P$. We can also define $Q_\infty : [0, T] \to \Re$ by

$$Q_\infty(t) = -\frac{1}{\varepsilon}\int_0^t [p_\infty(\tau) - s(\tau)]\,d\tau.$$

It is easy to show that $Q_\infty \in \mathcal{L}$ and hence that $(x_\infty, v_\infty, Q_\infty, p_\infty) \in \mathcal{F}$.

Thus there exists a strategy $(x_\infty, v_\infty, Q_\infty, p_\infty) \in \mathcal{F} \subseteq \mathcal{M} \times \mathcal{L} \times \mathcal{L} \times \mathcal{K}$.

10.9 Summary

For a solar car with a perfectly efficient battery and drive system, travelling on a flat road, the necessary conditions for an optimal strategy give three control modes:

power	maximum power
hold	maintain a constant speed
regen	maximum regenerative braking.

The optimal control sequence is power–hold–regen. For a long journey, most of the time should be spent travelling at a constant speed.

If we assume that there is always enough solar power to keep the car moving, yet never so much that it is impossible the use it all, then we have shown that it is possible to construct a feasible solution and that an optimal solution exists.

11 An inefficient battery

In this chapter we examine the effect of an inefficient battery on the optimal strategy. We assume that the battery has constant energy efficiency. The result is a strategy with two holding speeds—a lower holding speed used when the battery is discharging, and an upper holding speed used when the battery is charging. In later chapters we will replace this simple battery model with more realistic battery models, and get a slightly different strategy. Nevertheless, the two-speed strategy derived in this chapter provides useful insight—it is better to speed up slightly rather than store energy inefficiently.

This chapter is based on a paper by Howlett, Pudney, Tarnopolskaya & Gates (1996).

11.1 Problem formulation

If we apply energy E to a battery with constant energy efficiency $\eta_B \in [0, 1]$, the effective increase in stored energy is $\eta_B E \le E$. We can model such a battery by setting the current corresponding to battery power b to

$$I(b) = \begin{cases} \dfrac{b}{\varepsilon} & b \ge 0 \\ \dfrac{\eta_B b}{\varepsilon} & b < 0 \end{cases}$$

where ε is the battery emf. The new problem has state equations

$$\frac{dx}{dt} = v,$$

$$\frac{dv}{dt} = \frac{1}{m}\left[\frac{p}{v} - R(v)\right],$$

and

$$\frac{dQ}{dt} = -I(b)$$

where $p(t) = s(t) + b(t)$. The normalised Hamiltonian and adjoint equation can be formed as before, and are

$$H = v + \eta\,[p - \varphi(v)] - CI(b) \tag{11.1}$$

and

$$\frac{d\eta}{dt} = \frac{1}{mv}\,[\eta\varphi'(v) - 1]\,. \tag{11.2}$$

Grouping the terms that depend on the control b, the Hamiltonian can now be written as

$$H = \begin{cases} [\eta - \eta_D]\; b + \ldots & b \geq 0 \\ [\eta - \eta_C]\; b + \ldots & b < 0 \end{cases}$$

where $\eta_D = C/\varepsilon$ and $\eta_C = \eta_B C/\varepsilon$. The value of b that maximises the Hamiltonian depends on the value of η. This time there are five cases to consider:

power	$\eta_D < \eta \;\Rightarrow\; b = P_T - s$
discharge	$\eta = \eta_D \;\Rightarrow\; b \in [0, P_T - s]$
solar	$\eta_C < \eta < \eta_D \;\Rightarrow\; b = 0$
charge	$\eta = \eta_C \;\Rightarrow\; b \in [-P_R - s, 0]$
regen	$\eta < \eta_C \;\Rightarrow\; b = -P_R - s$

The power, solar and regen cases correspond respectively to maximum power, solar power only, and maximum regenerative braking.

The discharge and charge cases are singular, and can only be maintained on a non-trivial interval if $d\eta/dt = 0$. During a discharge phase power is drawn from the battery. If a discharge phase is to be maintained on a non-trivial interval then (11.2) gives

$$\varphi'(v) = \frac{1}{\eta_D}\,. \tag{11.3}$$

But φ' is a strictly increasing function of v, and so (11.3) has a unique solution $v = V$.

During a charge phase power is applied to the battery. If a charge phase is to be maintained on a non-trivial interval then (11.2) gives

$$\eta_B\varphi'(v) = \frac{1}{\eta_D}\,. \tag{11.4}$$

Equation (11.4) also has a unique solution, $v = W$. The two singular cases both require constant speed operation, with the discharge speed V and charge speed W related by

$$\varphi'(V) = \eta_B \varphi'(W) \tag{11.5}$$

and, because φ' is strictly increasing, $V \leq W$.

If the battery is perfectly efficient then $\eta_B = 1$ and $V = W$. In this special case the discharge, solar and charge modes correspond to the single hold mode derived in the previous two chapters.

11.2 Control transitions in an optimal strategy

The optimal strategy depends on the evolution of the variable η. But η is continuous, since the adjoint variable π_2 and speed v are both continuous. Because η is continuous, only certain control transitions are possible. These are shown in Figure 11-1.

There are two critical values of η, corresponding to the two singular control modes:

$$\eta_D = \frac{1}{\varphi'(V)}$$

for the discharge mode and

$$\eta_C = \frac{\eta_B}{\varphi'(V)} = \frac{1}{\varphi'(W)}$$

for the charge mode.

By examining the behaviour of η at transition points it is possible to derive further conditions for transition. As with the simpler problem analysed in the previous chapter, Taylor series expansions in the vicinity of a transition point $t = t_0$ can be used to derive necessary conditions for a transition at that point.

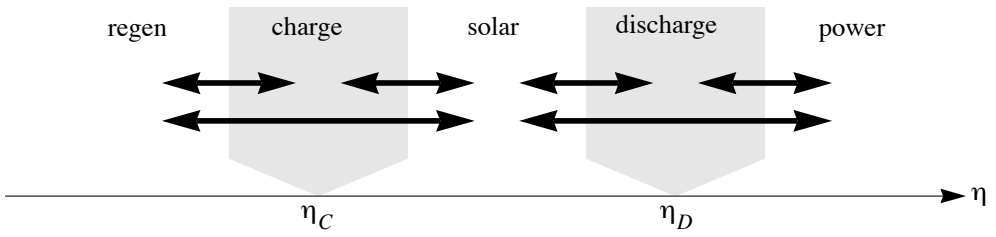

Figure 11-1: Since η is continuous, only certain control transitions are possible. The shaded regions correspond to singular control modes.

Transitions at $\eta = \eta_D$

At $\eta = \eta_D$ transitions may occur between any two of the following control modes:

- power with $p = P_T$ and $\eta > \eta_D$;
- discharge with $p = \varphi(V)$ and $\eta = \eta_D$; and
- solar with $p = s$ and $\eta < \eta_D$.

Let t_0 be the transition time and write $v_0 = v(t_0)$ and $\eta_0 = \eta(t_0)$. Let

$$p_0 = p(t_0) = \lim_{t \to t_0} p(t)$$

and

$$p'_0 = p'(t_0) = \lim_{t \to t_0} p'(t).$$

Because $p(t)$ is not necessarily continuous at $t = t_0$ we will use one-sided limits when required. For t near t_0 the Taylor series expansion of η is dominated by the first non-zero term, and hence:

- if $v_0 \neq V$ then

$$\eta \approx \eta_D + \left[\frac{1}{mv_0}\right] \frac{\varphi'(v_0) - \varphi'(V)}{\varphi'(V)} (t - t_0)$$

- if $v_0 = V$ and $p_0 \neq \varphi(V)$ then

$$\eta \approx \eta_D + \frac{1}{2}\left[\frac{1}{mV}\right]^2 \frac{\varphi''(V)}{\varphi'(V)} [p - \varphi(V)] (t - t_0)^2$$

- if $v_0 = V$ and $p_0 = \varphi(V)$ then

$$\eta \approx \eta_D + \frac{1}{6}\left[\frac{1}{mV}\right]^2 \frac{\varphi''(V)}{\varphi'(V)} p_0' (t - t_0)^3.$$

Table 11-1 indicates regions near $\eta = \eta_D$ where the value of η is valid—that is, where the Taylor series expansion satisfies the conditions for operation in the given mode. The table can be used to determine the possible transitions at $\eta = \eta_D$. For example, if $v_0 < V$ then the only feasible mode at times $t < t_0$ is power, and the only feasible mode at times $t > t_0$ is solar. The only possible transition at speeds $v_0 < V$ are from power to solar.

	solar $\eta < \eta_D$		discharge $\eta = \eta_D$		power $\eta > \eta_D$	
	$t < t_0$	$t > t_0$	$t < t_0$	$t > t_0$	$t < t_0$	$t > t_0$
$v_0 > V$	✓	×	×	×	×	✓
$v_0 = V$	a	b	✓	✓	✓	✓
$v_0 < V$	×	✓	×	×	✓	×

*Table 11-1: Regions near $\eta = \eta_D$ where the value of η is valid. Transitions to or from discharge V can only occur if $v_0 = V$. Transition **a** requires $s < \varphi(V)$ or $[s_0 = \varphi(V)] \wedge [s'_0 > 0]$; transition **b** requires $s < \varphi(V)$ or $[s_0 = \varphi(V)] \wedge [s'_0 < 0]$*

Transitions at $\eta = \eta_C$

At $\eta = \eta_C$ transitions may occur between any two of the following control modes:

- solar with $p = s$ and $\eta > \eta_C$;
- charge with $p = \varphi(W)$ and $\eta = \eta_C$; and
- regen $p = -P_R$ and $\eta < \eta_C$.

For t near t_0 the Taylor series expansion for η is dominated by the first non-zero term:

- if $v_0 \neq W$ then

$$\eta \approx \eta_C + \left[\frac{1}{mv_0}\right] \frac{\varphi'(v_0) - \varphi'(W)}{\varphi'(W)} [t - t_0]$$

- if $v_0 = W$ and $p_0 \neq \varphi(W)$ then

$$\eta \approx \eta_C + \frac{1}{2}\left[\frac{1}{mW}\right]^2 \frac{\varphi''(W)}{\varphi'(W)} [p - \varphi(W)] [t - t_0]^2$$

- if $v_0 = W$ and $p_0 = \varphi(W)$ then

$$\eta \approx \eta_C + \frac{1}{6}\left[\frac{1}{mW}\right]^2 \frac{\varphi''(W)}{\varphi'(W)} p_0' [t - t_0]^3.$$

Table 11-2 indicates regions near $\eta = \eta_C$ where the value of η is valid. As before, the table can be used to determine the possible transitions at $\eta = \eta_C$. Once again, there are restrictions on transitions to and from solar.

	regen $\eta < \eta_C$		charge $\eta = \eta_C$		solar $\eta > \eta_C$	
	$t < t_0$	$t > t_0$	$t < t_0$	$t > t_0$	$t < t_0$	$t > t_0$
$v_0 > W$	✓	×	×	×	×	✓
$v_0 = W$	✓	✓	✓	✓	a	b
$v_0 < W$	×	✓	×	×	✓	×

*Table 11-2: Regions near $\eta = \eta_C$ where the value of η is valid. Transitions to or from charge W can only occur if $v_0 = W$. Transition **a** requires $s > \varphi(V)$ or $[s_0 = \varphi(V)] \wedge [s'_0 > 0]$; transition **b** requires $s > \varphi(V)$ or $[s_0 = \varphi(V)] \wedge [s'_0 < 0]$.*

The possible control transitions in an optimal strategy are summarised in Figure 11-2. For example, a change from regen requires $v \geq W$ before the change, and you can change to charge with $v = W$ or to solar with $v \geq 0$. From solar you can change to power with $v \geq V$, to discharge with $v = V$, to charge with $v = W$, or to regen with $v \leq W$.

Some transitions are not feasible if the initial and final speeds of the car are zero:

- Transitions to power require $v_0 \geq V$. Following such a transition the speed of the car will remain above V, and no further transitions will be possible.
- Transitions from regen require $v_0 \geq W$, and can only occur if the initial speed of the car $v(0) \geq W$.

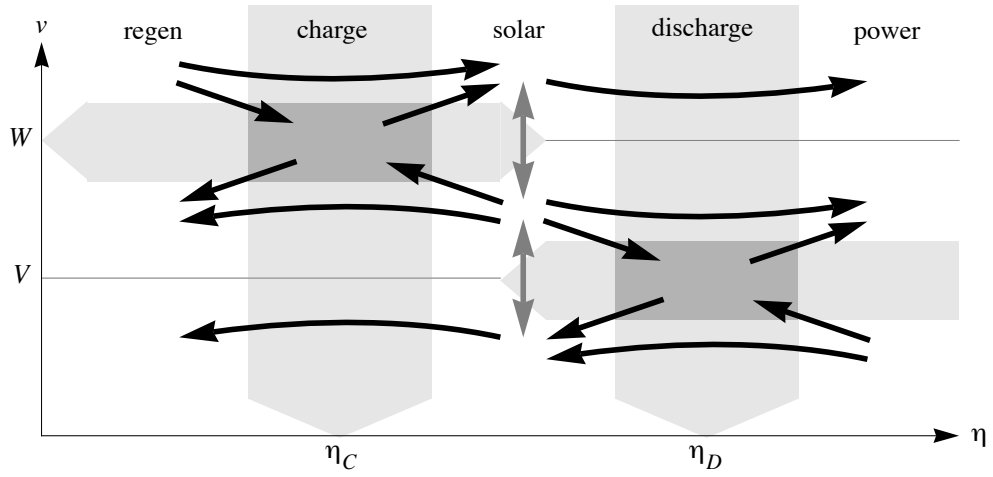

Figure 11-2: Possible control transitions in an optimal strategy. The grey arrows indicate that solar power can sometimes be used to increase or decrease speed through $v = V$ or $v = W$.

11.3 Calculation of transition points

Transition points are determined by the evolution of η. The points at which the critical values of η occur can be determined directly by solving the differential equation

$$\frac{d\eta}{dt} = \frac{1}{mv}[\eta\varphi'(v) - 1] \tag{11.6}$$

or indirectly by solving an equivalent integral equation.

Discharge–solar–charge transitions

Consider the solar phase in a discharge–solar–charge sequence. If the solar phase starts at time t_i and finishes at time t_f then

$$v_i = v(t_i) = V,$$

$$\eta_i = \eta(t_i) = \eta_D,$$

$$v_f = v(t_f) = W,$$

$$\eta_f = \eta(t_f) = \eta_C.$$

For each speed segment $v\colon [t_i, t_f] \to \Re$ equation (11.6) can be rewritten as a first-order linear differential equation

$$\frac{d\eta}{dt} - \frac{\varphi'(v)}{mv}\eta = -\frac{1}{mv}. \tag{11.7}$$

Equation (11.7) can be solved using the integrating factor $e^{\theta(t)}$, where $\theta\colon (-\infty, t_f] \to \Re$ is given by

$$\theta(t) = -\int_t^{t_f} \frac{\varphi'(v(\tau))}{mv(\tau)}\,d\tau.$$

The integrating factor is defined with t_f regarded as known because numerical solutions of (11.6) converge only if time is run backwards. Integrating (11.7) from $t = t_i$ to $t = t_f$ gives

$$\eta_C - \eta_D \exp[\theta(t_i)] = \int_{t_i}^{t_f} \frac{1}{\varphi'(v)} \frac{d}{dt}\{\exp[\theta(t)]\}\,dt.$$

Integrating by parts then gives the transition equation

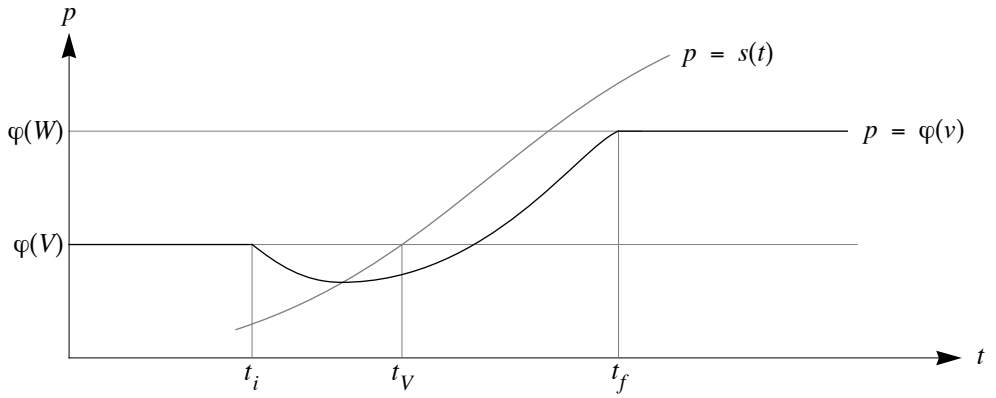

Figure 11-3: Transitions for a typical discharge–solar–charge sequence. Speed initially decreases during the solar phase.

$$\int_{t_i}^{t_f} \exp\left[\theta(t)\right] \frac{d}{dt}\left[\frac{1}{\varphi'(v)}\right] dt = 0 \qquad (11.8)$$

which can be solved for t_i, since $v(t_f) = W$ and t_f is assumed known. For (11.8) to have a solution it is necessary that

$$\frac{d}{dt}\left[\frac{1}{\varphi'(v)}\right] = \frac{-\varphi''(v)}{[\varphi'(v)]^2}\frac{dv}{dt}$$

take both positive and negative values in the interval $[t_i, t_f]$. But $\varphi''(v) > 0$, so acceleration dv/dt must take both negative and positive values in the interval.

From Table 11-1, the sequence discharge–solar–charge can only occur if solar power is increasing. Suppose $s'(t) > 0$ throughout the interval. The transition from discharge to solar at $t = t_i$ requires $s_i = s(t_i) < \varphi(V)$, so v must first decrease from the initial value $v_i = V$ and then increase to the final value $v_f = W$. Equation (11.8) guarantees that there is at most one solution point $t = t_i$ in the region where $s(t) < \varphi(V)$.

A typical discharge–solar–charge sequence is illustrated in Figure 11-3. Notice that the change from discharge to solar occurs with $s < \varphi(V)$; you have to know in advance that s will increase. At the end of this chapter we will construct an optimal journey, and show that in practice the time interval $t_V - t_i$ is less than a minute.

Charge–solar–discharge transitions

Now consider the solar phase in a charge–solar–discharge sequence. The transition equation (11.8) still applies. This time, however, the sequence can only occur if solar power is decreasing. Suppose $s'(t) < 0$ throughout the solar interval $[t_i, t_f]$. The

transition from charge to solar at $t = t_i$ requires $s_i = s(t_i) > \varphi(V)$, so v must first increase from the initial value $v_i = W$ and then decrease to the final value $v_f = V$. Once again, (11.8) guarantees that there is at most one solution point $t = t_i$ in the region where $s(t) > \varphi(V)$.

11.4 Existence of transition points

The transition equation (11.8) gives a necessary condition for switching into a solar phase. Under certain conditions it is possible to show that the transition equation has a solution.

Consider the transition from discharge to solar as solar power increases, and suppose that solar power is given by the continuous function

$$s(t) = \begin{cases} \varphi(V_0) & t < p \\ \sigma(t) & p \le t \le q \\ \varphi(W_0) & q < t \end{cases}$$

where $\sigma(t)$ is monotone increasing on the interval $[p, q]$ and where $V_0 < V < W < W_0$, as shown in Figure 11-4.

How does η behave when $p = s$? In the region $t > q$ the power to the drive system is $p(t) = \varphi(W_0)$, and so

$$\frac{d\eta}{dv} = \frac{\eta\varphi'(v) - 1}{\varphi(W_0) - \varphi(v)}.$$

Integrating this equation gives

$$\eta = \frac{C - v}{\varphi(W_0) - \varphi(v)}$$

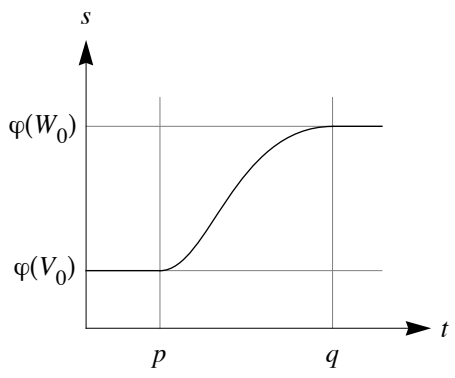

Figure 11-4: If solar power increases continuously and monotonically from a constant level $\varphi(V_0) < \varphi(V)$ to a constant level $\varphi(W_0) > \varphi(W)$ then it is possible to show that the transition equation has a solution.

where C is a constant. Setting $C = W_0$ generates an η curve

$$h(v) = \frac{W_0 - v}{\varphi(W_0) - \varphi(v)} \tag{11.9}$$

with

$$\lim_{v \uparrow W_0} h(v) = \frac{1}{\varphi'(W_0)} = \kappa_0 .$$

Note that $dh/dv < 0$ for $v < W_0$, and so $h(v) \downarrow \kappa_0$ as $v \uparrow W_0$. Surrounding η curves can be analysed by setting

$$C = W_0 + \delta .$$

Each value of δ generates a curve

$$h_\delta(v) = h(v) + \frac{\delta}{\varphi(W_0) - \varphi(v)} .$$

If $\delta > 0$ then $h_\delta(v) > h(v)$ and $h_\delta(v) \to \infty$ as $v \uparrow W_0$. Alternatively, if $\delta < 0$ then $h_\delta(v) < h(v)$ and $h_\delta(v) \to -\infty$ as $v \uparrow W_0$. But $v \uparrow W_0$ as $t \to \infty$, and so

- $h_\delta \to \infty$ as $t \to \infty$ for all $\delta > 0$,
- $h_0 \to \kappa_0$ as $t \to \infty$, and
- $h_\delta \to -\infty$ as $t \to \infty$ for all $\delta < 0$.

These three curves are illustrated in Figure 11-5.

During the solar phase η must decrease from $\eta(t_i) = \eta_D$ to $\eta(t_f) = \eta_C$ with $v(t_f) = W$ and

$$\left.\frac{d\eta}{dt}\right|_{t_f} = 0 . \tag{11.10}$$

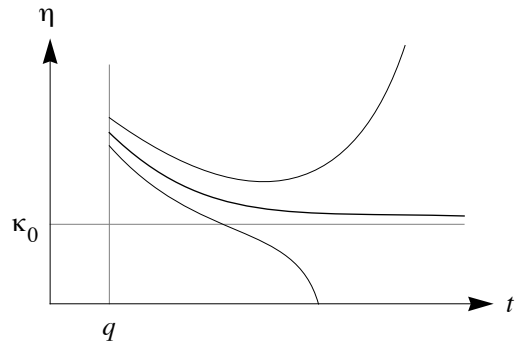

Figure 11-5: Curves h_δ. The middle curve corresponds to $\delta = 0$, the upper curve to $\delta > 0$, and the lower curve to $\delta < 0$.

The η curve given by (11.9) is critical—only curves lying above this critical curve can satisfy condition (11.10). The critical curve can be extended back into the region $t < q$ in the following way. Choose $\tau < q$, then let $v_\tau(t)$ be the speed profile with $v(\tau) = V$ and let

$$\eta_\tau^\dagger(t) = h(v_\tau(t)) = \frac{W_0 - v_\tau(t)}{\varphi(W_0) - \varphi(v_\tau(t))}$$

in the region $t > q$. The curve $\eta_\tau^\dagger$ satisfies the differential equation (11.6) in the region $t > q$ and has the additional property that $\eta_\tau^\dagger(t) \downarrow \kappa_0$ as $t \to \infty$. For each τ there is a uniquely defined speed curve v_τ and a corresponding unique curve $\eta_\tau^\dagger$ in the region $t > q$. Each curve $\eta_\tau^\dagger$ can be extended back into the interval $[\tau, q]$ by solving the differential equation

$$\frac{d\eta}{dt} = \frac{1}{mv_\tau(t)}[\varphi'(v_\tau(t))\eta - 1] \tag{11.11}$$

with boundary condition $\eta(q) = \eta_\tau^\dagger(q)$. It is now possible to show that there is a special point $\tau = \omega$ and a corresponding special curve $\eta_\omega^\dagger$ such that $\eta_\omega^\dagger(\omega) = \eta_D$. Let $t = t_v$ denote the unique solution to the equation $s(t) = \varphi(V)$. The proof is in three parts:

- Lemma 11-1 shows that if $\tau = \tau_V$ then $\eta_\tau^\dagger(\tau) < \eta_D$.
- Lemma 11-2 shows that if $\tau \in [p, t_V]$ and $\eta_\tau^\dagger(\tau) < \eta_D$ then $\eta_\tau^\dagger$ decreases throughout the interval $[\tau, q]$.
- Lemma 11-3 shows that if $\eta_p^\dagger(p) < \eta_D$ then there exist $\zeta < p$ such that $\eta_\zeta^\dagger(\zeta) > \eta_D$.

The first two lemmas imply that if there is a point ω such that $\eta_\omega^\dagger(\omega) = \eta_D$ then it must lie in the region $(-\infty, t_V)$. The third lemma, combined with a continuity argument, shows that if the point ω does not lie in the interval $[p, t_V]$ then it must lie in the interval $(-\infty, p)$. It can then be shown that the curve $\eta_\omega^\dagger$ divides the (t, η) plane into two regions, and that in the uppermost region there is a uniquely defined solar interval $[t_i, t_f]$ with $v(t_i) = V$, $\eta(t_i) = \eta_D$, $v(t_f) = W$ and $\eta(t_f) = \eta_C$.

Lemma 11-1 *Let $t = t_V$ denote the unique solution to the equation $s(t) = \varphi(V)$. If $\tau = t_V$ then $\eta_\tau^\dagger(\tau) < \eta_D$.*

Proof From (11.11),

$$\frac{d\eta}{dt} - \frac{\varphi'(v_\tau)}{mv_\tau}\eta = -\frac{1}{mv_\tau}.$$

If we define

$$\theta_\tau(t) = -\int_t^q \left[\frac{\varphi'(v_\tau(\rho))}{mv_\tau(\rho)}\right] d\rho$$

then integrating from $t = \tau$ to $t = q$ gives

$$\eta(q) - \eta(\tau)\exp\left[\theta_\tau(\tau)\right] = \int_\tau^q \frac{1}{\varphi'(v_\tau(\rho))}\frac{d}{d\rho}\left\{\exp\left[\theta_\tau(\rho)\right]\right\} d\rho.$$

But $v_\tau(\rho) \geq V$ for all $\rho \in (\tau, q)$, and so $1/\varphi'(v_\tau(\rho)) \leq 1/\varphi'(V) = \eta_D$. Since

$$\frac{d}{d\rho}\left\{\exp\left[\theta_\tau(\rho)\right]\right\} < 0$$

it follows that

$$\int_\tau^q \frac{1}{\varphi'(v_\tau(\rho))}\frac{d}{d\rho}\left\{\exp\left[\theta_\tau(\rho)\right]\right\} d\rho > \int_\tau^q \eta_D \frac{d}{d\rho}\left\{\exp\left[\theta_\tau(\rho)\right]\right\} d\rho$$

and hence

$$\eta(q) - \eta(\tau)\exp\left[\theta_\tau(\tau)\right] > \eta_D - \eta_D \exp\theta_\tau(\tau).$$

Since $\eta(q) < \eta_D$ it follows that $\eta(\tau) < \eta_D$. Thus $\eta_\tau^\dagger(\tau) = \eta(\tau) < 1$ when $\tau = t_V$.
□

Lemma 11-2 *If* $\tau \in [p, t_V]$ *and* $\eta_\tau^\dagger(\tau) < \eta_D$ *then the curve* $\eta_\tau^\dagger$ *decreases throughout the interval* $[\tau, q]$.

Proof Since $d\eta_\tau^\dagger/dt$ is continuous and since

$$\frac{d}{dt}\eta_\tau^\dagger\Big|_q < 0$$

it follows that $d\eta_\tau^\dagger/dt < 0$ for all $t < q$ and sufficiently close to q. Let $t = t_\tau$ be the point where $s(t) = \varphi(v_\tau(t))$. Suppose there is some point $r \in (t_\tau, q)$ with

$$\frac{d}{dt}\eta_\tau^\dagger\Big|_r = 0$$

and $d\eta_\tau^\dagger / dt < 0$ for all $t \in (r, q)$. From (11.6),

$$\frac{d^2\eta}{dt^2} = \frac{1}{mv}\{\frac{d\eta}{dt}\varphi'(v) + \left[\eta\varphi''(v) - \frac{\eta\varphi'(v) - 1}{v}\right]\frac{dv}{dt}\}$$

and since

$$\frac{d}{dt}\eta_\tau^\dagger\Big|_r = 0$$

and

$$\frac{dv_\tau}{dt}\Big|_r > 0$$

it follows that

$$\frac{d^2}{dt^2}\eta_\tau^\dagger\Big|_r = \frac{\eta_\tau^\dagger(r)\ \varphi''(v_\tau(r))}{mv_\tau(r)}\ \frac{dv_\tau}{dt}\Big|_r > 0.$$

But

$$\frac{d}{dt}\eta_\tau^\dagger\Big|_r = 0,$$

implies $\eta_\tau^\dagger(t) > \eta_\tau^\dagger(r)$ for all $t > r$ and sufficiently close to r. This contradicts the assumption that $d\eta_\tau^\dagger / dt < 0$ for $t > r$. Thus $d\eta_\tau^\dagger / dt < 0$ for all $t \in (t_\tau, q)$.

If $\eta_\tau^\dagger(\tau) < \eta_D$ then equation (11.11) shows that

$$\frac{d}{dt}\eta_\tau^\dagger\Big|_\tau < 0.$$

Since $d\eta_\tau^\dagger / dt$ is continuous and since

$$\frac{d}{dt}\eta_\tau^\dagger\Big|_\tau < 0$$

it follows that $d\eta_\tau^\dagger / dt < 0$ for all $t > \tau$ and sufficiently close to τ. Suppose there is some point $r \in (\tau, t_\tau)$ with

$$\frac{d}{dt}\eta_\tau^\dagger\Big|_r = 0$$

and $d\eta_\tau^\dagger / dt < 0$ for all $t \in (\tau, r)$. A similar argument to the one used above shows that $d\eta_\tau^\dagger / dt < 0$ for all $t \in (r, t_\tau)$.

Hence $d\eta_\tau^\dagger / dt < 0$ for all $t \in [\tau, t_\tau) \cup (t_\tau, q]$ and, by continuity, $d\eta_\tau^\dagger / dt \le 0$ for $t = t_\tau$. Thus $\eta_\tau^\dagger(t)$ is strictly monotone decreasing on the interval $[\tau, q]$.
□

When $\tau = p$ the condition $\eta_p^\dagger(p) < \eta_D$, from Lemma 11-1 with $\tau = p$, implies that the curve $\eta_p^\dagger$ is strictly monotone decreasing on the interval $[p, q]$, and any point τ with $\eta_\tau^\dagger(\tau) > \eta_D$ must lie in the region $t < p$. In this region we have $s(t) = \varphi(V_0)$ and the curve $\eta_\tau^\dagger$ satisfies the differential equation (11.11) with

$$\eta(p) = \eta_\tau^\dagger(p)$$

and so

$$\eta = \frac{v - V_0 + D}{\varphi(v) - \varphi(V_0)} \tag{11.12}$$

where D is a constant. Setting

$$D = \eta_\tau^\dagger(p)\,[\varphi(v_\tau(p)) - \varphi(V_0)] - [v_\tau(p) - V_0] \tag{11.13}$$

generates a curve $\eta = k(v)$ with

$$k(v_\tau(p)) = \eta_\tau^\dagger(p)$$

and with $dk/dv > 0$ for $v \in [v_\tau(p), V]$. Substituting $v = v_\tau$ and (11.13) into (11.12) gives

$$\eta_\tau^\dagger(t) = \frac{[v_\tau(t) - v_\tau(p)] + \eta_\tau^\dagger(p)\,[\varphi(v_\tau(p)) - \varphi(V_0)]}{\varphi(v_\tau(t)) - \varphi(V_0)} \tag{11.14}$$

in the region $t < p$.

Lemma 11-3 *If $\eta_p^\dagger(p) < \eta_D$ then there exists $\zeta < p$ such that $\eta_\zeta^\dagger(\zeta) > \eta_D$.*

Proof At the start of the solar phase the speed of the car is $v_\tau(\tau) = V$. From (11.14),

$$\eta_\tau^\dagger(\tau) = \frac{[V - v_\tau(p)] + \eta_\tau^\dagger(p)\,[\varphi(v_\tau(p)) - \varphi(V_0)]}{\varphi(V) - \varphi(V_0)}.$$

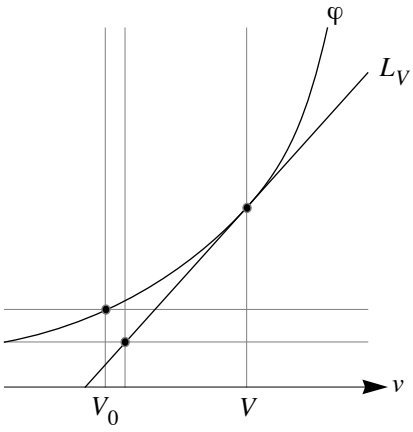

Figure 11-6: If L_V is the tangent to φ at speed V, and if $V_0 < V$, then there exist $\delta > 0$ so that $L_V(V_0 + \delta) < \varphi(V_0)$.

In the interval $t \le p$ the speed $v_\tau(p) \downarrow V_0$ as $\tau \downarrow -\infty$, and so $\varphi(v_\tau(p)) > \varphi(V_0)$ and

$$\eta_\tau^\dagger(\tau) > \frac{V - v_\tau(p)}{\varphi(V) - \varphi(V_0)}.$$

Let $L_v(w) = \varphi(v) + \varphi'(v)(w - v)$ for any two speeds v and w. Since $V_0 < V$ there exists $\delta > 0$ so that $L_V(V_0 + \delta) < \varphi(V_0)$, as shown in Figure 11-6. Suppose the speed of the car at time p is $v_\tau(p) = V_0 + \delta$. Then

$$\begin{aligned} V - (V_0 + \delta) &= \frac{L_V(V) - L_V(V_0 + \delta)}{\varphi'(V)} \\ &= \frac{\varphi(V) - L_V(V_0 + \delta)}{\varphi'(V)}. \end{aligned}$$

But $L_V(V_0 + \delta) < \varphi(V_0)$ and so

$$\frac{V - (V_0 + \delta)}{\varphi(V) - \varphi(V_0)} > \frac{1}{\varphi'(V)} = \eta_D$$

and there exists $\tau = \zeta$ such that $\eta_\zeta^\dagger(\zeta) > \eta_D$.

□

Because $\eta_\tau^\dagger(\tau)$ depends continuously on τ there must be some point $\omega \in (\zeta, t_V)$ with $\eta_\omega^\dagger(\omega) = \eta_D$. Typical curves s, v_ω and $\eta_\omega^\dagger$ are shown in Figure 11-7.

The special curve $\eta_\omega^\dagger(t)$ divides the (t, η) plane into two regions. Let $\tau \in (\omega, t_V)$ be a proposed transition time and consider the curve η_τ satisfying the differential equation

$$\frac{d\eta_\tau}{dt} = \frac{1}{m v_\tau(t)} [\varphi'(v_\tau(t))\eta_\tau - 1]$$

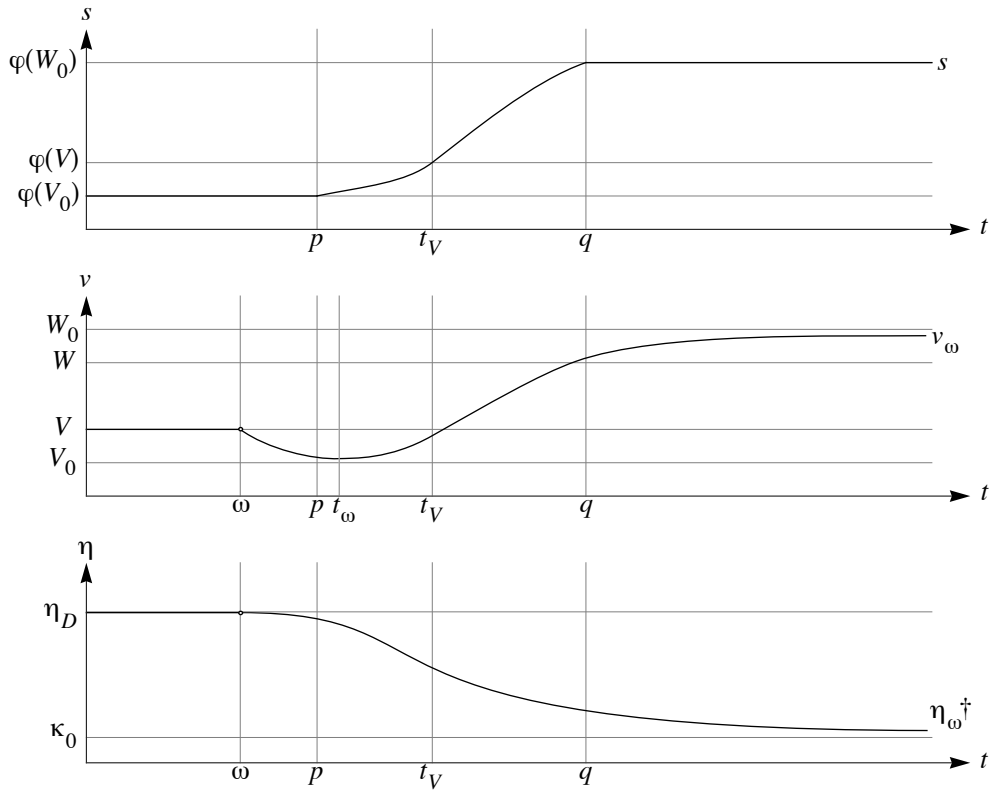

Figure 11-7: Typical curves s, v_ω and $\eta_\omega^\dagger$.

with $\eta_\tau(\tau) = \eta_D$. The fundamental existence and uniqueness theorem for first-order differential equations can be used to show that:

- the curve η_τ lies above the special curve $\eta_\omega^\dagger$
- the curve η_τ has a minimum turning point at $(t, \eta) = (\mu(\tau), \kappa(\tau))$ with $\eta_\tau(t) \uparrow \infty$ as $t \uparrow \infty$;
- μ: $(\omega, t_V) \to (t_V, \infty)$ is a one-to-one correspondence;
- $\mu(\tau)$ depends continuously on τ and decreases as τ increases;
- κ: $(\omega, t_V) \to (\kappa_0, \eta_D)$, where $\kappa_0 = 1/\varphi'(W_0)$, is a one-to-one correspondence; and
- $\kappa(\tau)$ depends continuously on τ and increases as τ increases.

When $\tau < \omega$ the curve η_τ lies below the special curve $\eta_\omega^\dagger$. Furthermore, $d\eta_\tau/dt < 0$ for all $t > \tau$ and $\eta_\tau(t) \downarrow -\infty$ as $t \uparrow \infty$.

The family of curves η_τ is illustrated in Figure 11-8.

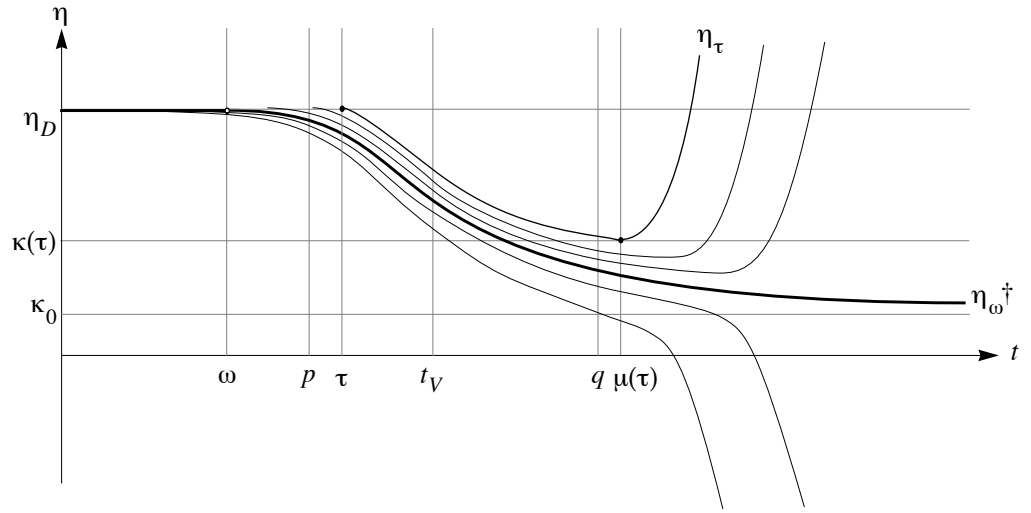

Figure 11-8: Curves η_τ *for various* $\tau \in (\omega, t_V)$.

If $\eta_C \in (\kappa_0, \eta_D)$ there is a transition time $\tau \in (\omega, t_V)$ such that $\kappa(\tau) = \eta_C$. By setting $t_i = \tau$, $t_f = \mu(\tau)$, $v(t) = v_\tau(t)$ and $\eta(t) = \eta_\tau(t)$ it can be seen that there is a uniquely defined control interval $[t_i, t_f]$ and a corresponding η curve with $\eta(t_i) = \eta_D$ and $\eta(t_f) = \eta_C$.

11.5 Example

The best way to illustrate the procedure for constructing an optimal strategy is with an example. Suppose a solar car race starts two hours after sunrise, travels for nine hours, and finishes two hours before sunset. We wish to maximise the distance travelled.

The parameters for the example are given in Table 11-3. The car parameters are based on those of the top cars in the 1993 and 1996 World Solar Challenges.

Parameter	Value
solar power	$s(t) = 1700 \sin(\pi t / (13 \times 3600))$ W
maximum drive power	$P_T = 3000$ W
maximum regenerative braking power	$P_R = 3000$ W
mass	$m = 250$ kg
acceleration due to gravity	$g = 9.8$ m s^{-2}
number of wheels	$N = 3$

Table 11-3: Parameters for a solar racing car.

Parameter	Value
resistance coefficients	$c_{rr1} = 0.005$ $c_{rr2} = 0.052\,\mathrm{kg\,s^{-1}}$ $C_dA = 0.095\,\mathrm{m^2}$
air density	$\rho = 1.22\,\mathrm{kg\,m^{-3}}$
battery efficiency	$\eta_B = 0.85$

Table 11-3: Parameters for a solar racing car.

The strategy for the journey is power–discharge–solar–charge–solar–discharge–solar–regen. The charge phase is used during the middle of the day when $s(t) > \varphi(W)$. The final two phases, solar and regen, are positioned so that the car stops at the correct finishing time.

For a given discharge speed V, the charge speed W can be determined from (11.5). The two holding speeds and the control strategy then determine the entire journey, and hence the distance travelled and the energy used. Increasing the hold speeds increases the distance travelled and the energy used; decreasing the hold speeds decreases the distance travelled and the energy used. By selecting an appropriate discharge speed V it is possible to construct a journey that maximises distance for any desired energy consumption, or that minimises energy consumption for any desired distance.

An optimal journey with $V = 23.6$ (85km/h) and $W = 25.9$ (93.3km/h) is shown in Figure 11-9. The *solar speed* curve $\varphi^{-1}(s)$, shown as a dotted line, indicates the holding speed that could be maintained using only the available solar power s. The functions v and η were calculated using an adaptive Runge-Kutta scheme to solve the relevant differential equations.

Three of the transition points require no detailed calculation:

- power–discharge occurs when $v = V$;
- solar–charge occurs when $v = W$; and
- solar–discharge occurs when $v = V$.

The final solar and regen phases must be positioned so that $V(T) = 0$. Let τ be the time at which the final solar phase commences, with $v(\tau) = V$ and $\eta(\tau) = \eta_D$. The final transition to regen occurs when $\eta(t) = \eta_C$, and can be found by solving the appropriate differential equations for v and η. The appropriate transition time τ is found by searching for the time τ that gives $v(T) = 0$. Brent's algorithm was used to perform the search.

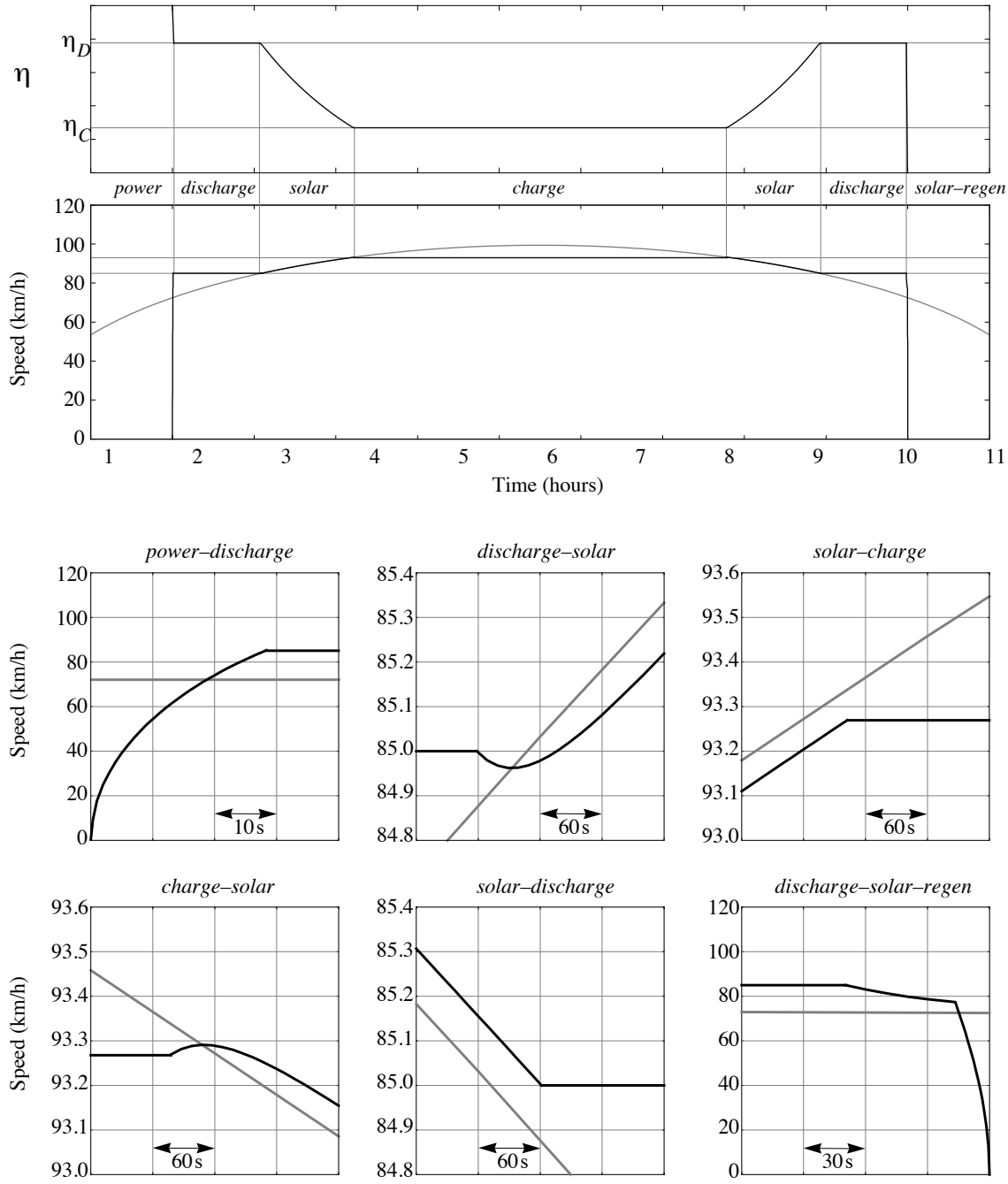

Figure 11-9: Optimal strategy for the example journey. The top two graphs show the η and v curves. The second graph also shows solar speed $\varphi^{-1}(s)$ (dotted). Details of the six transitions are shown in the six smaller graphs.

The remaining two transitions, discharge–solar and charge–solar, are more difficult to calculate. For the discharge–solar transition it is necessary to search for a transition time τ and associated curves v_τ and η_τ, described in section 11.4, so that $v(\tau) = V$, $v[\mu(\tau)] = W$, $\eta(\tau) = \eta_D$ and $\eta[\mu(t)] = \eta_C$. The search is complicated by the behaviour of the differential equations for v and η; the numerical solution for v converges only if t increases, whereas the numerical solution for η converges only if t decreases. This difficulty can be overcome by calculating the speed profile v for $t \in [\tau, \mu(\tau)]$ with $v(\tau) = V$ and t increasing, and then using the resulting values of v to calculate η for $t \in [\tau, \mu(\tau)]$ with $\eta[\mu(\tau)] = \eta_C$ and t decreasing. This procedure is repeated for various candidate τ until a solution is found with $\eta(\tau) = \eta_D$. A similar procedure is used to calculate the transition from charge to solar. Efficient numerical algorithms were developed and used to calculate the transitions shown in Figure 11-9.

11.6 Summary

For the simplified solar car problem with a constant efficiency battery, the optimal driving strategy uses five driving modes:

- maximum power;
- discharging at a lower critical speed V;
- solar power;
- charging at an upper critical speed W; and
- maximum regenerative braking.

For typical clear-sky irradiance the optimal control sequence is power–discharge–solar–charge–solar–discharge–solar–regen. The two holding speeds V and W are related to the efficiency of the energy storage system η_B by the equation

$$\frac{\varphi'(V)}{\varphi'(W)} = \eta_B.$$

If the energy efficiency of the battery is less than perfect then $\eta_B < 1$ and $V < W$. For reasonably efficient batteries, however, the two holding speeds are sufficiently close that differences between the optimal strategy and a constant speed strategy are small.

If solar irradiance is assumed known then standard numerical procedures can be used to calculate precise control transition points for an optimal journey.

12 Gradients

Up until now we have assumed that the road is level. In this chapter we introduce non-constant gradients to the model. Our assumptions are:

- solar irradiance does not depend on location,
- the car has a single battery with constant energy efficiency, and
- the battery is sufficiently large that battery power and charge constraints are never binding.

Gradients do not change the form of the solution; the optimal strategy still has a lower hold speed used when the battery is discharging and an upper hold speed used when the battery is charging.

This chapter is based on a paper by Howlett & Pudney (1998).

12.1 Problem formulation

The state equations for the new problem are

$$\frac{dx}{dt} = v, \tag{12.1}$$

$$\frac{dv}{dt} = \frac{1}{m}\left[\frac{p}{v} - R(v) + G(x)\right], \tag{12.2}$$

and

$$\frac{dQ}{dt} = -I(b) \tag{12.3}$$

where G is the force on the car due to the gradient of the road, given by the formula

$$G(x) = -mg\sin\theta(x)$$

where θ is the angle of slope of the road.

For a battery with constant energy efficiency $\eta_B \in [0, 1]$, the current corresponding to battery power b is

$$I(b) = \begin{cases} \dfrac{b}{\varepsilon} & b \geq 0 \\ \dfrac{\eta_B b}{\varepsilon} & b < 0 \end{cases}$$

where ε is the battery emf. The normalised Hamiltonian for the simplified problem is

$$H = \pi_1 v + \frac{\pi_2}{m}\left[\frac{p}{v} - R(v) + G(x)\right] - CI(b)$$

with corresponding adjoint equations

$$\frac{d\pi_1}{dt} = -\frac{\pi_2}{m}G'(x), \tag{12.4}$$

$$\frac{d\pi_2}{dt} = \frac{\pi_2}{m}\left[\frac{p}{v^2} + R'(v)\right] - \pi_1 \tag{12.5}$$

By defining

$$\eta = \frac{\pi_2}{mv}$$

and

$$\varphi(v) = vR(v)$$

we can rewrite the Hamiltonian and adjoint equations as

$$H = \pi_1 v + \eta\left[p - \varphi(v) + vG(x)\right] - CI(b) \tag{12.6}$$

$$\frac{d\pi_1}{dt} = -\eta v G'(x) \tag{12.7}$$

$$\frac{d\eta}{dt} = \frac{\eta_T}{mv}\left\{\left[\varphi'(v) - G(x)\right]\eta - \pi_1\right\}. \tag{12.8}$$

Grouping the terms that depend on the control, the Hamiltonian can be rewritten as

$$H = \begin{cases} [\eta - \eta_D]\, b + \ldots & b \geq 0 \\ [\eta - \eta_C]\, b + \ldots & b < 0 \end{cases}$$

where $\eta_D = C/\varepsilon$ and $\eta_C = \eta_B C/\varepsilon$.

12.2 Necessary conditions for an optimal strategy

The optimal control maximises the Hamiltonian, and so depends on the value of η. The usual five cases apply:

power	$\eta_D < \eta \Rightarrow b = P_T - s$
discharge	$\eta = \eta_D \Rightarrow b \in [0, P_T - s]$
solar	$\eta_C < \eta < \eta_D \Rightarrow b = 0$
charge	$\eta = \eta_C \Rightarrow b \in [-P_R - s, 0]$
regen	$\eta < \eta_C \Rightarrow b = -P_R - s$

The singular discharge mode requires $\eta = \eta_D$. If this condition is maintained on a non-trivial interval then

$$\frac{d\pi_1}{dt} = -\eta_D v G'(x) = -\eta_D \frac{d}{dt}[G(x)]$$

and so

$$\pi_1 = -\eta_D G(x) + A \qquad (12.9)$$

where A is a constant of integration. But $d\eta/dt = 0$; substituting (12.9) into (12.8) gives $\eta_D \varphi'(v) = A$. Since $\varphi(v)$ is convex, this equation has a unique solution $v = V$, and the discharge mode corresponds to speed holding with

$$b(t) = \varphi(V) - VG(x(t)) - s(t).$$

Similarly, the singular charge mode requires $\eta = \eta_C$. If this condition is maintained on a non-trivial interval then

$$\pi_1 = -\eta_C G(x) + B,$$

where B is a constant of integration, and so $\eta_C \varphi'(v) = B$. This equation has a unique solution $v = W$, so the charge mode corresponds to speed holding with

$$b(t) = \varphi(W) - WG(x(t)) - s(t).$$

The optimal driving modes are the same as for level track. Unlike level track, however, it is not obvious that there is only one discharge speed and only one charge speed, with a simple relationship between these two speeds. We will show that the optimal strategy has these features in the next section.

12.3 How many holding speeds?

To show that there is only one discharge speed and only one charge speed we need to consider three types of transitions:

- transitions between discharge and charge using a solar phase,
- discharge–power–discharge transitions; and
- charge–regen–charge transitions.

Transitions using solar

Consider an optimal journey with

- discharge intervals (α_i, β_i) with $v = V_i$
- charge intervals (γ_j, δ_j) with $v = W_j$, and
- solar between these intervals.

The charge in the battery at the end of the journey will be

$$Q(T) = Q(0) + \frac{1}{\varepsilon}\sum_i \left[\int_{\alpha_i}^{\beta_i} (s(t) - [\varphi(V_i) - V_i G(x(t))])\, dt\right] + \frac{\eta_B}{\varepsilon}\sum_j \left[\int_{\gamma_j}^{\delta_j} (s(t) - [\varphi(W_j) - W_j G(x(t))])\, dt\right].$$

For $t \in [\alpha_i, \beta_i]$ we have

$$x(t) = x(\alpha_i) + V_i[t - \alpha_i],$$

and for $t \in [\gamma_j, \delta_j]$ we have

$$x(t) = x(\gamma_j) + W_j[t - \gamma_j].$$

Suppose we wish to maximise the distance travelled in a fixed time T, subject to a charge constraint $Q(T) \geq 0$. The cost function to be maximised is

$$J = \int_0^T v(t)dt.$$

Necessary conditions for a solution can be found by forming a Lagrangean

$$L = J + \lambda\varepsilon Q$$

and then applying the Kuhn-Tucker conditions

$$\frac{\partial L}{\partial V_i} = \frac{\partial L}{\partial W_j} = 0. \tag{12.10}$$

Figure 12-1 shows a discharge phase surrounded by solar phases. The relationship between the holding speed V_i and the distance travelled is given by

$$J = \int_0^{\alpha_i} v dt + V_i(\beta_i - \alpha_i) + \int_{\beta_i}^{T} v dt$$

with

$$\frac{\partial J}{\partial V_i} = v(\alpha_i)\frac{d\alpha_i}{dV_i} + (\beta_i - \alpha_i) + V_i\left(\frac{d\beta_i}{dV_i} - \frac{d\alpha_i}{dV_i}\right) - v(\beta_i)\frac{d\beta_i}{dV_i}.$$

Since $v(\alpha_i) = v(\beta_i) = V_i$ we have

$$\frac{\partial J}{\partial V_i} = \beta_i - \alpha_i$$

for each interval (α_i, β_i). The relationship between the holding speed V_i and the final battery charge is given by

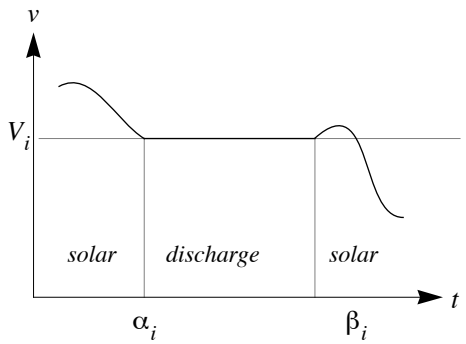

Figure 12-1: A discharge phase between two solar phases.

$$\varepsilon Q(T) = \ldots + \int_{\alpha_i}^{\beta_i} (s(t) - [\varphi(V_i) - V_i G(x(t))])\, dt + \ldots$$

$$= \ldots + \int_{\alpha_i}^{\beta_i} s(t)dt - \varphi(V_i)(\beta_i - a_i) + \int_{x(\alpha_i)}^{x(\beta_i)} G(x)dx + \ldots$$

and hence

$$\frac{\partial}{\partial V_i}[\varepsilon Q(T)] = s(\beta_i)\frac{d\beta_i}{dV_i} - s(\alpha_i)\frac{d\alpha_i}{dV_i}$$

$$- \varphi'(V_i)(\beta_i - \alpha_i) - \varphi(V_i)\left[\frac{d\beta_i}{dV_i} - \frac{d\alpha_i}{dV_i}\right]$$

$$+ \left[G(x(\beta_i))\frac{d}{dV_i}x(\beta_i) - G(x(\alpha_i))\frac{d}{dV_i}x(\alpha_i)\right].$$

But

$$\frac{d\alpha_i}{dV_i} = mV_i[s(\alpha_i) - \varphi(V_i) + V_i G(x(\alpha_i))]^{-1}$$

$$\frac{d\beta_i}{dV_i} = mV_i[s(b_i) - \varphi(V_i) + V_i G(x(\beta_i))]^{-1}$$

$$\frac{d}{dV_i}x(\alpha_i) = \frac{d}{d\alpha_i}x(\alpha_i)\frac{d\alpha_i}{dV_i} = V_i\frac{d\alpha_i}{dV_i}$$

$$\frac{d}{dV_i}x(\beta_i) = \frac{d}{d\beta_i}x(\beta_i)\frac{d\beta_i}{dV_i} = V_i\frac{d\beta_i}{dV_i}$$

which gives

$$\frac{\partial}{\partial V_i}[\varepsilon Q(T)] = -\varphi'(V_i)(\beta_i - \alpha_i)\,.$$

The partial derivative of the Lagrangean function is therefore

$$\frac{\partial L}{\partial V_i} = \frac{\partial J}{\partial V_i} + \lambda\frac{\partial}{\partial V_i}[\varepsilon Q(T)]$$

$$= [1 - \lambda\varphi'(V_i)](\beta_i - \alpha_i)$$

For each charge interval (γ_j, δ_j) a similar argument gives

$$\frac{\partial L}{\partial W_j} = [1 - \lambda\eta_B\varphi'(W_j)]\,(\delta_j - \gamma_j)\,.$$

The Kuhn-Tucker conditions (12.10) give the relationship between the holding speeds:

$$\varphi'(V_i) = \varphi'(W_j) = \frac{1}{\lambda}.$$

Thus there are only two distinct holding speeds, V and W, related by

$$\varphi'(V) = \eta_B\varphi'(W).$$

Discharge–power–discharge transitions

We use a different method to show that a discharge–power–discharge sequence has the same holding speed on each of the discharge intervals.

Suppose we switch from discharge with $\eta = \eta_D$ to power with $\eta > \eta_D$ and back to discharge with $\eta = \eta_D$. Assume that the power phase occurs on a time interval (a, b). During the power phase the Hamiltonian is

$$H = \pi_1 v + \eta\,[P_T - \varphi(v) + vG(x)] - \eta_D\,[P_T - s(t)] \qquad (12.11)$$

with

$$\frac{dH}{dt} = \eta_D s'(t)$$

and hence

$$H = H_a + \eta_D\,[s(t) - s_a]\,.$$

At $t = a$ equation (12.9) gives

$$\pi_1 = \eta_D\,[\varphi'(V_a) - G(x_a)]\,.$$

Substituting this into (12.11) gives

$$H_a - \eta_D s_a = \eta_D V_a^2 R'(V_a). \qquad (12.12)$$

At $t = b$ a similar substitution gives

$$H_b - \eta_D s_b = \eta_D V_b^2 R'(V_b). \qquad (12.13)$$

But $H_b = H_a + \eta_D\,(s_b - s_a)$, and so $H_b - \eta_D s_b = H_a - \eta_D s_a$. Equating the right hand sides of (12.12) and (12.13) gives $V_b = V_a$.

A discharge–power–discharge sequence must therefore start and finish at the same speed. This can only occur if the road incline is so steep that the speed of the car remains constant during the power phase, or if speed both increases and decreases during the power phase.

Charge–regen–charge transitions

Suppose we switch from charge with $\eta = \eta_C$ to regen with $\eta < \eta_C$ and back to charge with $\eta = \eta_C$. The regen phase occurs on the interval (a, b). During the regen phase the Hamiltonian is

$$H = \pi_1 v + \eta\,[-P_R - \varphi(v) + G(x)] + \eta_C\,[s(t) + P_R]$$

with

$$\frac{dH}{dt} = \eta_C s'(t),$$

and hence

$$H = H_a + \eta_C\,[s(t) - s_a]\,.$$

At $t = a$,

$$H_a - \eta_C s_a = \eta_C V_a^2 R'(V_a).$$

At $t = b$,

$$H_a - \eta_C s_a = \eta_C V_b^2 R'(V_b).$$

A charge–regen–charge sequence must also start and finish at the same speed. This can only occur if the road decline is so steep that the speed of the car does not decrease during the regen phase, or if speed both decreases and increases during the regen phase.

12.4 Transitions

Transitions between optimal driving modes depend on the evolution of the adjoint variable η. There are two critical values: $\eta = \eta_D$ and $\eta = \eta_C$.

Transitions at $\eta = \eta_D$

At $\eta = \eta_D$ transitions may occur between any two of the following control modes:

- power with $p = P_T$ and $\eta > \eta_D$;

- discharge V with $p = \varphi(V)$ and $\eta = \eta_D$; and
- solar with $p = s$ and $\eta < \eta_D$.

Let t_0 be the transition time and write $v_0 = v(t_0)$ and $\eta_0 = \eta(t_0)$. Let

$$p_0 = p(t_0) = \lim_{t \to t_0} p(t)$$

and

$$p'_0 = p'(t_0) = \lim_{t \to t_0} p'(t).$$

Because $p(t)$ is not necessarily continuous at $t = t_0$ we again use one-sided limits when required. For t near t_0 the function η can be approximated by a Taylor series:

- if $\varphi'(v_0) - G(x_0) \neq \pi_1(t_0)/\eta_D$ then

$$\frac{\eta}{\eta_D} \approx 1 + \frac{1}{mv_0}\left[\left[\varphi'(v_0) - G(x_0)\right] - \frac{\pi_1(t_0)}{\eta_D}\right](t - t_0) \tag{12.14}$$

- if $\varphi'(v_0) - G(x_0) = \pi_1(t_0)/\eta_D$ and $p_0 \neq \varphi(v_0) - v_0 G(x_0)$ then

$$\frac{\eta}{\eta_D} = 1 + \frac{\varphi''(v_0)}{2}\left[\frac{1}{mv_0}\right]^2 \left[p_0 - \varphi(v_0) + v_0 G(x_0)\right](t - t_0)^2 \tag{12.15}$$

- if $\varphi'(v_0) - G(x_0) = \pi_1(t_0)/\eta_D$ and $p_0 = \varphi(v_0) - v_0 G(x_0)$ then

$$\frac{\eta}{\eta_D} \approx 1 + \frac{\varphi''(v_0)}{6}\left[\frac{1}{mv_0}\right]^2 \left[p'_0 + v_0^2 G'(x_0)\right](t - t_0)^3. \tag{12.16}$$

These three equations can be used to derive conditions for specific transitions at $\eta = \eta_D$.

A transition from power requires $\eta > \eta_D$ for $t < t_0$. There are two possible cases:

- $\varphi'(v_0) - G(x_0) < \pi_1(t_0)/\eta_D$
- $\varphi'(v_0) - G(x_0) = \pi_1(t_0)/\eta_D$ and $P_T > \varphi(v_0) - v_0 G(x_0)$

The condition $P_T > \varphi(v_0) - v_0 G(x_0)$ is satisfied when full power increases the speed of the car. It will not be satisfied on sufficiently steep inclines.

A transition to power requires $\eta > \eta_D$ for $t > t_0$. There are two possible cases:

- $\varphi'(v_0) - G(x_0) > \pi_1(t_0)/\eta_D$

- $\varphi'(v_0) - G(x_0) = \pi_1(t_0)/\eta_D$ and $P_T > \varphi(v_0) - v_0 G(x_0)$

A transition from solar requires $\eta < \eta_D$ for $t < t_0$. There are three possible cases:

- $\varphi'(v_0) - G(x_0) > \pi_1(t_0)/\eta_D$
- $\varphi'(v_0) - G(x_0) = \pi_1(t_0)/\eta_D$ and $s_0 < \varphi(v_0) - v_0 G(x_0)$
- $\varphi'(v_0) - G(x_0) = \pi_1(t_0)/\eta_D$ and $s_0 = \varphi(v_0) - v_0 G(x_0)$ and $s'_0 > v_0^2 G'(x_0)$

A transition to solar requires $\eta < \eta_D$ for $t > t_0$. There are three possible cases:

- $\varphi'(v_0) - G(x_0) < \pi_1(t_0)/\eta_D$
- $\varphi'(v_0) - G(x_0) = \pi_1(t_0)/\eta_D$ and $s_0 < \varphi(v_0) - v_0 G(x_0)$
- $\varphi'(v_0) - G(x_0) = \pi_1(t_0)/\eta_D$ and $s_0 = \varphi(v_0) - v_0 G(x_0)$ and $s'_0 < v_0^2 G'(x_0)$

A transition to or from discharge requires $v_0 = V$.

Transitions at $\eta = \eta_C$

When $\eta = \eta_C$ transitions may occur between the following control modes:

- solar with $p = s$ and $\eta > \eta_C$
- charge W with $p = \varphi(W)$ and $\eta = \eta_C$; and
- regen with $p = -P_R$ and $\eta < \eta_C$.

The analysis of transitions is similar to that at $\eta = \eta_D$. For t near the transition time t_0, the Taylor series approximation to η is:

- if $\varphi'(v_0) - G(x_0) \neq \pi_1(t_0)/\eta_C$ then

$$\frac{\eta}{\eta_C} \approx 1 + \frac{1}{mv_0}\left[\left[\varphi'(v_0) - G(x_0)\right] - \frac{\pi_1(t_0)}{\eta_C}\right](t - t_0) \tag{12.17}$$

- if $\varphi'(v_0) - G(x_0) = \pi_1(t_0)/\eta_C$ and $p_0 \neq \varphi(v_0) - v_0 G(x_0)$ then

$$\frac{\eta}{\eta_C} = 1 + \frac{\varphi''(v_0)}{2}\left[\frac{1}{mv_0}\right]^2 \left[p - \varphi(v_0) + v_0 G(x_0)\right](t - t_0)^2 \tag{12.18}$$

- if $\varphi'(v_0) - G(x_0) = \pi_1(t_0)/\eta_C$ and $p_0 = \varphi(v_0) - v_0 G(x_0)$ then

$$\frac{\eta}{\eta_C} \approx 1 + \frac{\varphi''(v_0)}{6}\left[\frac{1}{mv_0}\right]^2 [p'_0 + v_0^2 G'(x_0)]\,(t - t_0)^3. \qquad (12.19)$$

A transition from solar requires $\eta > \eta_C$ for $t < t_0$. There are three possible cases:

- $\varphi'(v_0) - G(x_0) < \pi_1(t_0)/\eta_D$
- $\varphi'(v_0) - G(x_0) = \pi_1(t_0)/\eta_D$ and $s_0 > \varphi(v_0) - v_0 G(x_0)$
- $\varphi'(v_0) - G(x_0) = \pi_1(t_0)/\eta_D$ and $s_0 = \varphi(v_0) - v_0 G(x_0)$ and $s'_0 < v_0^2 G'(x_0)$

A transition to solar requires $\eta > \eta_C$ for $t > t_0$. There are three possible cases:

- $\varphi'(v_0) - G(x_0) > \pi_1(t_0)/\eta_D$
- $\varphi'(v_0) - G(x_0) = \pi_1(t_0)/\eta_D$ and $s_0 > \varphi(v_0) - v_0 G(x_0)$
- $\varphi'(v_0) - G(x_0) = \pi_1(t_0)/\eta_D$ and $s_0 = \varphi(v_0) - v_0 G(x_0)$ and $s'_0 > v_0^2 G'(x_0)$

A transition from regen requires $\eta < \eta_C$ for $t < t_0$. There are two possible cases:

- $\varphi'(v_0) - G(x_0) > \pi_1(t_0)/\eta_C$
- $\varphi'(v_0) - G(x_0) = \pi_1(t_0)/\eta_D$ and $-P_R < \varphi(v_0) - v_0 G(x_0)$

The condition $-P_R < \varphi(v_0) - v_0 G(x_0)$ is satisfied when full regenerative braking decreases the speed of the car. It will not be satisfied on sufficiently steep declines.

A transition to regen requires $\eta < \eta_C$ for $t > t_0$. There are two possible cases:

- $\varphi'(v_0) - G(x_0) < \pi_1(t_0)/\eta_D$
- $\varphi'(v_0) - G(x_0) = \pi_1(t_0)/\eta_D$ and $-P_R < \varphi(v_0) - v_0 G(x_0)$

A transition to or from charge requires $v_0 = W$.

The possible transitions are summarised in Figure 12-2.

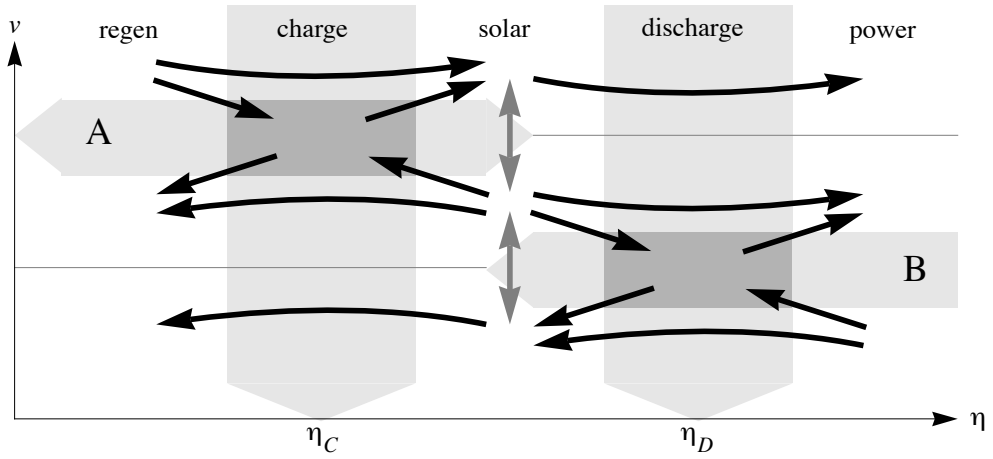

Figure 12-2: Possible control transitions in an optimal strategy. The shaded region A corresponds to speeds v_0 satisfying $\varphi'(v_0) - G(x_0) = \pi_1(t_0)/\eta_C$. The shaded region B corresponds to speeds satisfying $\varphi'(v_0) - G(x_0) = \pi_1(t_0)/\eta_D$. Compare this diagram to Figure 11-2.

12.5 Construction of an optimal strategy

Perfectly efficient battery

If the battery is perfectly efficient then the discharge speed V and the charge speed W are equal, and there is a single holding speed for the journey. The solar mode, used between discharge and charge, is no longer required, and an optimal journey has only three driving modes: power, hold and regen.

To construct an optimal control sequence we need to distinguish between steep and non-steep gradients. An incline is steep at speed v if maximum power is not sufficient to maintain speed v on the incline. Similarly, a decline is steep at speed v if maximum regenerative braking is not sufficient to maintain speed v on the decline.

If the road has no steep gradients for the range of speeds required for a particular journey then the speed of the car will always increase during a power phase and decrease during a regen phase. The only possible strategy for a journey starting and finishing at rest and satisfying the transition conditions is power–hold–regen.

As the journey hold speed increases, the time required to complete the journey and the energy left in the battery both decrease. The optimal hold speed will leave no energy in the battery at the end of the journey. The optimal journey can be found using a numerical differential equation solver to calculate a power–hold–regen journey (x, v, Q, p) for any given hold speed V. A numerical root finder can then be used to find the hold speed V^* that finishes with the final battery charge $Q(X) = 0$.

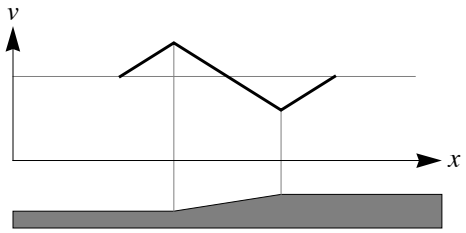

Figure 12-3: Power phase for a steep incline. The speed of the car increases until the base of the incline, decreases while on the incline, then increases back to the holding speed.

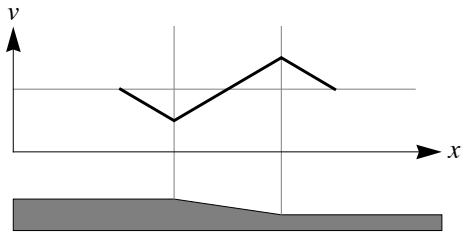

Figure 12-3: Regen phase for a steep decline. The speed of the car decreases until the base of the decline, increases while on the incline, then decreases back to the holding speed.

On a steep incline, full power is not sufficient to maintain the hold speed V. Previous work on train control has shown that the optimal strategy is to change control from hold to power before the incline, as shown in Figure 12-3. A similar strategy applies to steep declines; the control should be changed to regen before the decline, as shown in Figure 12-3. The switching calculations required for steep gradients are described in the book on energy-efficient train control by Howlett & Pudney (1995).

Inefficient battery

If the battery has efficiency $\eta_B < 1$ then the optimal strategy has five control modes and two possible hold speeds, and so the conditions for switching are more complex. Rather than continue analysing this model, we will move forward in the next chapter using more realistic battery models.

12.6 Summary

On a level road, the strategy for a car with a simple inefficient battery uses two holding speeds. The lower of the two speeds is used when the battery is being discharged; the upper speed is used when the battery is being charged.

Gradients do not effect the form of this solution, but they can disrupt the typical power–discharge–solar–charge–solar–discharge–regen sequence. Furthermore, the conditions for changing from one mode to the next are complex.

13 Realistic battery models

In previous chapters we have assumed that the battery has constant energy efficiency, and shown that an optimal driving strategy uses one speed while the battery is discharging and a slightly higher speed while the battery is charging to balance resistance losses against energy losses in the battery.

In this chapter we consider more realistic battery models. The necessary conditions for an optimal driving strategy no longer have simple solutions. However, we can show that the speed of the car must stay close to a critical speed that varies continuously with solar power, but still within a narrow speed range.

13.1 Problem formulation for an ohmic battery

Figure 13-1 shows a discharge polarisation curve for a typical battery. In the centre, unshaded, region the polarisation is primarily ohmic, as described in Chapter 5. If the battery is operated in this region then battery voltage can be approximated by the linear function

$$V = \varepsilon_D - IR_D \qquad I \geq 0$$

where ε_D is a discharge emf and R_D is the internal resistance of the battery while discharging. If current is restricted to the region of ohmic polarisation then $V > 0$.

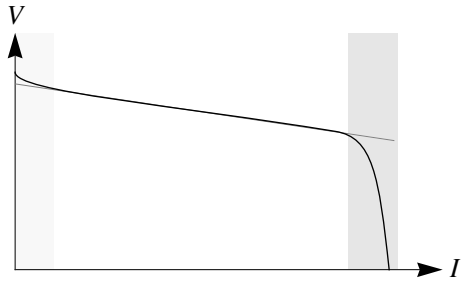

Figure 13-1: A typical discharge polarisation curve. In the first shaded region the polarisation is primarily activation polarisation. In the second (unshaded) region the polarisation is primarily ohmic. In the final region reactant transport rates cause additional polarisation.

If we use a similar model when the battery is being charged we have

$$V = \begin{cases} \varepsilon_D - IR_D & I \geq 0 \\ \varepsilon_C - IR_C & I < 0 \end{cases}$$

where $e_C \geq e_D$ is the voltage offset while charging and R_C is the internal resistance of the battery while charging.

The power from or to the battery is

$$b(I) = \begin{cases} [\varepsilon_D - IR_D]I & I \geq 0 \\ [\varepsilon_C - IR_C]I & I < 0 \end{cases}.$$

Rearranging this equation gives

$$I(b) = \begin{cases} \dfrac{1}{2R_D}\left[\varepsilon_D - \sqrt{\varepsilon_D^2 - 4R_D b}\right] & b \geq 0 \\ \dfrac{1}{2R_C}\left[\varepsilon_C - \sqrt{\varepsilon_C^2 - 4R_C b}\right] & b < 0 \end{cases}.$$

If the car has a single battery with these characteristics then the solar car problem has state equations

$$\frac{dx}{dt} = v, \tag{13.1}$$

$$\frac{dv}{dt} = \frac{1}{m}\left[\frac{p}{v} - R(v)\right], \tag{13.2}$$

and

$$\frac{dQ}{dt} = -I(b) \tag{13.3}$$

where $p(t) = s(t) + b(t)$. These are the same equations as in previous chapters; only the expression for $I(b)$ has changed.

We wish to minimise the time taken for the journey. As with the previous models, the Hamiltonian for the problem can be normalised to give

$$H(t, \xi, u, \pi, 0) = v + \frac{\pi_2}{m}\left[\frac{p}{v} - R(v)\right] - CI(b)$$

with the normalised adjoint equation

$$\frac{d\pi_2}{dt} = \frac{\pi_2}{m}\left[\frac{p}{v^2} + R'(v)\right] - 1 . \tag{13.4}$$

If we once again let

$$\eta = \frac{\pi_2}{mv}$$

and

$$\varphi(v) = vR(v)$$

then the Hamiltonian can be written as

$$H = v + \eta\,[p - \varphi(v)] - CI(b)$$

with the adjoint equation

$$\frac{d\eta}{dt} = \frac{1}{mv}\,[\eta\varphi'(v) - 1] . \tag{13.5}$$

13.2 Necessary conditions for an optimal strategy

The optimal control maximises the Hamiltonian. Grouping the terms depending on the control, and substituting $p = s + b$, the Hamiltonian can be written as

$$H = \begin{cases} \eta b + \dfrac{C}{2R_D}\sqrt{\varepsilon_D^2 - 4R_D b} + \ldots & b \geq 0 \\ \eta b + \dfrac{C}{2R_C}\sqrt{\varepsilon_C^2 - 4R_C b} + \ldots & b < 0 \end{cases}$$

The control b^* required to maximise the Hamiltonian depends on the value of the adjoint variable η. The Hamiltonian is maximised when

$$\frac{\partial H}{\partial b} = \begin{cases} \eta - \dfrac{C}{\sqrt{\varepsilon_D^2 - 4R_D b}} & b \geq 0 \\ \eta - \dfrac{C}{\sqrt{\varepsilon_C^2 - 4R_C b}} & b < 0 \end{cases} = 0 .$$

Solving for b^* gives three optimal driving modes:

discharge $\eta > \eta_D$

$$\Rightarrow \quad b^* = \frac{1}{4R_D}\left[\varepsilon_D^2 - \left(\frac{C}{\eta}\right)^2\right] > 0$$

solar $\eta \in [\eta_C, \eta_D] \quad \Rightarrow \quad b^* = 0$

charge $\eta < \eta_C$

$$\Rightarrow \quad b^* = \frac{1}{4R_C}\left[\varepsilon_C^2 - \left(\frac{C}{\eta}\right)^2\right] < 0$$

where the critical values of η are $\eta_D = C/\varepsilon_D$ and $\eta_C = C/\varepsilon_C$. These critical values are similar to the values obtained using the simpler battery model; that is, we have $\eta_C = \eta_B \eta_D$ for some $0 < \eta_B < 1$.

The optimal control b^* varies continuously with η, as shown in Figure 13-2. The Hamiltonian corresponding to various values of η is illustrated in Figure 13-3.

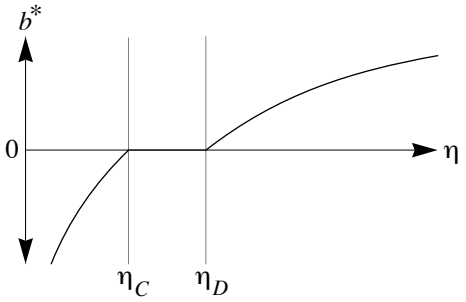

Figure 13-2: The optimal battery power b^* increases with η.

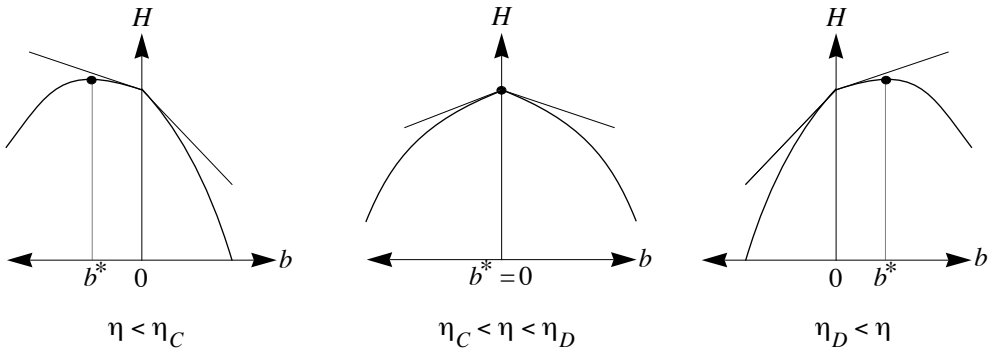

Figure 13-3: Maximising the Hamiltonian for various values of η.

13.3 Construction of an optimal journey

An optimal journey can be found by substituting the optimal control into the state and adjoint equations. The resulting system is

$$\frac{dx}{dt} = v$$

$$\frac{dv}{dt} = \begin{cases} \frac{1}{mv}\left[s + \frac{1}{4R_D}\left[\varepsilon_D^2 - \left(\frac{C}{\eta}\right)^2 \right] - \varphi(v) \right] & \eta_D < \eta \\ \frac{1}{mv}\left[s - \varphi(v) \right] & \eta_C \le \eta \le \eta_D \\ \frac{1}{mv}\left[s + \frac{1}{4R_C}\left[\varepsilon_C^2 - \left(\frac{C}{\eta}\right)^2 \right] - \varphi(v) \right] & \eta < \eta_C \end{cases}$$

$$\frac{dQ}{dt} = \begin{cases} -\frac{1}{2R_D}\left[\varepsilon_D - \frac{C}{\eta} \right] & \eta_D < \eta \\ 0 & \eta_C \le \eta \le \eta_D \\ -\frac{1}{2R_C}\left[\varepsilon_C - \frac{C}{\eta} \right] & \eta < \eta_C \end{cases}$$

$$\frac{d\eta}{dt} = \frac{1}{mv}\left[\eta\varphi'(v) - 1 \right]$$

with boundary conditions $x(0) = 0$, $x(T) = X$ and $v(0) = v(T) = 0$. The value of the constant C can be adjusted to satisfy the final charge constraint. For any given value of C this system defines a two-point boundary value problem, but one that is difficult to solve in practice, particularly for journeys that last many hours. Instead, we can find a practical strategy by examining the phase portrait of the differential equations that determine the optimal strategy.

The optimal control can be rewritten in terms of speed v and the adjoint variable π_2 as

$$b^*(v, \pi_2) = \begin{cases} \frac{1}{4R_D}\left[\varepsilon_D^2 - \left(\frac{mvC}{\pi_2}\right)^2 \right] & \eta_D < \frac{\pi_2}{mv} \\ 0 & \eta_C \le \frac{\pi_2}{mv} \le \eta_D \\ \frac{1}{4R_C}\left[\varepsilon_C^2 - \left(\frac{mvC}{\pi_2}\right)^2 \right] & \frac{\pi_2}{mv} < \eta_C \end{cases}.$$

Substituting the control b^* into the state equation (13.3) and adjoint equation (13.4) gives the system of equations

$$\begin{aligned} \frac{dv}{dt} &= f(v, \pi_2) \\ \frac{d\pi_2}{dt} &= g(v, \pi_2) \end{aligned} \tag{13.6}$$

where

$$\begin{aligned} f(v, \pi_2) &= \frac{1}{mv}\left[s + b^*(v, \pi_2) - \varphi(v)\right] \\ g(v, \pi_2) &= \frac{\pi_2}{mv^2}\left[s + b^*(v, \pi_2) + v^2 R'(v)\right] - 1\,. \end{aligned}$$

Using the adjoint variable π_2 instead of η gives us an *exact* system (Plaat 1971), which simplifies the process of constructing a phase portrait for the system. To show that (13.6) is exact we must show that

$$\frac{\partial f}{\partial v} + \frac{\partial g}{\partial \pi_2} = 0\,.$$

The partial derivatives are

$$\begin{aligned} \frac{\partial f}{\partial v} &= -\frac{1}{mv^2}\left[s + b^*(v, \pi_2) - \varphi(v)\right] + \frac{1}{mv}\left[\frac{\partial}{\partial v} b^*(v, \pi_2) - \varphi'(v)\right] \\ \frac{\partial g}{\partial \pi_2} &= \frac{1}{mv^2}\left[s + b^*(v, \pi_2) + v^2 R'(v)\right] + \frac{\pi_2}{mv^2}\frac{\partial}{\partial \pi_2} b^*(v, \pi_2)\,. \end{aligned}$$

Straightforward algebra gives

$$\frac{\partial f}{\partial v} + \frac{\partial g}{\partial \pi_2} = \frac{1}{mv^2}\left[v\frac{\partial}{\partial v} b^* + \pi_2 \frac{\partial}{\partial \pi_2} b^*\right].$$

The partial derivatives of b^* are

$$\frac{\partial}{\partial v} b^* = \begin{cases} -\dfrac{1}{2R_C}\left(\dfrac{mC}{\pi_2}\right)^2 v & \eta_D < \dfrac{\pi_2}{mv} \\ 0 & \eta_C \le \dfrac{\pi_2}{mv} \le \eta_D \\ -\dfrac{1}{2R_D}\left(\dfrac{mC}{\pi_2}\right)^2 v & \dfrac{\pi_2}{mv} < \eta_C \end{cases}$$

and

$$\frac{\partial}{\partial \pi_2} b^* = \begin{cases} \dfrac{(mvC)^2}{2R_C}\dfrac{1}{\pi_2^3} & \eta_D < \dfrac{\pi_2}{mv} \\ 0 & \eta_C \le \dfrac{\pi_2}{mv} \le \eta_D, \\ \dfrac{(mvC)^2}{2R_D}\dfrac{1}{\pi_2^3} & \dfrac{\pi_2}{mv} < \eta_C \end{cases}$$

and so

$$\frac{\partial f}{\partial v} + \frac{\partial g}{\partial \pi_2} = 0$$

and (13.6) is exact. Furthermore, the Hamiltonian H is such that

$$f = \frac{\partial H}{\partial \pi_2}$$

and

$$g = -\frac{\partial H}{\partial v}$$

and so H is an integral of the system and the level curves of H are trajectories of the system (Plaat 1971).

The level curves of the Hamiltonian H can be used to construct a phase portrait of the system. Critical points $(v^*, \pi_2{}^*)$ have

$$\frac{d}{dt} v^* = \frac{d}{dt} \pi_2{}^* = 0,$$

which give

$$s + b^* = \varphi(v^*)$$

and

$$\frac{\pi_2{}^*}{mv^*} = \frac{1}{\varphi'(v^*)}.$$

At a critical point $(v^*, \pi_2{}^*)$ we have

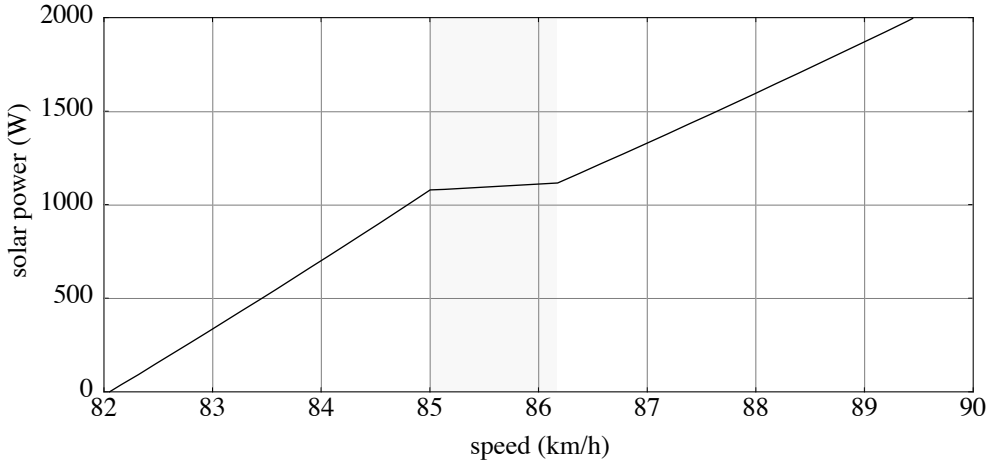

Figure 13-4: The solar power required to give a critical speed v^* is a strictly increasing function. The shaded region is between the highest discharge speed and the lowest charge speed, and has $b^*(v^*) = 0$.

$$b^*(v^*) = \begin{cases} \dfrac{1}{4R_D}\left[\varepsilon_D^2 - (C\varphi'(v^*))^2\right] & C\varphi'(v^*) < \varepsilon_D \\ 0 & \varepsilon_D \le C\varphi'(v^*) \le \varepsilon_C. \\ \dfrac{1}{4R_C}\left[\varepsilon_C^2 - (C\varphi'(v^*))^2\right] & \varepsilon_C < C\varphi'(v^*) \end{cases}$$

This function is decreasing, and so the equation $s + b^*(v^*) = \varphi(v^*)$ has a unique solution for each value of solar power s.

The critical speed v^* varies with solar power. The speed v_D satisfying

$$C\varphi'(v_D) = \varepsilon_D \tag{13.7}$$

is the highest critical speed with $b^* \ge 0$. Similarly, the speed v_C satisfying

$$C\varphi'(v_C) = \varepsilon_C$$

is the lowest critical speed with $b^* \le 0$.

The solar power s required to give a critical speed v^* is given by

$$s(v^*) = \varphi'(v^*) - b^*(v^*)$$

and, as shown in Figure 13-4, is a strictly increasing function. In this example the battery parameters are $\varepsilon_D = 1.63n$, $R_D = 0.00650n$, $\varepsilon_C = 1.67n$ and $R_C = 0.0106n$, where $n = 83$ is the number of cells. The parameters are from a least-squares fit to measurements taken from a silver-zinc battery. The rest of the car parameters are those

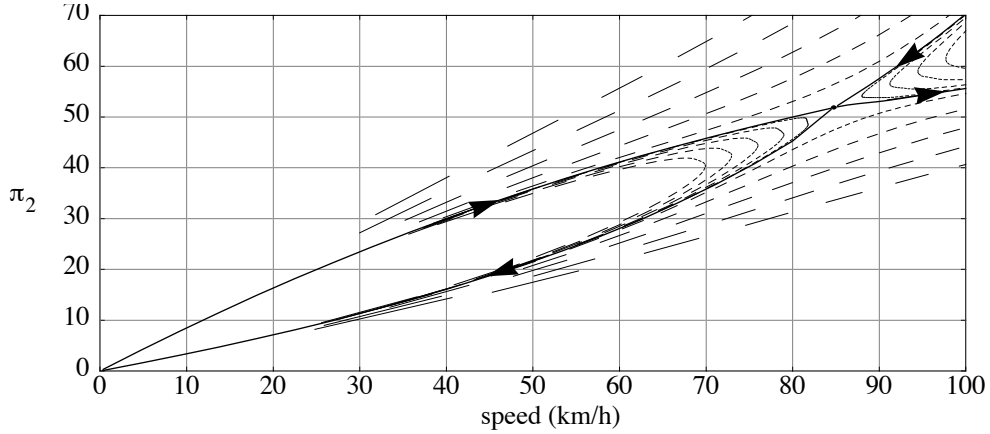

Figure 13-5: For each value of solar power the vector field (v, π_2) *has a unique saddle point* (v^*, π_2^*)*. Points surrounding the saddle point quickly evolve to either large* v *or to* $v = 0$*; the line segments on the* (v, π_2) *trajectories indicate one-second time steps.*

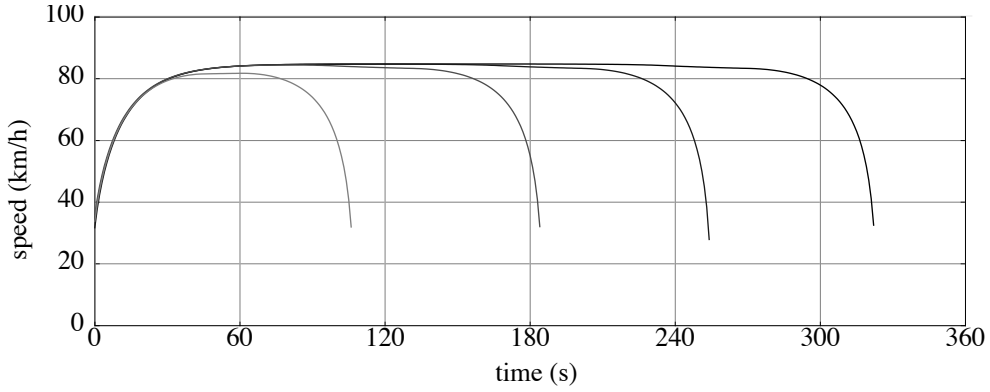

Figure 13-6: Optimal speed profiles passing through the point $(v, \pi_2) = (v^* - \delta, \pi_2^* - 2\delta)$ *for* $\delta \in \{1, 0.1, 0.01, 0.001\}$*. Any journey lasting more than a few minutes must travel at a speed very close to the critical speed* v^* *for most of the journey. (The graphs do not extend to* $v = 0$ *because the simple method I used to calculate the trajectories did not handle the singularity.)*

given in Table 11-3. The highest discharge speed v_D for the example has been set to 85km/h and the constant C calculated using equation (13.7). Because s is a strictly increasing function of v^* there is a unique critical speed v^* for any given solar power s.

For a given solar power s the critical point (v^*, π_2^*) is a saddle point. Surrounding points quickly evolve to either large v or to $v = 0$. Examples of (v, π_2) trajectories when $s = 1000$ are shown in Figure 13-5. For a journey to last more than a few minutes the trajectory must pass very close to the critical point, and the speed of the car must be very close to the critical speed v^* for most of the journey. Figure 13-6 shows some example speed profiles.

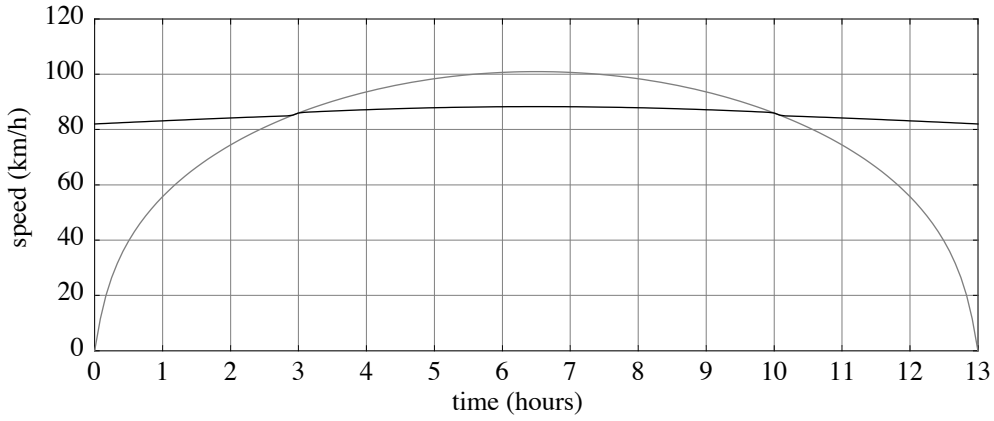

Figure 13-7: Critical speed v^* for a sunrise to sunset journey. The grey curve starting and finishing at $v = 0$ is $\varphi^{-1}(s)$, the speed the car would travel using solar power alone.

When solar power is not constant the critical speed v^* will change with s, as shown in Figure 13-4. Any long journey must travel at a speed close to v^*. Figure 13-7 shows a journey at speed v^* that starts at sunrise and finishes at sunset. The grey curve $\varphi^{-1}(s)$, which starts and finishes at $v = 0$, is the speed the car would travel if the battery was not used. The area between the two curves is the net energy applied to the battery during the journey; it is clearly negative, so this journey will result in a net drop in battery charge. The speed of the journey can be adjusted to satisfy the final charge constraint by adjusting the value of the constant C.

13.4 Two ohmic batteries

If the car has two ohmic batteries then the problem has state equations

$$\frac{dx}{dt} = v, \tag{13.8}$$

$$\frac{dv}{dt} = \frac{1}{m}\left[\frac{p}{v} - R(v)\right], \tag{13.9}$$

$$\frac{dQ_1}{dt} = I_1(b_1) \tag{13.10}$$

and

$$\frac{dQ_2}{dt} = I_2(b_2) \tag{13.11}$$

where $p(t) = s(t) + b_1(t) + b_2(t)$ and where the current corresponding to battery power p_i is

$$I_i(b_i) = \begin{cases} \dfrac{1}{2R_{iD}}\left[e_{iD} - \sqrt{e_{iD}^2 - 4R_{iD}b_i}\right] & b_i \geq 0 \\ \dfrac{1}{2R_{iC}}\left[e_{iC} - \sqrt{e_{iC}^2 - 4R_{iC}b_i}\right] & b_i < 0 \end{cases}.$$

The Hamiltonian for this system is

$$H(t, \xi, u, \pi, 0) = v + \eta\,[p - \varphi(v)] - C_1 I_1(b_1) - C_2 I_2(b_2)$$

with the adjoint equation

$$\frac{d\eta}{dt} = \frac{1}{mv}\,[\eta\varphi'(v) - 1]\,.$$

Grouping the terms depending on the control, the Hamiltonian can be written as

$$H = H_1(b_1) + H_2(b_2) + \ldots$$

where

$$H_i(b_i) = \begin{cases} \eta b_i + \dfrac{C_i}{2R_{iD}}\sqrt{\varepsilon_{iD}^2 - 4R_{iD}b_i} & b_i \geq 0 \\ \eta b_i + \dfrac{C_i}{2R_{iC}}\sqrt{\varepsilon_{iC}^2 - 4R_{iC}b_i} & b_i < 0 \end{cases}$$

The Hamiltonian is maximised when

$$\frac{\partial H}{\partial p_i} = \begin{cases} \eta - \dfrac{C_i}{\sqrt{\varepsilon_{iD}^2 - 4R_{iD}b_i}} & b_i \geq 0 \\ \eta - \dfrac{C_i}{\sqrt{\varepsilon_{iC}^2 - 4R_{iC}b_i}} & b_i < 0 \end{cases} = 0$$

Solving for b_i gives three optimal modes for each battery:

discharge $\quad \eta > \eta_{iD}$

$$\Rightarrow \quad b_i = \frac{1}{4R_{iD}}\left[\varepsilon_{iD}^2 - \left(\frac{C_i}{\eta}\right)^2\right] > 0$$

off $\quad \eta \in [\eta_{iC}, \eta_{iD}] \quad \Rightarrow \quad b_i = 0$

charge $\eta < \eta_{iC}$

$$\Rightarrow \quad b_i = \frac{1}{4R_{iC}}\left[\varepsilon_{iC}^2 - \left(\frac{C_i}{\eta}\right)^2\right] < 0$$

where the critical values of η are $\eta_{iD} = C_i/e_{iD}$ and $\eta_{iC} = C_i/e_{iC}$.

As with the single ohmic battery, we can write the optimal controls in terms v and π_2 as

$$b_i^* = \begin{cases} \dfrac{1}{4R_{iD}}\left[\varepsilon_{iD}^2 - \left(\dfrac{C_i mv}{\pi_2}\right)^2\right] & \dfrac{C_i mv}{\varepsilon_{iD}} < \pi_2 \\ 0 & \dfrac{C_i mv}{\varepsilon_{iC}} \le \pi_2 \le \dfrac{C_i mv}{\varepsilon_{iD}} \\ \dfrac{1}{4R_C}\left[\varepsilon_{iC}^2 - \left(\dfrac{C_i mv}{\pi_2}\right)^2\right] & \pi_2 < \dfrac{C_i mv}{\varepsilon_{iC}} \end{cases}.$$

Substituting the optimal control into the state equations gives

$$\frac{dv}{dt} = \frac{1}{mv}\left[s + b_1^* + b_2^* - \varphi(v)\right] \tag{13.12}$$

and

$$\frac{d\pi_2}{dt} = \frac{1}{mv^2}\left[s + b_1^* + b_2^* + v^2 R'(v)\right]. \tag{13.13}$$

Critical points (v^*, π_2^*) with

$$\frac{d}{dt}v^* = \frac{d}{dt}\pi_2^* = 0$$

must therefore satisfy

$$s + b_1^* + b_2^* = \varphi(v)$$

and, substituting this into (13.3),

$$\frac{\pi_2}{mv} = \frac{1}{\varphi'(v)}.$$

At a critical point (v^*, π_2^*) the optimal control is

$$b_i^*(v^*) = \begin{cases} \dfrac{1}{4R_{iD}}\left[\varepsilon_{iD}^2 - (C_i\varphi'(v^*))^2\right] & C_i\varphi'(v^*) < \varepsilon_{iD} \\ 0 & \varepsilon_{iD} \le C_i\varphi'(v^*) \le \varepsilon_{iC}. \\ \dfrac{1}{4R_C}\left[\varepsilon_{iC}^2 - (C_i\varphi'(v^*))^2\right] & \varepsilon_{iC} < C_i\varphi'(v^*) \end{cases}$$

As with the single ohmic battery, these functions b_i^* are decreasing, and so there is a unique solution v^* to the equation

$$s + b_1^*(v^*) + b_2^*(v^*) = \varphi(v^*)$$

for each value of solar power s. Once again, points surrounding the critical point quickly evolve to have either large v or else $v = 0$. Any journey lasting more than a few minutes must have the speed of the car very close to the critical speed v^*, which varies with solar power s. In practice, following the critical speed will give a journey that is close to optimal.

For a car with a single battery, the value of the single parameter C determines the optimal speed curve and the final battery charge. To find an optimal journey we must find the value of C that empties the battery as the car crosses the finish line. For the car with two batteries there are two parameters, C_1 and C_2, that determine the optimal speed profile and the charge profile for each battery. These two parameters independently control the two battery power profiles. To find an optimal strategy we must find values for C_1 and C_2 that empty each battery just as the car crosses the finish line.

13.5 Silver-zinc battery

We now consider the silver-zinc battery model developed in Chapter 5. The main features of this model are:

- current I depends on power but not on charge, and
- I' is positive and strictly increasing over the range of possible battery powers.

A typical current graph is shown in Figure 13-8. For the silver-zinc batteries used by Aurora in the 1996 and 1999 World Solar Challenges we approximated this curve by a quadratic

$$I(b) = b\left[c_1 + c_2 b\right]$$

where c_1 and c_2 are constants. To take into account the capacity efficiency of the battery we modified the model to

$$I(b) = \begin{cases} b\left[c_1 + c_2 b\right] & b \geq 0 \\ \eta_B b\left[c_1 + c_2 b\right] & b < 0 \end{cases}$$

where η_B is the capacity efficiency of the battery. The battery used in the Aurora car had $c_1 = 7.61 \times 10^{-3}$, $c_2 = 5.06 \times 10^{-7}$ and $\eta_B = 0.97$.

The normalised Hamiltonian and adjoint equation for a car with a single such battery are

$$H = v + \frac{\pi_2}{m}\left[\frac{p}{v} - R(v)\right] - CI(b)$$

and

$$\frac{d\pi_2}{dt} = \frac{\pi_2}{m}\left[\frac{p}{v^2} + R'(v)\right] - 1.$$

To find the necessary conditions for an optimal strategy we will once again define

$$\eta = \frac{\pi_2}{mv}$$

to give

$$H = v + \eta\left[p - \varphi(v)\right] - CI(b).$$

Grouping the terms depending on the control b gives

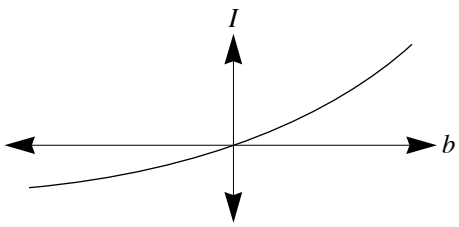

Figure 13-8: A typical current graph.

$$H = \begin{cases} \eta b - Cb[c_1 + c_2 b] & b \geq 0 \\ \eta b - \eta_B Cb[c_1 + c_2 b] & b < 0 \end{cases}$$

which is maximised when

$$\frac{\partial H}{\partial b} = \begin{cases} \eta - C[c_1 + 2c_2 b] & b \geq 0 \\ \eta - \eta_B C[c_1 + 2c_2 b] & b < 0 \end{cases} = 0.$$

The Hamiltonian is similar to that shown in Figure 13-3. Solving for b^* gives the usual three control modes:

discharge $\quad \eta > Cc_1 \Rightarrow b^* = \dfrac{\eta - Cc_1}{2Cc_2} > 0$

solar $\quad \eta \in [\eta_B Cc_1, Cc_1] \Rightarrow b^* = 0$

charge $\quad \eta < \eta_B Cc_1 \Rightarrow b^* = \dfrac{\eta - \eta_B Cc_1}{2\eta_B Cc_2} < 0$

The optimal control is therefore

$$b^* = \begin{cases} \dfrac{\eta - \eta_D}{2Cc_2} & \eta_D < \eta \\ 0 & \eta_C \leq \eta \leq \eta_D \\ \dfrac{\eta - \eta_C}{2\eta_B Cc_2} & \eta < \eta_C \end{cases}$$

where $\eta_D = Cc_1$ and $\eta_C = \eta_B Cc_1$.

As with the ohmic models used earlier in this chapter, the system

$$\frac{dv}{dt} = \frac{1}{mv}[s + b^* - \varphi(v)]$$
$$\frac{d\pi_2}{dt} = \frac{1}{mv^2}[s + b^* + v^2 R'(v)] - 1$$

is exact and the level curves of the Hamiltonian are trajectories of the system. At critical points $(v^*, \pi_2{}^*)$ we once again have

$$s + b^* = \varphi(v^*)$$

and

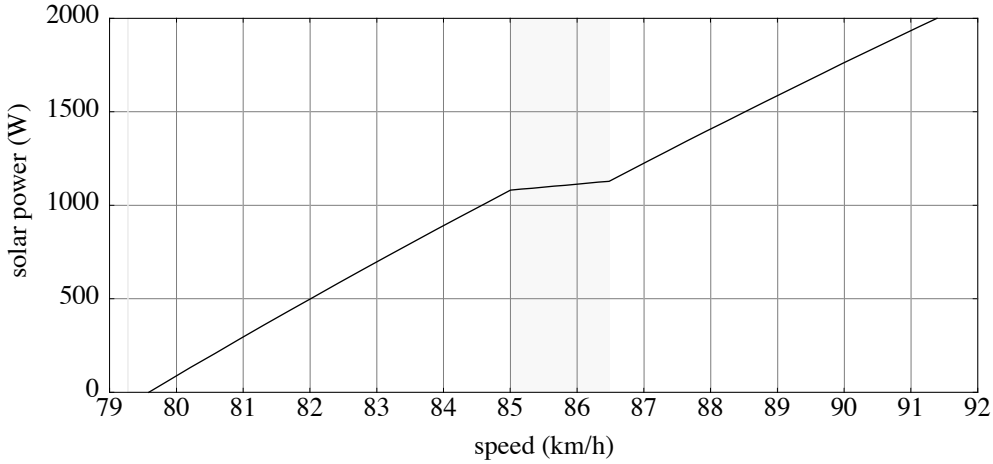

Figure 13-9: The solar power required to give a critical speed v^* is a strictly increasing function. The shaded region has control $b^* = 0$. During a typical day solar power will vary between 0W and 1500W; the corresponding critical speed will vary by less than 10km/h.

$$\frac{\pi_2^*}{mv^*} = \frac{1}{\varphi'(v^*)}$$

and so

$$b^*(v^*) = \begin{cases} \dfrac{1 - Cc_1\varphi'(v^*)}{2Cc_2} & Cc_1 < \dfrac{1}{\varphi'(v^*)} \\ 0 & \eta_B Cc_1 \le \dfrac{1}{\varphi'(v^*)} \le Cc_1. \\ \dfrac{1 - \eta_B Cc_1\varphi'(v^*)}{2Cc_2} & \dfrac{1}{\varphi'(v^*)} < \eta_B Cc_1 \end{cases}$$

The solar power required to travel at a critical speed v^* is shown in Figure 13-9. The phase portrait is similar to that shown in Figure 13-5. As with the ohmic battery, optimal trajectories must stay very close to the critical point for any journey lasting more than a few minutes.

Figure 13-10 shows some sample journeys. Solar power is constant with $s = 1000$. The strategy is discharge–solar–charge. The critical speed v^* is 84.57km/h. To stay near this speed requires 1067W, so the section of the journey with v near v^* occurs during a long discharge phase.

Figure 13-11 shows phase diagram separatrices for $s \in \{400, 1200, 2000\}$. The battery capacity efficiency has been reduced to $\eta_B = 0.8$ so that the solar phase, indicated by the shaded region, can be seen clearly. Typically, the capacity efficiency of a battery will be better than 0.97.

On a long journey the car will spend almost all of its time near the critical point. On a typical day solar power will increase during the morning and decrease during the afternoon. When solar power is low the critical speed v^* will be in the discharge region of the phase plane. As solar power increases the critical speed will move through the solar region into the charge region. During the afternoon, as solar power drops, the critical speed will drop back through the solar region into the discharge region.

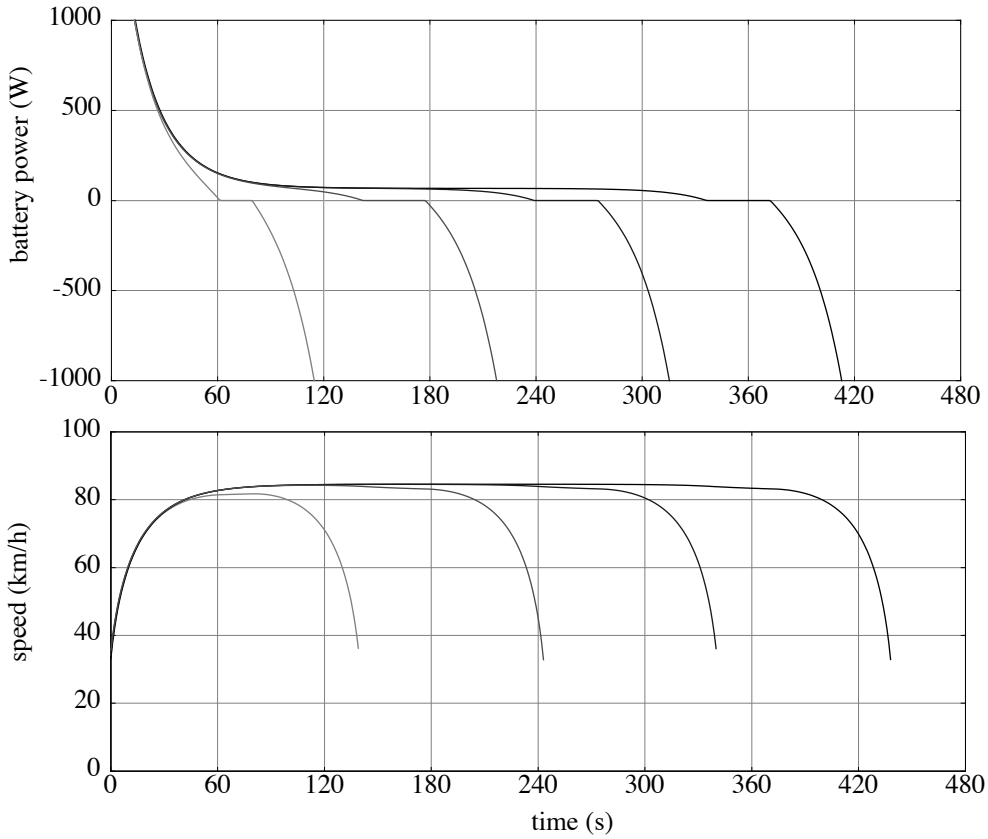

Figure 13-10: Optimal speed profiles passing through the point $(v, \pi_2) = (v^* - \delta, \pi_2 - 2\delta)$ *for* $\delta \in \{1, 0.1, 0.01, 0.001\}$. *Solar power is* $s = 1000$. *The upper graph shows a portion of the optimal control. As with the ohmic battery model, any journey lasting more than a few minutes must travel at speeds close to the critical speed* v^* *for most of the journey.*

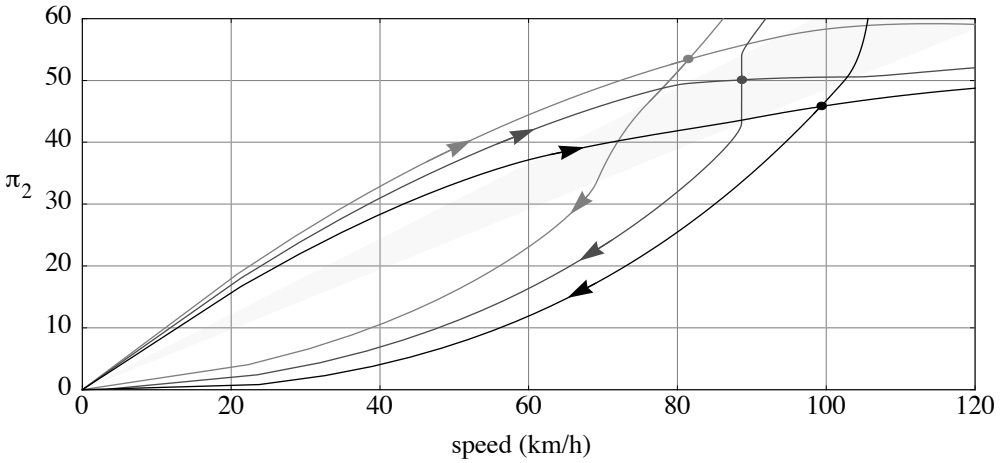

Figure 13-11: Phase diagram separatrices for solar power $s \in \{400, 1200, 2000\}$ *. The critical speed, indicated by a dot, increases with solar power. The shaded region indicates the solar phase of the discharge–solar–charge strategy. Battery capacity efficiency is* $\eta_B = 0.8$ *to make the solar region visible.*

13.6 Summary

With the more realistic ohmic battery model and the silver-zinc model developed for the Aurora car it is much more difficult to calculate a precise optimal strategy. However, we have shown that any practical strategy must closely follow the trajectory of a critical speed that occurs at a stationary point of the system of state equations. The critical speed increases with solar power.

The ohmic battery model and the silver-zinc model both give similar strategies. Unlike the strategies derived using the simple battery model, speed varies continuously with solar power. Nevertheless, the range of speeds is still small, and there is still a short period between discharging and charging where the batteries are not used.

14 Drive losses

So far we have assumed that the drive system is perfectly efficient. In practice there are power losses in the drive system during power and regenerative braking. The magnitude of these losses depends on the speed of the car and on the power being applied to or generated by the drive system.

To analyse the effect of drive system losses on the optimal strategy, we will first consider the simplest case where

- solar irradiance does not depend on location,
- the acceleration of the car does not depend on location,
- the car has a single, perfectly efficient battery, and
- the battery is sufficiently large that battery power and charge constraints are never binding.

In this simplest case the optimal strategy is, as expected, essentially speed-holding. On an undulating road, however, speed variations can be used to reduce power losses and improve performance.

14.1 Problem formulation

Sources of power loss in an electric drive system include electrical resistance in the motor, air drag, bearing friction and losses in the control electronics. As described in Chapter 6, the total power loss in the drive system has the form

$$L(p_{\text{out}}, v) = p_{\text{in}} - p_{\text{out}} = a_0 + a_1 v + a_2 v^2 + a_3 v^3 + k\left(\frac{p_{\text{out}}}{v}\right)^2$$

where p_{in} is the power applied to the drive system, p_{out} is the power output of the drive system, v is the speed of the car, and a_0, a_1, a_2, a_3, k are constants.

Drive losses can be taken into account by including them in the state equations and re-solving the optimal control problem. To simplify the analysis, let the control be the drive output power p_{out} rather than drive input power p_{in} or battery power b. If the car has a perfectly efficient battery then on a level road the problem has state equations

$$\frac{dx}{dt} = v,$$

$$\frac{dv}{dt} = \frac{1}{m}\left[\frac{p_{\text{out}}}{v} - R(v)\right],$$

and

$$\frac{dQ}{dt} = -\frac{b}{\varepsilon}$$

where ε is the emf of the battery and where the power b flowing from the battery is

$$\begin{aligned} b &= p_{\text{in}} - s \\ &= p_{\text{out}} + L(p_{\text{out}}, v) - s. \end{aligned}$$

Unlike previous formulations, battery power b now depends on the speed of the car. The new Hamiltonian is

$$H = \pi_1 v + \frac{\pi_2}{m}\left[\frac{p_{\text{out}}}{v} - R(v)\right] - \frac{\pi_3}{\varepsilon}\left[p_{\text{out}} + L(p_{\text{out}}, v) - s\right]$$

and has adjoint equations

$$\begin{aligned} \frac{d\pi_1}{dt} &= -\frac{\partial H}{\partial x} = 0 \\ \frac{d\pi_2}{dt} &= -\frac{\partial H}{\partial v} = -\pi_1 + \frac{\pi_2}{m}\left[\frac{p_{\text{out}}}{v^2} + R'(v)\right] + \frac{\pi_3}{\varepsilon}\frac{\partial}{\partial v}L(p_{\text{out}}, v) \\ \frac{d\pi_3}{dt} &= -\frac{\partial H}{\partial Q} = 0. \end{aligned}$$

The normalised Hamiltonian is

$$H = v + \frac{\pi_2}{m}\left[\frac{p_{\text{out}}}{v} - R(v)\right] - C\left[p_{\text{out}} + L(p_{\text{out}}, v) - s\right]$$

where C is a constant, with the normalised adjoint equation

$$\frac{d\pi_2}{dt} = -1 + \frac{\pi_2}{m}\left[\frac{p_{\text{out}}}{v^2} + R'(v)\right] + C\frac{\partial}{\partial v}L(p_{\text{out}}, v) \quad .$$

The optimal control maximises the Hamiltonian. Collecting the terms depending on the control gives

$$H = \frac{\pi_2}{mv} p_{\text{out}} - C\left[p_{\text{out}} + k\left(\frac{p_{\text{out}}}{v}\right)^2 \right] + \ldots .$$

The maximum value of the Hamiltonian occurs when

$$\frac{\partial H}{\partial p_{\text{out}}} = \frac{\pi_2}{mv} - C\left[1 + \frac{2kp_{\text{out}}}{v^2} \right] = 0$$

and so the optimal control is

$$p_{\text{out}} = \frac{v^2}{2k}\left[\frac{\pi_2}{Cmv} - 1 \right].$$

Substituting the optimal control into the equations of motion and the adjoint equation gives

$$\frac{dv}{dt} = \frac{1}{m}\left\{ \frac{v}{2k}\left[\frac{\pi_2}{Cmv} - 1 \right] - R(v) \right\} \tag{14.1}$$

and

$$\begin{aligned} \frac{d\pi_2}{dt} &= -1 + \frac{\pi_2}{m}\left\{ \frac{1}{2k}\left[\frac{\pi_2}{Cmv} - 1 \right] + R'(v) \right\} \\ &\quad + C\left\{ a_1 + 2a_2 v + 3a_3 v^2 - \frac{v}{2k}\left[\frac{\pi_2}{Cmv} - 1 \right]^2 \right\} \\ &= -1 + \frac{\pi_2}{m}\left\{ R'(v) + \frac{1}{2k} \right\} + C\left\{ a_1 + 2a_2 v + 3a_3 v^2 - \frac{v}{2k} \right\}. \end{aligned} \tag{14.2}$$

This system of equations does not depend explicitly on solar power; in fact, it is autonomous.

14.2 Constructing a phase portrait

The optimal strategy follows a trajectory governed by the equations

$$\frac{dv}{dt} = f(v, \pi_2)$$

and

$$\frac{d\pi_2}{dt} = g(v, \pi_2)$$

where

$$f(v, \pi_2) = \frac{1}{m}\left\{\frac{v}{2k}\left[\frac{\pi_2}{Cmv} - 1\right] - R(v)\right\}$$

$$g(v, \pi_2) = \frac{\pi_2}{m}\left\{R'(v) + \frac{1}{2k}\right\} + C\left\{a_1 + 2a_2 v + 3a_3 v^2 - \frac{v}{2k}\right\} - 1.$$

As in the previous chapter, this system is exact since

$$\frac{\partial f}{\partial v} + \frac{\partial g}{\partial \pi_2} = 0,$$

and at any given value of solar power s the Hamiltonian is an integral of the system. The behaviour of the adjoint equations is independent of solar power, so for convenience we set $s = 0$. The Hamiltonian is therefore

$$H = v + \frac{\pi_2}{m}\left\{\frac{v}{2k}\left[\frac{\pi_2}{Cmv} - 1\right] - R(v)\right\} - C\frac{v^2}{2k}\left[\frac{\pi_2}{Cmv} - 1\right]$$
$$- C\left\{a_0 + a_1 v + a_2 v^2 + a_3 v^3 + \frac{v^2}{4k}\left[\frac{\pi_2}{Cmv} - 1\right]^2\right\}.$$

Optimal trajectories in the (v, π_2) plane follow the level curves of H. For a given value H_0 and speed v, the value of π_2 is given by the quadratic equation

$$c_2\pi_2^2 + c_1\pi_2 + c_0 = 0$$

where

$$c_2 = \frac{1}{4Cm^2k}$$

$$c_1 = -\frac{1}{m}\left\{\frac{v}{2k} + R(v)\right\}$$

$$c_0 = v - C\left\{a_0 + a_1 v + a_2 v^2 + a_3 v^3 - \frac{v^2}{4k}\right\} - H_0$$

Level curves of the Hamiltonian H are shown in Figure 14-1. Solar power s affects only the value of H on each level curve.

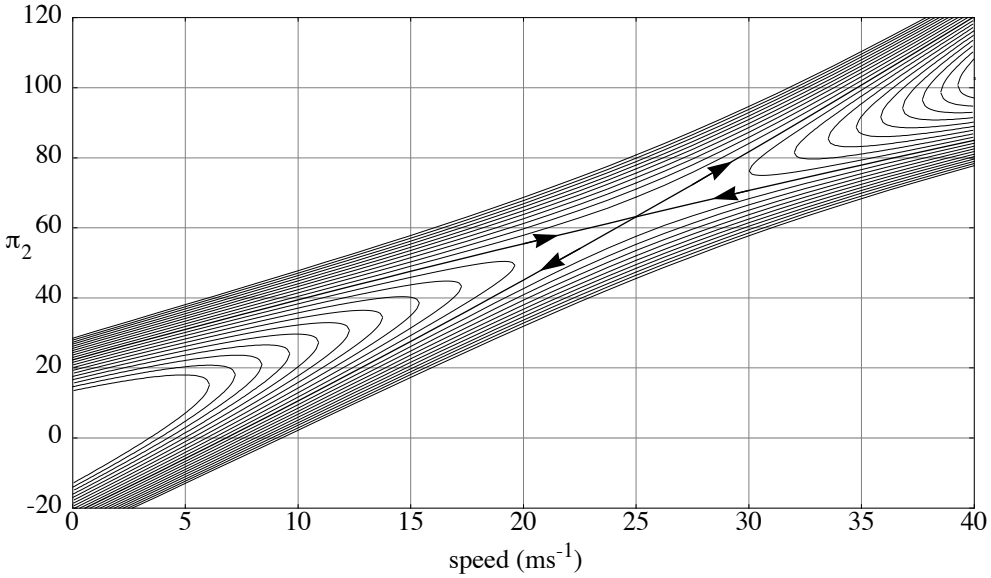

Figure 14-1: Level curves of the Hamiltonian. The fixed point is a saddle point.

The system has a singular point (v^*, π_2^*); from (14.1) we get

$$\pi_2^* = Cm\,[2kR(v^*) + v^*]$$

and from (14.2) we deduce that v^* satisfies

$$C\,\{\,[2kR(v^*) + v^*]\left[R'(v^*) + \frac{1}{2k}\right]\} + C\,\{a_1 + 2a_2v^* + 3a_3v^{*2} - \frac{v^*}{2k}\} - 1 = 0.$$

With the Aurora parameters, this cubic has only one root in the region $v^* \geq 0$. The singular point is a saddle point; nearby curves quickly evolve to either large v or to $v = 0$. In Figure 14-1 the value of C was calculated to give $v^* = 25$.

Separatrices divide the (v, π_2) plane into four regions. Trajectories in the lower left region correspond to journeys with low initial and final speed. Optimal journeys can be found by solving the differential equations forwards and backwards from an initial point $(v^* - \delta_v, \pi_2^* - \delta_\pi)$. Some example trajectories are shown in Figure 14-2. Power increases gradually to avoid high losses at low speed, then drops back to the level required to maintain an almost-constant speed.

14.3 A practical strategy for a long journey

For a journey that lasts more than a few minutes, the state trajectory must pass very close to the fixed point. The fixed speed v^* does not depend on time, so the optimal journey will be close to a constant-speed journey.

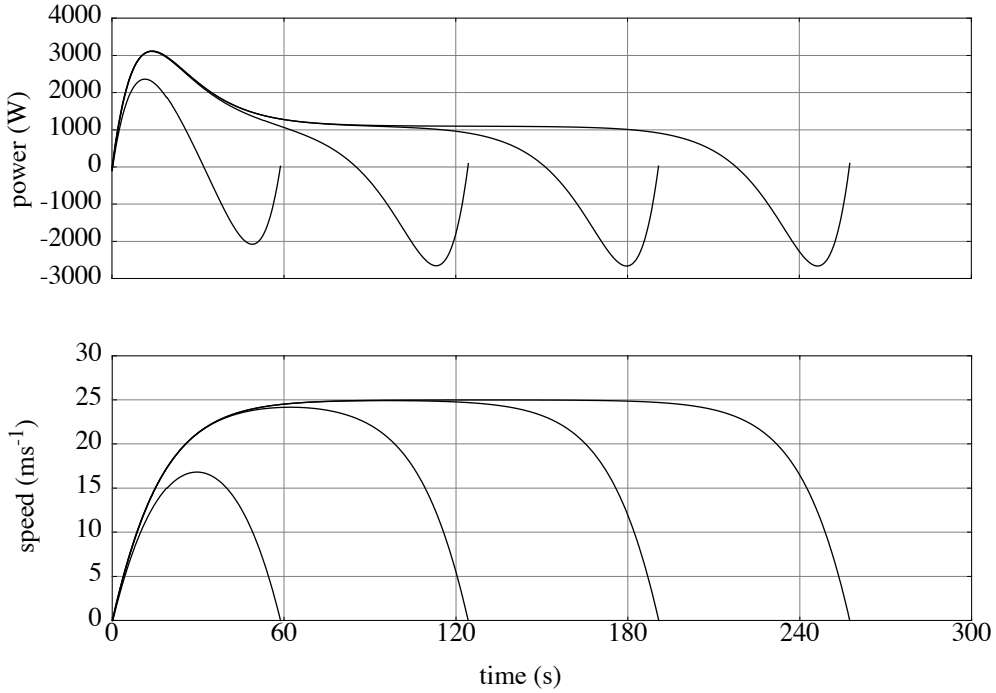

Figure 14-2: Power and speed graphs for trajectories passing close to the fixed point. The longer trajectories are closer to the separatrices, and pass closer to the fixed point.

14.4 Gradients

If the road is not level then the problem has state equations

$$\frac{dx}{dt} = v,$$

$$\frac{dv}{dt} = \frac{1}{m}\left[\frac{p_{\text{out}}}{v} - R(v) + G(x)\right],$$

and

$$\frac{dQ}{dt} = -\frac{1}{\varepsilon}\left[p_{\text{out}} + L\left(p_{\text{out}}, v\right) - s\right].$$

This time only the adjoint variable π_3 will be constant, so we can normalise the equations to make $\pi_3 = 1$. The normalised Hamiltonian is

$$H = \pi_1 v + \frac{\pi_2}{m}\left[\frac{p_{\text{out}}}{v} - R(v) + G(x)\right] - \left[p_{\text{out}} + L(p_{\text{out}}, v) - s\right]$$

and has corresponding normalised adjoint equations

$$\frac{d\pi_1}{dt} = -\frac{\pi_2}{m}G'(x)$$

$$\frac{d\pi_2}{dt} = -\pi_1 + \frac{\pi_2}{m}\left[\frac{p_{\text{out}}}{v^2} + R'(v)\right] + \frac{\partial}{\partial v}L(p_{\text{out}}, v).$$

Grouping the terms depending on the control, the Hamiltonian can be written as

$$H = \frac{\pi_2}{m}\left[\frac{p_{\text{out}}}{v}\right] - \left[p_{\text{out}} + k\left(\frac{p_{\text{out}}}{v}\right)^2\right] + \ldots.$$

As on the level road, the maximum value of the Hamiltonian occurs with the optimal control

$$p_{\text{out}} = \frac{v^2}{2k}\left[\frac{\pi_2}{mv} - 1\right].$$

Substituting the optimal control into the adjoint equations gives

$$\frac{dv}{dt} = \frac{1}{m}\left\{\frac{v}{2k}\left[\frac{\pi_2}{mv} - 1\right] - R(v) + G(x)\right\}$$

$$\frac{d\pi_1}{dt} = -\frac{\pi_2}{m}G'(x)$$

$$\frac{d\pi_2}{dt} = -\pi_1 + \frac{\pi_2}{m}\left[\frac{1}{2k} + R'(v)\right] + a_1 + 2a_2 v + 3a_3 v^2 - \frac{v}{2k}.$$

Figure 14-3 shows an optimal speed curve over a hill. The hill is 10m high and has a maximum slope of just over 3%. The curve was found using a shooting method. The initial speed of the car is 85km/h. The initial value of π_2 was chosen to give $dv/dt = 0$ at the beginning of the journey. The other adjoint variable π_1 was then chosen to give a trajectory with distance as large as possible before speed diverged.

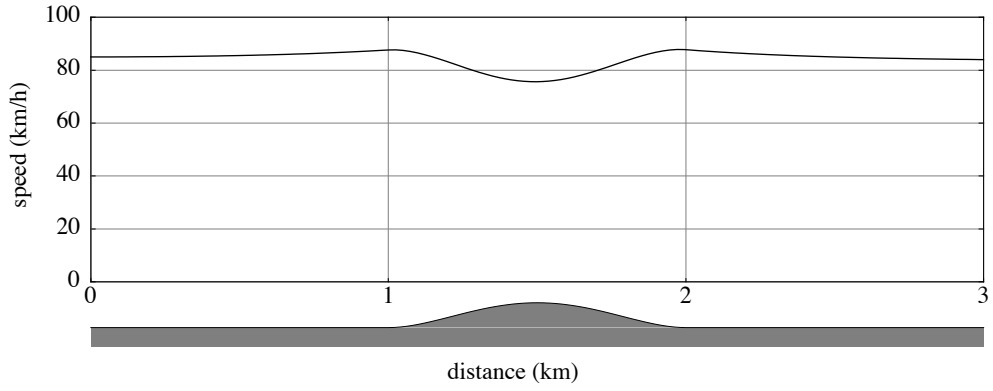

Figure 14-3: Optimal speed over a hill.

14.5 Summary

The optimal strategy for a car with perfectly efficient batteries and a perfectly efficient drive system is to travel at a constant speed. If we introduce drive losses into the model, the practical strategy for a level road is essentially the same, apart from a gradual application of power at the beginning of the journey and a gradual use of regenerative braking at the end.

On an undulating road, however, power losses in the drive system can be reduced by increasing the speed of the car on the approach to an incline, then reducing the speed while climbing. This anticipation of hills is similar to that required for the optimal control of trains on steep gradients (Howlett & Pudney 1995).

15 Spatially varying irradiance

So far we have assumed that solar power does not depend on the location of the car. For a car with a perfectly efficient battery, a constant speed strategy is best. When the battery is not perfectly efficient, such as with the simple constant efficiency model and the more realistic ohmic and silver zinc models, the optimal speed of the car varies to compensate for losses in the battery—that is, the car is driven slightly faster while charging and slightly slower while discharging.

A constant speed strategy is the most energy-efficient. If solar power varies with location, however, variations in speed may collect enough additional energy to increase the overall speed of the car. This principle is easily demonstrated with an extreme example. Suppose the car is sitting at the start line in full sun, but the rest of the track will be completely dark for the entire race. If the batteries are empty at the start of the race then the car must wait at the start line until it has stored enough energy to drive through the darkness to the finish line. (How long should it wait?) But even this is not the most extreme scenario—suppose the race heads south, but the darkness is moving north. The car must travel north with the light until it collects enough energy to turn around and head for the finish line!

In this chapter we consider the solar car problem where solar power depends on location as well as on time.

15.1 Problem formulation

Suppose solar power s varies with both time and location. If the car has a single battery with constant energy efficiency $0 \le \eta_B \le 1$ then

$$I(b) = \begin{cases} \dfrac{b}{\varepsilon} & b \ge 0 \\ \dfrac{\eta_B b}{\varepsilon} & b < 0 \end{cases}$$

where ε is the battery emf. The adjoint equations for the problem are

$$\frac{d\pi_1}{dt} = -\frac{\pi_2}{mv}\frac{\partial s}{\partial x}$$

$$\frac{d\pi_2}{dt} = -\pi_1 + \frac{\pi_2}{m}\left[\frac{p}{v^2} + R'(v)\right].$$

If we once again let $\eta = \pi_2/mv$ then the adjoint equations can be rewritten as

$$\frac{d\pi_1}{dt} = -\eta\frac{\partial s}{\partial x} \tag{15.1}$$

$$\frac{d\eta}{dt} = \frac{1}{mv}[\eta\varphi'(v) - \pi_1] \tag{15.2}$$

The Hamiltonian is

$$H(t, \xi, u, \pi, 0) = \begin{cases} [\eta - \eta_D]\, b + \ldots & b \geq 0 \\ [\eta - \eta_C]\, b + \ldots & b < 0 \end{cases}$$

where $\eta_D = C/e$ and $\eta_C = \eta_B\eta_D$.

15.2 Necessary conditions for an optimal strategy

The maximum value of the Hamiltonian depends on the value of η. There are five cases to consider:

power	$\eta_D < \eta \Rightarrow b = P_T - s$
discharge	$\eta = \eta_D \Rightarrow b \in [0, P_T - s]$
solar	$\eta_C < \eta < \eta_D \Rightarrow b = 0$
charge	$\eta = \eta_C \Rightarrow b \in [-P_R - s, 0]$
regen	$\eta < \eta_C \Rightarrow b = -P_R - s$

The discharge and charge phases are singular. If discharge is maintained on a non-trivial interval then (15.2) gives

$$\pi_1 = \eta_D\varphi'(v).$$

Differentiating both sides and substituting from (15.1) gives

$$\varphi''(v)\frac{dv}{dt} = -\frac{\partial s}{\partial x}$$

and so

$$v\varphi''(v)\frac{dv}{dt} = -\frac{\partial s}{\partial x}\frac{dx}{dt}.$$

If we let

$$\psi(v) = v^2 R'(v)$$

then

$$\psi'(v)\frac{dv}{dt} = -\frac{\partial s}{\partial x}\frac{dx}{dt}.$$

Taking antiderivatives with respect to t gives

$$\psi(v) + s(t, x) - \int\frac{\partial s}{\partial t}dt = A \tag{15.3}$$

where A is a constant.

If a charge phase is maintained on a non-trivial interval then $\pi_1 = \eta_C\varphi'(v)$, which leads to

$$\psi(v) + \eta_B\left[s(t, x) - \int\frac{\partial s}{\partial t}dt\right] = B \tag{15.4}$$

where B is a constant.

If s depends only on time then (15.3) and (15.4) reduce to

$$\psi(v) = A$$

and

$$\psi(v) = B.$$

The analysis in Chapter 10 showed that the solutions V and W to these two equations are related by the equation

$$\varphi'(V) = \eta_B\varphi'(W).$$

If s depends only on location then (15.3) and (15.4) reduce to

$$\psi(v) + s(x) = A \tag{15.5}$$

and

$$\psi(v) + \eta_B s(x) = B. \tag{15.6}$$

Over short time intervals, say less than an hour, solar power can be considered as depending on location only, and equations (15.5) and (15.6) used to develop an appropriate short-term strategy. By reformulating the problem with location as the independent variable it is possible to find the relationship between A and B. This will be done in the next chapter.

15.3 Construction of an optimal strategy

Single, perfectly efficient battery

If the car has a single, perfectly efficient battery then there are only three driving modes: power, hold and regen. The singular hold phase with $\eta = \eta^*$ must be maintained for most of the journey. During the hold phase, (15.2) gives

$$\pi_1 = \eta^* \varphi'(v).$$

Differentiating both sides and substituting from (15.1) as before gives the key equation

$$\frac{dv}{dt} = -\frac{1}{\varphi''(v)}\frac{\partial s}{\partial x}. \tag{15.7}$$

Given an initial speed, this equation can be solved numerically to give an optimal speed profile for the hold phase. The corresponding control profile can be found by using the equation of motion and (15.7) to give

$$\frac{1}{mv^2}\left[p_1 + s(t, x) - \varphi(v)\right] = -\frac{1}{\varphi''(v)}\frac{\partial s}{\partial x}$$

which can be rearranged to give

$$p_1 = \varphi(v) - s(t, x) - \frac{mv^2}{\varphi''(v)}\frac{\partial s}{\partial x}.$$

The energy drop in the battery can be controlled by varying the initial speed—increasing the initial speed will increase the average speed for the journey and increase the energy drop in the battery.

Figure 15-1 shows three optimal speed profiles, corresponding to three levels of energy use, for a journey with spatially varying irradiance. Notice that the speed of the car increases as solar power drops, reducing the time spent with low solar power.

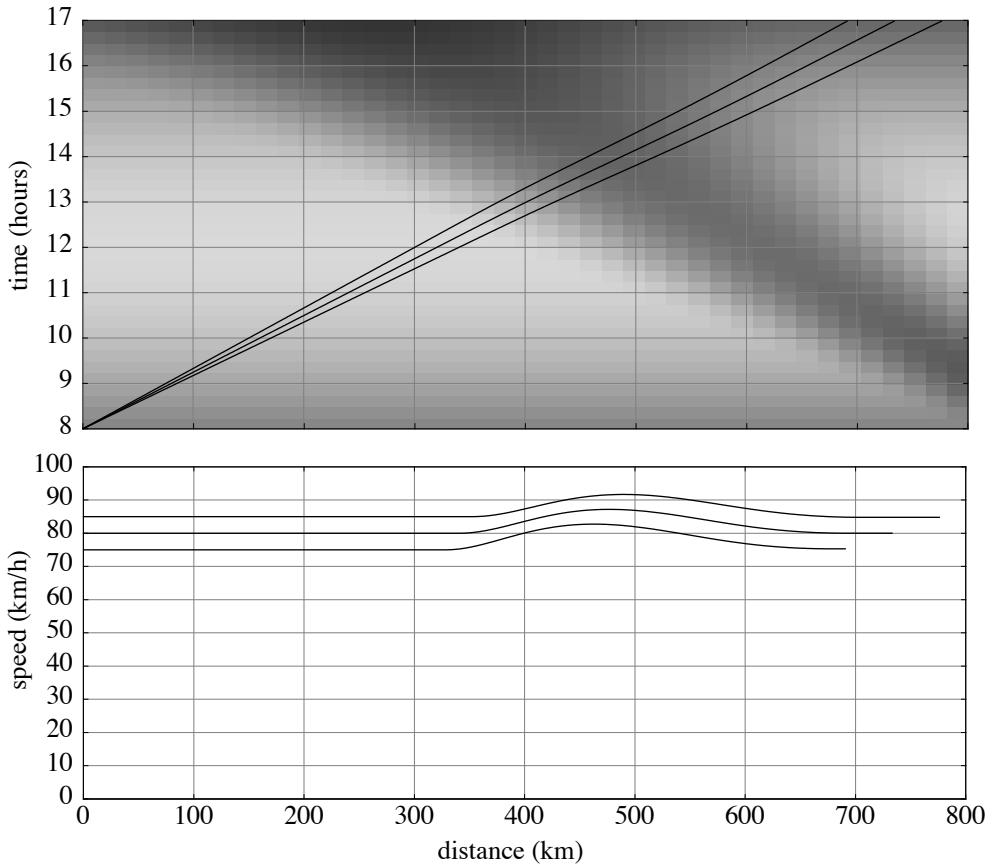

Figure 15-1: Optimal journeys starting at 75, 80 and 85km/h. The shading behind the top graph indicates solar power. The diagonal dark strip represents an expanding cloud band moving in the opposite direction to the car.

Single battery with constant energy efficiency

If the car has a single battery with constant energy efficiency then there are five driving modes: power, discharge, solar, charge and regen. The key equation (15.7) applies during both the discharge and charge modes.

15.4 Solution of a 'dark route' problem

An extreme example of a problem with spatially varying irradiance is the problem mentioned in the introduction to the chapter, where the start line is in full sun but the remainder of the route is in complete darkness. Suppose we have to complete the race with no net drop in stored energy, that the solar power at the start line is a constant s, and that the battery has constant energy efficiency η_B. The optimal strategy for the race is to wait on the start line for some time T_C, then drive to the finish line at some constant speed V.

Ignoring the power phase, the total time for the journey, including the time spent charging, will be $T = T_C + X/V$. The energy collected on the start line will be

$$E_C = \eta_B s T_C$$

and the energy used to drive distance X at speed V will be

$$E_D = \frac{X\varphi(V)}{V} = XR(V).$$

The maximum value of the hold speed V will occur when $E_C = E_D$ and so

$$XR(V) = \eta_B s T_C.$$

The total time for the journey will therefore be

$$T = \frac{XR(V)}{\eta_B s} + \frac{X}{V}.$$

The minimum value of T occurs when

$$\frac{XR'(V)}{\eta_B s} - \frac{X}{V^2} = 0$$

and hence when

$$\psi(V) = \eta_B s.$$

The optimal speed does not depend on the length of the track! Using the car parameters in Table 11-3 with 1000 W of solar power at the start line, the optimal journey has $V = 18.9$, or 68 km/h.

15.5 Stationary brightness factor

Suppose

$$s(t, x) = \kappa(x) s_0(t)$$

where κ is a location dependent 'brightness' factor, corresponding to a sky uniformly covered by clouds that vary in transmittance as the car moves along the route. The adjoint equations are

$$\frac{d\pi_1}{dt} = -\eta s_0(t)\kappa'(x) \tag{15.8}$$

and

$$\frac{d\eta}{dt} = \frac{1}{mv}\left[\eta\varphi'(v) - \pi_1\right]. \tag{15.9}$$

The Hamiltonian and five control modes are as before, with singular discharge and charge phases. If discharge is maintained on a non-trivial interval then (15.3) becomes

$$\psi(v) + s_0(t)\kappa(x) - \int s_0'(t)\kappa(x)dt = A$$

or

$$\psi(v) + \int s_0(t)\kappa'(x)dx = A$$

where A is a constant. If a charge phase is maintained on a non-trivial interval then $\pi_1 = \eta_C\varphi'(v)$, which leads to

$$\psi(v) + \eta_B\left[s_0(t)\kappa(x) - \int s_0'(t)\kappa(x)dt\right] = B$$

or

$$\psi(v) - \eta_B\int s_0(t)\kappa'(x)dx = B$$

where B is a constant.

15.6 Summary

If solar power is a known function of time and location then the key equation

$$\frac{dv}{dt} = -\frac{1}{\varphi''(v)}\frac{\partial s}{\partial x}$$

describes the optimal speed profile for a car with a perfectly efficient battery on a level road. This equation can be solved numerically.

In the next chapter we will show that with spatial variations in solar power, the speed of the car should be increased when solar power is low and decreased when solar power is high so that the extra energy collected exceeds the energy losses due to the speed variations.

16 Short-term strategy

In the previous chapter we saw that if solar power depends only on location then the necessary conditions for the discharge and charge phases are

$$\psi(v) + s(x) = A$$

and

$$\psi(v) + \eta_B s(x) = B.$$

These equations are particularly relevant for the short-term strategy; over short time intervals—say, less than an hour—solar power can be considered a function of location only. By reformulating the problem with distance as the independent variable we can derive a relationship between A and B.

16.1 Problem formulation

Suppose solar power $s\colon [0, X] \to \Re$ is known for the distance interval $[0, X]$. We wish to minimise the time taken to traverse the interval. We will use the simple battery model and assume that the road is level. Using distance as the independent variable, the state equations for the problem are

$$\frac{dt}{dx} = \frac{1}{v},$$

$$\frac{dv}{dx} = \frac{1}{mv}\left[\frac{p}{v} - R(v)\right]$$

and

$$\frac{dQ}{dx} = -I(b)$$

with

$$I(b) = \begin{cases} \dfrac{b}{\varepsilon} & b \geq 0 \\ \dfrac{\eta_B b}{\varepsilon} & b < 0 \end{cases}$$

where ε is the battery voltage. The normalised Hamiltonian for the problem is

$$H = \frac{1}{v}\left\{-1 + \frac{\pi_2}{m}\left[\frac{p}{v} - R(v)\right] - CI(b)\right\}$$

with normalised adjoint equation

$$\frac{d\pi_2}{dx} = \frac{1}{v^2}\left\{\frac{\pi_2}{m}\left[\frac{p}{v} - R(v)\right] - CI(b) - 1\right\} + \frac{\pi_2}{mv}\left[\frac{p}{v^2} + R'(v)\right].$$

If we once again let $\eta = \pi_2/mv$ and $\varphi(v) = vR(v)/\eta_T$ then

$$H = \frac{1}{v}\left\{\eta\left[p - \varphi(v)\right] - CI(b) - 1\right\}$$

and

$$\frac{d\eta}{dx} = \frac{1}{mv^3}\left\{\eta\left[p + \psi(v)\right] - CI(b) - 1\right\}$$

where

$$\psi(v) = v^2 R'(v)$$

16.2 Necessary conditions for an optimal strategy

The Hamiltonian can be rewritten as

$$H = \begin{cases} \left[\eta - \eta_D\right] b + \ldots & b \geq 0 \\ \left[\eta - \eta_C\right] b + \ldots & b < 0 \end{cases}$$

where $\eta_D = C/\varepsilon$ and $\eta_C = \eta_B \eta_D$. The maximum value of the Hamiltonian depends on the value of η. As usual, there are five cases to consider:

power $\quad \eta_D < \eta \Rightarrow b = P_T - s$

discharge $\quad \eta = \eta_D \Rightarrow b \in [0, P_T - s]$

solar $\quad \eta_C < \eta < \eta_D \Rightarrow b = 0$

charge $\eta = \eta_C \Rightarrow b \in [-P_R - s, 0]$

brake $\eta < \eta_C \Rightarrow b = -P_R - s$

If a discharge phase is maintained on a non-trivial interval then $\eta = \eta_D$ and

$$\frac{d\eta}{dx} = \frac{1}{mv^3}\{\eta_D[s(x) + \psi(v)] - 1\} = 0$$

which gives

$$s(x) + \psi(v) = \frac{1}{\eta_D}.$$

For given $s(x)$ there is a unique speed v that satisfies this equation, since $\psi(v)$ is strictly increasing. As s increases the optimal speed decreases; by speeding up under cloud and slowing down in bright sunlight you collect enough extra energy to increase the overall average speed of the car.

If η_D is such that the optimal speed of the car is 100km/h when solar power is 1200W then the optimal speed at various levels of solar power is given by the graph in Figure 16-1.

If a charge phase is maintained on a non-trivial interval then $\eta = \eta_C$ and

$$\frac{d\eta}{dx} = \frac{1}{mv^3}\{\eta_C[s(x) + \psi(v)] - 1\} = 0$$

which gives

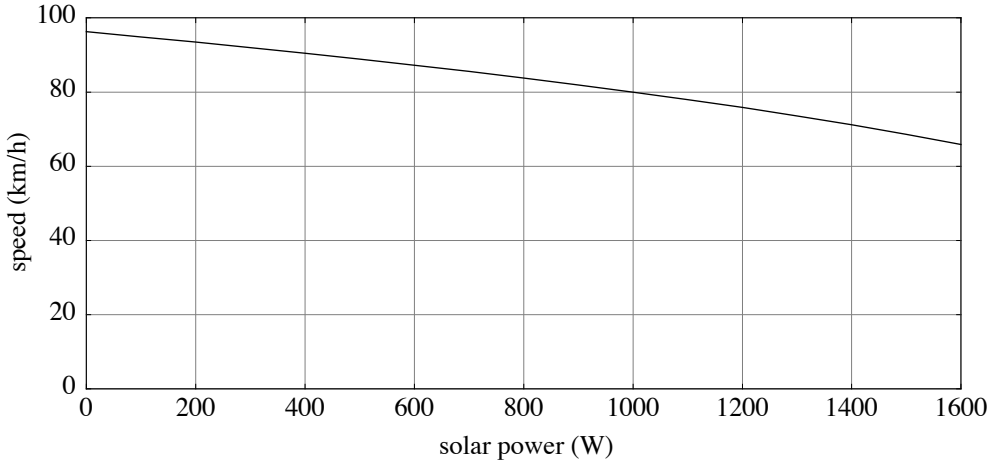

Figure 16-1: If solar power depends on distance only then the optimal speed decreases as solar power increases.

$$s(x) + \psi(v) = \frac{1}{\eta_C}.$$

16.3 Construction of a short-term strategy

The appropriate value of η_D for a short-term strategy depends on the total solar energy expected during the next, say, 50km. To find η_D we use the long-term strategy to determine the desired battery energy at the end of the 50km interval. For any candidate η_D and predicted solar profile s we can calculate a corresponding speed profile v and battery energy profile E. By adjusting η_D we can find the energy profile that finishes at the desired level.

16.4 Example

The difference between the optimal short-term strategy and a constant speed strategy can be quite small. Consider a 50km interval where solar power is 1200W on the first half of the interval and 600W on the second half of the interval. To make the problem simpler, assume that the car has a perfectly efficient battery. The optimal journey is compared to a constant speed journey in Table 16-1.

		optimal	constant speed
0–25km, 1200W	speed (km/h)	75.8	80.8
	time (s)	1186.7	1114.2
	energy (Wh)	123.1	72.9
25–50km, 600W	speed (km/h)	87.2	80.8
	time (s)	1031.7	1114.2
	energy (Wh)	-163.0	-112.8
Overall	speed (km/h)	81.1	80.8
	time (s)	2218.3	2228.4
	energy (Wh)	-39.9	-39.9

Table 16-1: Comparison of an optimal short-term strategy with a constant speed strategy. Both strategies use the same battery energy. The optimal strategy is 10 seconds faster over 50km.

16.5 Summary

On short time intervals we can consider solar power to be a function of distance only, in which case the extra energy collected by slowing down in bright sunlight and speeding up under clouds can more than compensate for the extra energy required to vary the speed. In practice, however, the difference between the optimal strategy and a constant speed strategy is negligible.

17 Stochastic irradiance

So far we have considered deterministic models of the solar car problem. We now reconsider the simplest solar car model, this time with a stochastic model of solar power.

This chapter is based on a paper by Boland, Gaitsgory, Howlett & Pudney (1998).

17.1 A simple stochastic solar car problem

Suppose we wish to drive a solar car as far as possible in n days, where n is known in advance. We know how much energy is stored in the battery, but do not know how much solar energy we will collect over the next n days. How far should we drive today?

The solar energy collected each day can be modelled by a sequence $\{S_i\}$ with

$$S_i = \bar{S}_i + \xi_i$$

where the deterministic term $\bar{S}_i$ is the mean solar energy for day i, and where $\{\xi_i\}$ is a stochastic sequence modelled by a Markov transition matrix (Boland 1995).

The optimal driving strategy for a solar car with perfectly efficient energy storage and known solar power is a constant speed strategy. If the time spent driving is the same each day, and if we travel at a constant speed v_i on day i, then the distance travelled on day i will be $x(E_i)$, where x is an increasing function of the energy E used to drive the car on a given day, and has a decreasing derivative.

We use the index i to indicate the number of days remaining, so that B_1 is the energy in the battery at the beginning of the final day. The energy stored in the battery at the beginning of any day i depends on the battery energy at the beginning of the previous day and on the solar energy collected and energy used during the previous day. If we assume that the battery is perfectly efficient then the energy stored in the battery at the beginning of day i is

$$B_i = B_{i+1} + S_{i+1} - E_{i+1} = B_n + \sum_{j=i+1}^{n} S_j - E_j.$$

The energy in the battery at the end of the race is B_0.

The stored energy must also satisfy the battery constraints $0 \le B_i \le B_{\max}$ for $i = 0, \ldots, n-1$. We wish to maximise the total distance travelled in n days, and so must maximise

$$X = \sum_{i=1}^{n} x(E_i).$$

The initial battery energy, B_n, is known. The control is the energy used each day, $E = (E_n, \ldots, E_1)$.

17.2 Solution of the deterministic problem

If $\xi_i = 0$ for all i then the problem is deterministic—maximise

$$X = \sum_{i=1}^{n} x(E_i)$$

subject to $0 \le B_i \le B_{\max}$, with $B_i = B_{i-1} + \bar{S}_{i+1} - E_{i+1}$ and B_n known. This problem can be solved using Lagrange analysis. The Lagrangean for the problem is

$$J(E) = \sum_{i=1}^{n} \left\{ -x(E_i) + (\lambda_{i-1} - \mu_{i-1}) \left[B_n + \sum_{j=i}^{n} \bar{S}_j - E_j \right] - \lambda_{i-1} B_{\max} \right\}$$

where λ_i and μ_i, $i = 0, \ldots, n-1$, are non-negative Lagrange multipliers corresponding to the battery constraints $B_i \le B_{\max}$ and $B_i \ge 0$. An optimal strategy must satisfy the Kuhn-Tucker conditions

$$\frac{\partial J}{\partial E_i} = -x'(E_i) - \sum_{j=1}^{i} (\lambda_{j-1} - \mu_{j-1}) = 0$$

for $i = 1, \ldots, n$. The Kuhn-Tucker condition for the final day gives

$$(\lambda_0 - \mu_0) = -x'(E_1). \tag{17.1}$$

Substituting into the Kuhn-Tucker conditions for the previous days gives the recursion

$$(\lambda_i - \mu_i) = x'(E_{i+1}) - x'(E_i) \qquad i = 1, \ldots, n-1 .$$

If the none of the battery constraints are active until the end of the final day then the complementary slackness conditions

$$\lambda_i [B_i - B_{\max}] = 0$$

and

$$\mu_i B_i = 0$$

give $\lambda_i = \mu_i = 0$ for $i = 1, \ldots, n-1$, and hence $x'(E_i) = x'(E_{i+1})$. But x' is a strictly decreasing function, and so

$$E_1 = E_2 = \ldots = E_n = \frac{1}{n}\left[B_n + \sum_{j=1}^{n} \bar{S}_j \right]$$

An optimal strategy therefore requires an equal amount of energy to be used each day.

Equation (17.1) shows us that to get a solution with $E_1 > 0$ we must have $(\lambda_0 - \mu_0) < 0$, which requires $\mu_0 > 0$ and hence $B_0 = 0$. Thus an optimal strategy must also finish with an empty battery.

The optimal strategy with an inefficient battery requires the car to be driven within a narrow speed band instead of at a single constant speed. For a typical battery, with an energy efficiency of 85%, the optimal speed varies by less than 5km/h. Solar cars usually have batteries large enough that charge constraints are encountered only on the final day of a journey.

17.3 Modelling Adelaide's solar irradiation

Climatic variables can be decomposed into two components, a deterministic one and a stochastic one. In essence, the deterministic component 'is derived from the Earth's revolution and rotation and has quite predictable seasonal and diurnal variations' (Yoshida & Terai 1990/91). If the weather followed only the deterministic component, it would not vary from year to year. The stochastic component comprises fluctuations about the deterministic component. These give the day-to-day weather fluctuations, while the deterministic component gives the seasonal trends. Vergara-Dominguez et al (1985), Hokoi et al (1990/91) and Yoshida and Terai (1990/91) use a small number of Fourier coefficients corresponding to some of the cyclical components such as the annual and diurnal variation to characterise the deterministic component. Phillips (1983) and Boland

(1995) carry this procedure a step further in determining other significant cyclical components. The latter goes on to determine the characteristics of the stochastic component formed by subtracting the contribution of the deterministic component from the original time series.

We can approximate the daily solar irradiation sequence using a Fourier series. The frequency spectrum, shown in Figure 17-1, shows that apart from the average the most significant frequency is the intuitive one of one cycle per year. In keeping with results given in Boland (1995) for other locations, the frequency of two cycles per year was also included. The deterministic component is given by

$$\bar{S}(t) = 17.58 + 10.04\cos(2\pi t/365) - 1.050\sin(2\pi t/365) + 0.025\cos(4\pi t/365) + 0.755\sin(4\pi t/365) \qquad (17.2)$$

The contributions at these frequencies are aggregated and then subtracted from the original time series. The resulting residuals were checked for persistence by calculating the partial autocorrelation values for different lags. The results are shown in Figure 17-2.

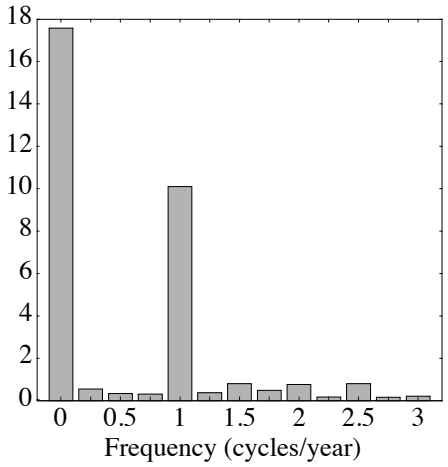

Figure 17-1: Spectrum of Adelaide's solar irradiation.

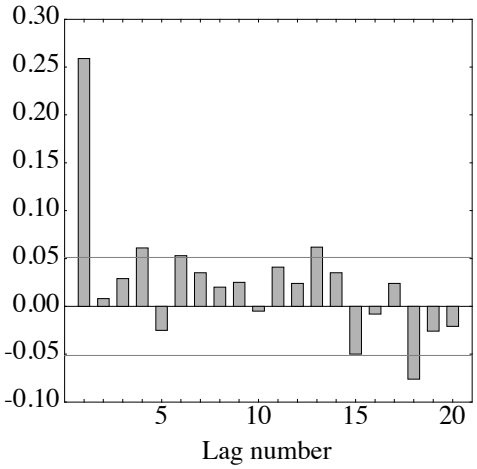

Figure 17-2: Partial autocorrelation function for the Adelaide solar irradiation residuals

It appears from these results that either a first-order autoregressive process (AR(1)) or a Markov Chain would be the appropriate model for these residuals. The histogram of these residuals is skewed, indicating that they do not come from a normal distribution, which implies that an AR(1) process would not be appropriate without performing a transformation on the residuals to enable them to follow a normal distribution. Thus it was decided to model the residuals as a Markov Chain. As a preliminary analysis it was decided to limit the possible states to two, these being greater than zero and less than zero. The next step is to calculate the transition matrix for this Markov process

$$P = \begin{bmatrix} p_{11} & p_{12} \\ p_{21} & p_{22} \end{bmatrix}$$

where p_{ij} denotes the probability of going from state i to state j. For Adelaide, South Australia, this matrix is

$$P = \begin{bmatrix} 0.5456 & 0.4544 \\ 0.3197 & 0.6803 \end{bmatrix}.$$

17.4 Solution of the stochastic problem

The stochastic problem can be tackled using dynamic programming. For finite time problems we define a value function V such that $V_i(B, S)$ is the expected maximum distance we can travel in the remaining i days if the battery contains energy B at the beginning of the day and if the solar energy collected during the previous day was S.

Suppose that solar energy is given by a Markov process with m possible values $s_1, \ldots, s_m$. The probability of a transition from energy s_i to energy s_j is denoted $P(s_i, s_j)$.

On the last day we maximise the distance travelled by using all of the battery energy and all of the solar energy. In practice we do this by watching the sky and adjusting our speed as we change our prediction of S_1, the solar energy we will receive during the day. We will assume that the distance attained on the last day will be the same as if we hand known S_1 in advance and travelled at the optimal speed all day. At the beginning of the last day, the distance we expect to travel is

$$V_1(B, S) = \sum_{j=1}^{m} P(S, s_j) x(B + s_j).$$

The expected maximum distance attainable with two days remaining is

$$V_2(B, S) = \max_E \left\{ x(E) + \sum_{j=1}^{m} P(S, s_j) V_1(B + s_j - E, s_j) \right\}$$

$$= \max_E \left\{ x(E) + \sum_{j=1}^{m} P(S, s_j) \sum_{k=1}^{m} P(s_j, s_k) x(B + s_j + s_k - E) \right\}$$

With two days remaining we should choose E to maximise

$$X_2(B, S, E) = x(E) + \sum_{j=1}^{m} P(S, s_j) \sum_{k=1}^{m} P(s_j, s_k) x(B + s_j + s_k - E) \qquad (17.3)$$

where S is the solar energy collected the previous day and B is the energy in the battery. The expected journey distance X_2 is maximised when

$$x'(E) - \sum_{j=1}^{m} P(S, s_j) \sum_{k=1}^{m} P(s_j, s_k) x'(B + s_j + s_k - E) = 0.$$

Because x is concave and strictly increasing,

$$\max_E \{X_2(B, S, E)\} \leq \max_E \{x(E) + x(E_1)\} \qquad (17.4)$$

where

$$E_1 = \sum_{j=1}^{m} P(S, s_j) \sum_{k=1}^{m} P(s_j, s_k) [B + s_j + s_k - E]$$

$$= B - E + \sum_{j=1}^{m} P(S, s_j) \sum_{k=1}^{m} P(s_j, s_k) [s_j + s_k].$$

The right hand side of (17.4) is maximised when

$$E = E_1 = \frac{1}{2} \left[B + \sum_{j=1}^{m} P(S, s_j) \sum_{k=1}^{m} P(s_j, s_k) [s_j + s_k] \right].$$

Equation (17.4) indicates that using the same energy each day gives an upper bound for the optimal solution.

Example 17-1 A two-day journey

The solar energy collected by a 1000 W panel in Adelaide, South Australia, during November can be modelled by a Markov process with two states $s_1 = 16.5 \times 10^6$ J and $s_2 = 27.7 \times 10^6$ J corresponding to residuals being below and above zero, and with the transition matrix

$$P = \begin{bmatrix} 0.5456 & 0.4544 \\ 0.3197 & 0.6803 \end{bmatrix}.$$

If we assume that the power required to drive the car is proportional to v^3 then the distance travelled in a day is

$$x(E) = kE^{1/3}$$

where $k = 2255.4$ is chosen to approximate the performance of a World Solar Challenge car, and where x is distance travelled in metres and E is the energy used in Joules. If the initial battery energy is $B_0 = 18.0 \times 10^6$ J then for a two-day journey we have

$$V_2(B_0, s_1) = 1413 \text{ km}, E = 30.1 \text{ MJ}, x(E) = 702 \text{ km}, \text{ and}$$
$$V_2(B_0, s_2) = 1437 \text{ km}, E = 31.7 \text{ MJ}, x(E) = 714 \text{ km}.$$

How far would we get if we were able to use half the expected total energy each day? If day 3 had solar energy s_1 then the expected total energy is 62.3 MJ and the expected total distance travelled is 1420 km; if day 3 had solar energy s_2 then the expected total energy is 65.5 MJ and the expected total distance travelled is 1443 km.

Example 17-2 A five-day journey

The dynamic programming method can be extended to any number of days. To make the problem manageable, the value function is tabulated at each stage and future evaluations are interpolated from the table. For a five-day journey the results are $V_5(B_0, s_1) = 3293$ and $V_5(B_0, s_2) = 3326$.

17.5 Efficient frontiers

If we plot expected return against risk we have drawn what financial managers call the 'efficient frontier'. We then choose a point on the curve corresponding to the level of risk we are prepared to accept.

We can use a similar idea to choose a strategy. First, we calculate the probability of each possible solar sequence. Sequences that give the same total energy can then be grouped, and their probabilities summed. We can then plot probability against solar energy or (deterministic) distance. The most likely distance is the base point. Greater distances have a lower probability, but greater glory. How much risk should we take? Perhaps the shape of the curve will help us decide.

There are two ways we can generate the expected total solar energy:

1. Generate all possible sequences, then use the Markov transition matrix to calculate the probability of each sequence, taking into account yesterday's solar energy. Group the sequences with the same total energy, summing the probabilities.
2. Use a binomial distribution of dull and bright days.

The expected distance travelled over the remaining n days is then

$$X = nx(\frac{B+E}{n})$$

where B is the initial battery energy and E is the total solar energy.

Markov method

Using the Markov transition matrix to calculate the energy probabilities for a five-day journey gives two sets of distance probabilities, as shown in Table 17-1.

	Yesterday dull		Yesterday bright	
x	$P[X = x]$	$P[X \geq x]$	$P[X = x]$	$P[X \geq x]$
3066	0.048	1.000	0.028	1.000
3176	0.135	0.952	0.100	0.972
3279	0.232	0.817	0.202	0.871
3376	0.272	0.585	0.273	0.670
3468	0.215	0.313	0.251	0.397
3555	0.097	0.097	0.146	0.146

Table 17-1: Distance probabilities for a five day journey, Markov method.

The distance probabilities for a two day journey are shown in Table 17-2.

	Yesterday dull		Yesterday bright	
x	$P[X = x]$	$P[X \geq x]$	$P[X = x]$	$P[X \geq x]$
1328	0.298	1.000	0.174	1.000
1419	0.393	0.702	0.363	0.826
1499	0.309	0.309	0.463	0.463

Table 17-2: Distance probabilities for a two day journey, Markov method.

Binomial method

The probability of a sunny day in Adelaide is $p = 0.587$. Given that the deterministic strategy depends solely on the total irradiation received during the journey, we need only calculate the probability of r sunny days in an n day journey, which is

$$P(r) = \binom{n}{r} p^r (1-p)^{n-r}.$$

We can use these probabilities to construct distance probabilities for a five day journey and for a two day journey.

x	$P[X = x]$	$P[X \geq x]$
3066	0.012	1.000
3176	0.085	0.988
3279	0.243	0.903
3376	0.345	0.660
3468	0.245	0.315
3555	0.070	0.070

Table 17-3: Distance probabilities for a five day journey, binomial method.

x	$P[X = x]$	$P[X \geq x]$
1328	0.169	1.000
1419	0.484	0.831
1499	0.347	0.347

Table 17-4: Distance probabilities for a two day journey, binomial method.

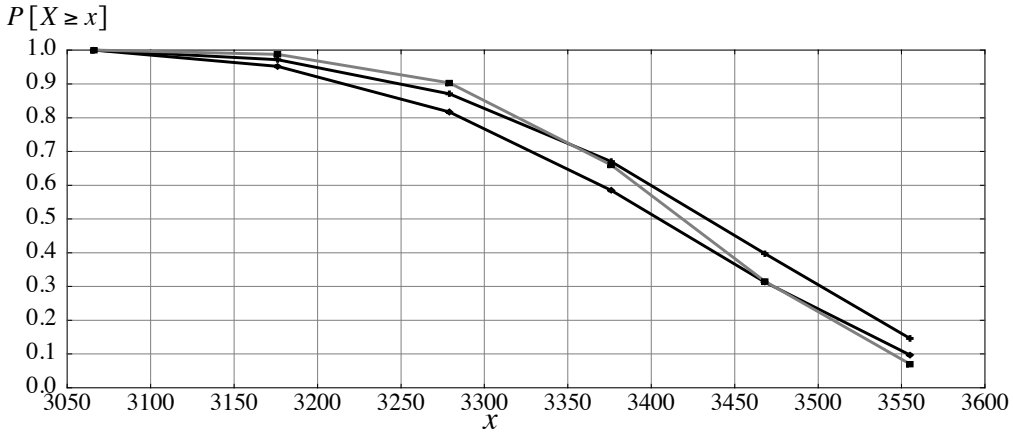

Figure 17-3: Probability of exceeding a given distance in five days. The two black curves are from the Markov method; the upper graph corresponds to yesterday being bright. The grey curve is from the binomial method.

Graphing the results

Figure 17-3 shows the probabilities of exceeding a given distance in five days, as given by each of the two methods. Looking at the upper Markov graph corresponding to a sunny day six we can see that we have an almost 90% chance of exceeding 3250km, but only a 30% chance of exceeding 3500km.

If we were prepared to take a 50% chance then our expected distance is 3440km. With five days to go we aim to drive 688km each day and set our speed accordingly, letting the batteries make up for any difference between the expected energy received and the actual energy received. At the end of each day we reassess our strategy by recalculating the efficient frontier using our actual battery energy.

17.6 Summary

By formulating a solar car problem with a stochastic model of daily solar irradiation we can calculate the probability of achieving a given total distance over the remaining days of a race. Knowing the risks, we can then choose a total distance to aim for and divide by the number of days remaining to give the distance we should drive today. At the end of each day we can reassess our situation and recalculate.

In practice, during a race you would use weather predictions as well as a stochastic irradiation model to predict the energy you will receive over the remainder of a race, and you would recalculate your options more often than once each day.

18 Calculating a practical strategy

Until now we have ignored several features of real solar racing, including:

- battery charge constraints,
- evening and morning charge sessions, and
- media stops.

When we take all of these into account, a truly optimal strategy is too hard to calculate. Instead, the practical strategies used by Aurora since 1993 have been based on the principles developed in this thesis.

18.1 Strategy principles

The principles used to develop a practical driving strategy for the World Solar Challenge are:

Speedholding
: For a car with a perfectly efficient drive system and a perfectly efficient battery, the most energy-efficient strategy is a constant speed strategy—even on an undulating road.

Sun chasing
: The amount of energy collected can be increased by varying the speed of the car to take advantage of spatial variations in irradiance. The car should be driven slower in intervals of increased irradiance and faster in intervals of decreased irradiance.

Battery pampering
: Inefficiencies in the battery mean that speed variations can be used to reduce battery losses. For a car with a perfectly

efficient drive system travelling at about 100km/h on a level road, the optimal speed increases by about 10km/h as solar power increases from zero to 2000W.

Looking at this slightly differently, if solar power increases by 200W then the speed of the car should be increased by 1km/h.

Riding the hills

If you imagine the power change due to gradient to be a change in solar power, you can use the same principle to calculate how you should change speed with gradient. The strategy calculations do not use detailed enough gradient information to do this, but we could do it as a short-term strategy: if the gradient causes us to increase battery power by 200W we would decrease our speed by 1km/h. This short-term strategy reduces drive losses too.

This scheme was tested on a simulated 500km journey with normally distributed gradients. The improvement was a few seconds.

And the result? With average weather, all of these strategies will get you to the finish line a couple of minutes earlier than if you had travelled at a constant speed. Nevertheless, the strategy software I developed for Aurora does take into account daily temporal variations and long-term spatial variations in solar irradiance.

18.2 Predicting irradiance

During the World Solar Challenge the irradiance for any location and time was predicted by interpolating between irradiance functions calculated for Darwin, Alice Springs and Adelaide.These three irradiance functions are based on the clear-sky irradiance functions for the three locations, multiplied by a constant brightness factor for each day. Daily brightness factor is simply the ratio of the measured daily irradiation to the predicted clear-sky irradiation. The problem of predicting irradiance up to five days in advance thus becomes one of predicting daily irradiation at three locations on the route.

The historical daily irradiation at any location can be approximated by a truncated Fourier series

$$I(d) = a_0 + \sum_{i=1}^{3} a_i \cos\frac{2\pi i d}{365} + b_i \sin\frac{2\pi i d}{365} \qquad (18.1)$$

where d is the day of the year and a_i and b_i are parameters that depend on the location of the car. The values of the parameters can be found by fitting the series to historical irradiation data (Boland, private communication). The parameters for Darwin, Alice Springs and Adelaide are given in the following table.

Location	a_0	a_1	a_2	a_3	b_1	b_2	b_3
Darwin	21.7	0.563	-1.12	0.195	-1.77	0.745	-0.389
Alice Springs	22.2	6.34	-0.886	0.139	-1.20	0.250	-0.236
Adelaide	18.0	10.6	0.325	-0.163	-0.803	0.689	0.849

Table 18-1: Fourier coefficients for calculating daily irradiation (MJ).

We can compare the historical irradiation data to the value from (18.1) to give a sequence of deviations $\Delta I_d = I_d - I(d)$, where I_d is the measured irradiation on day d.

If we now graph ΔI_d against ΔI_{d-1} we can see how the deviation depends on the deviation from the previous day. We can then fit a least-squares quadratic to this graph, and apply this function recursively to predict sequences of deviations.

The standard deviation of the error of this prediction scheme is about 20%, which is slightly better than assuming that the irradiation tomorrow will be ‘back to normal’ or ‘the same as today’.

During the 1999 World Solar Challenge I used satellite images and weather predictions from the Bureau of Meteorology to predict daily irradiation for the next day or two, and our daily irradiation prediction scheme to predict further.

18.3 Finding the optimal speed profile

Given a solar irradiance profile for the remainder of the race, the optimal speed profile can be found using a shooting method:

- pick a starting speed
- simulate forward until either the end of the route is reached or else the battery is empty

- if the end of the route was not reached then pick a lower speed and try again; if the end of the route was reached and there is energy left in the battery then pick a higher speed and try again.

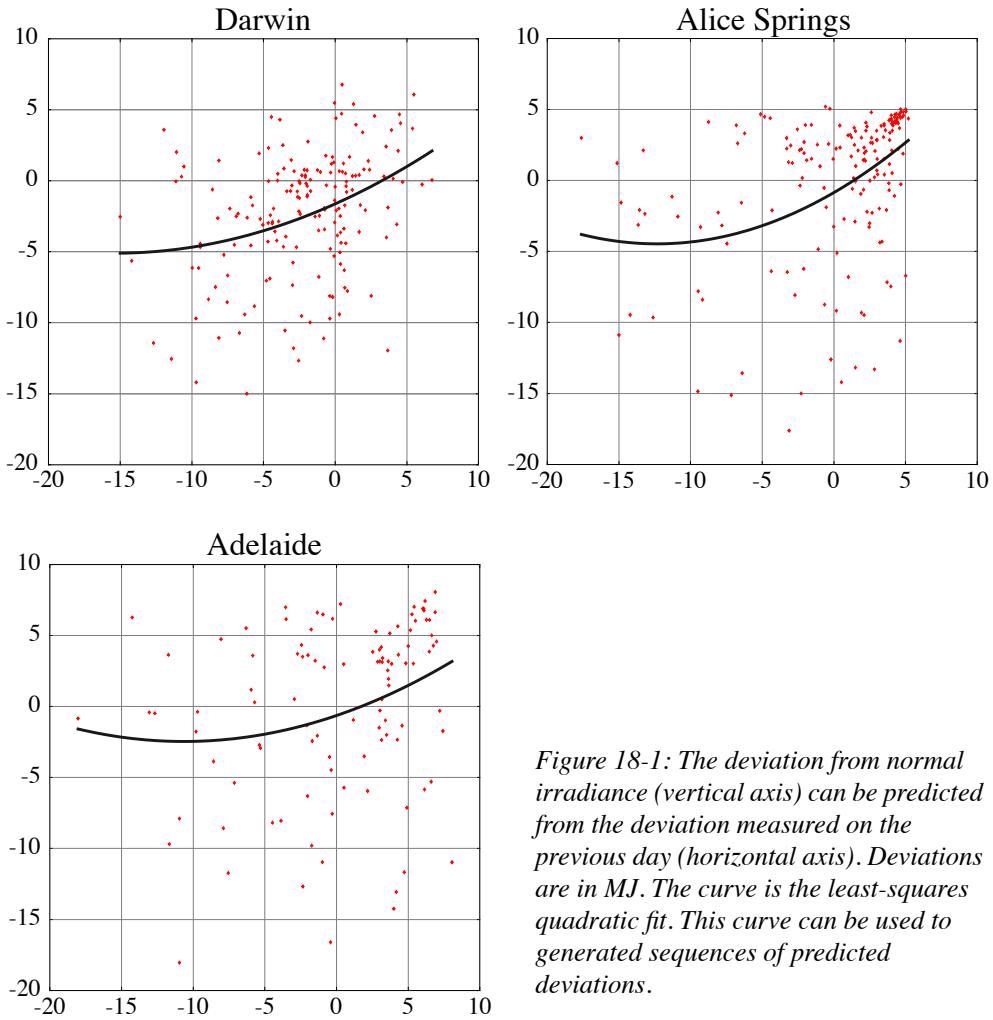

Figure 18-1: The deviation from normal irradiance (vertical axis) can be predicted from the deviation measured on the previous day (horizontal axis). Deviations are in MJ. The curve is the least-squares quadratic fit. This curve can be used to generated sequences of predicted deviations.

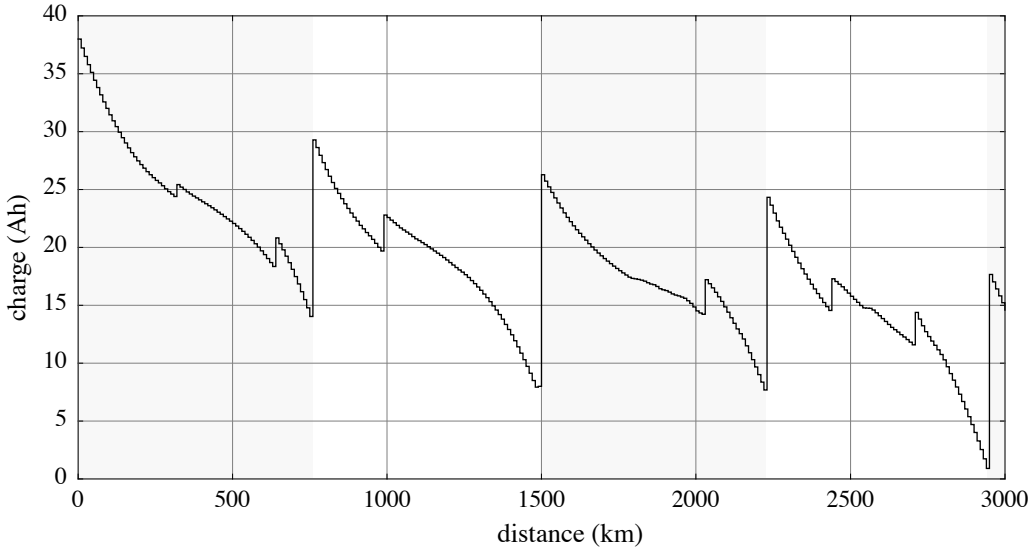

Figure 18-2: Charge prediction for the World Solar Challenge. The small vertical jumps occur at media stops, where the stationary car collects energy for half an hour. The larger vertical jumps occur at the end of each day, when the battery is charged from the setting sun and then again the next morning from the rising sun.

Figure 18-2 shows Aurora's predicted charge profile for the 1999 World Solar Challenge. based on historically average weather. The state of the journey is calculated at 10km intervals using a simple Euler method to solve the differential equations. The small vertical jumps are from 30 minutes of charging at media stops; the large jumps at the end of each day are from evening and morning charging.

The battery is empty at the end of day four, less than 100km from the finish line. If we had travelled faster during the first four days the battery would have emptied sooner. The overnight charge gives plenty of energy to complete the race early on day five.

18.4 Battery charge constraints

The charge profile in Figure 18-2 shows that the batteries used in the World Solar Challenge have over twice the capacity required to store the energy collected during an evening and morning charge session, and so a full battery constraint is rarely encountered. On the other hand, an optimal journey always has the battery empty near the end of the journey.

In November 1994 Aurora drove their Q1 solar car from Perth to Sydney. For this trip, the car had only a small 2000Wh lead-acid battery. The battery full and battery empty constraints were encountered every day. The car was driven from sunrise to sunset, so

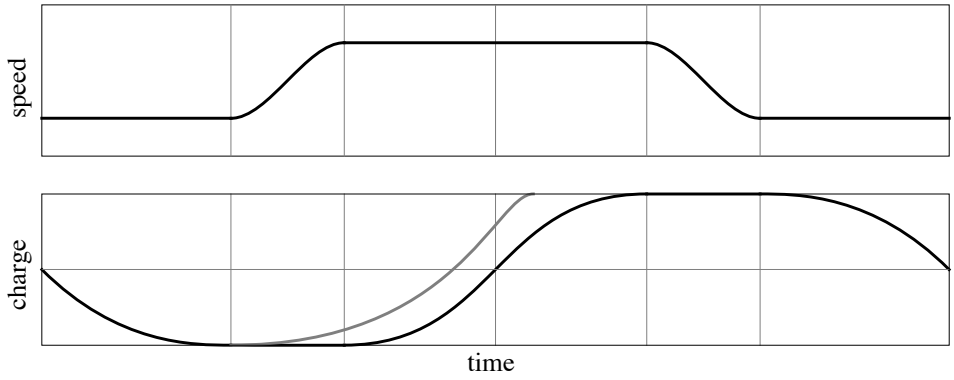

Figure 18-3: Daily charge profile for a long journey in a car with a small battery. The light grey charge profile shows what would happen if the car continued driving at the low speed.

there were no large recharge sessions. The ideal charge profile for such a journey is shown in Figure 18-3. The car starts each morning at sunrise with the battery half full, then drives at low speed so that the battery empties just as solar power becomes high enough to maintain the low speed. The car is then driven on solar power, with an empty battery, until it reaches the upper charging speed. This upper speed is selected so that the battery becomes full mid-afternoon, just as the solar power has dropped to the level required to sustain the upper speed. The car is then driven on solar power, with a full battery, until it reaches the lower speed which is maintained for the remainder of the day, finishing with the battery half full.

At any point on the journey the aim is to travel as far as possible at a constant speed before hitting a battery charge constraint. At the beginning of the day, the charge trajectory that does this will just touch the battery empty constraint then continue on at the same speed to hit the battery full constraint, as shown by the grey charge curve in the diagram. Travelling slower would give a charge trajectory that filled the battery sooner; travelling faster would have caused the battery to empty before the speed could be maintained using solar power. When the car reaches the battery empty constraint, it is possible to follow the constraint so that speed of the car increases, extending the range of the constant-speed strategy.

This method is based on an elegant formulation of the problem by Gates & Westcott (1996) where the total energy profile for the journey is represented by a curved tube with the tube width corresponding to the battery energy capacity. The optimal battery energy profile is found by stretching a string through the tube.

18.5 Following the battery charge profile

Errors in our modelling mean that the car will inevitably stray from any pre-computed journey profile. We compensate in two ways. First, we drive the car to follow the predicted charge profile instead of the predicted speed profile. Second, we recompute the profile whenever we stray too far.

By adjusting the speed of the car to stay on the charge profile we ensure that we will not empty the battery before the end of the race. If the car is performing better than we predicted then we will end up driving faster than we expected, which is not a bad thing. On the other hand, if the car is performing worse than we expected then we will travel slower than we predicted, but we will have enough energy in the battery to finish the race at a reasonable speed.

18.6 The 1999 World Solar Challenge

The next five pages are annotated telemetry logs from the 1999 World Solar Challenge. Our telemetry system took measurements in the solar car and relayed the measurements to a laptop computer in a support car.

The race data is presented as one page for each day. The graph on the left of each page shows three things:

- the shaded area indicates the remaining battery charge, as a percentage of full charge;
- the orange line indicates array power, with 100 indicating 1000W; and
- the blue line shows the approximate speed of the car, in km/h.

The measured speed fluctuated wildly because of instrumentation problems. The speed on the graph has been smoothed over five minute intervals, but is still not as stable as our true speed.

Telemetry was not working at the beginning of days four and five.

The race was very cloudy for the first three days, and so predicting the weather and strategy played a much greater role than if the weather had been clear.

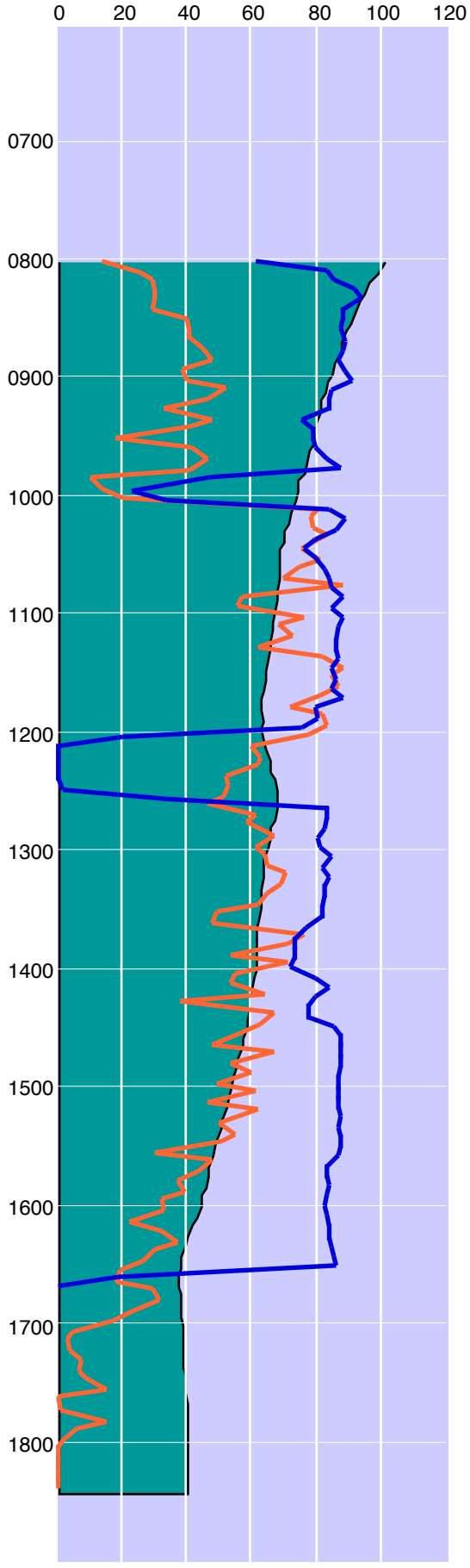

We start on The Esplanade in 7th position, behind Kanazawa, Solar Motions, Queens, Aoyama, Michigan and Minnesota.

Just before the end of the dual lanes we overtake SunShark to take the lead.

Roadworks 150km south of Darwin slow us to 30km/h. We are one of the few teams to escape tyre damage.

Katherine. Tamagawa arrive 11 minutes behind us, then NTU, OSU and Queens.

We notice that three array sections have been low since about 1130. The time we would lose if we stopped to find and repair the fault would be greater than any potential benefit, so we keep driving.

Dunmarra. We are in front by 25 minutes. Tamagawa, NTU and Queens all arrive before 1710.

The evening sun is blocked by a cloud. At this power level we cannot find any faults in the array.

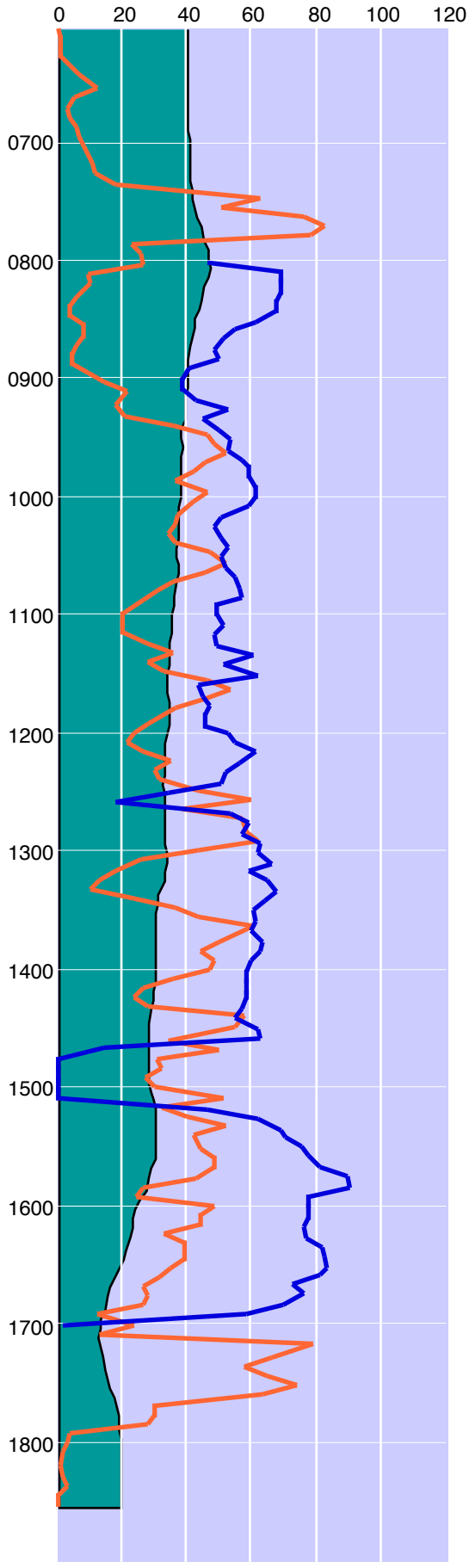

The morning charge session is cloudy except for half an hour at 0730. There are heavy clouds to the south. We did not get anywhere near the charge we were expecting, so will have to slow down.

The cloud is now very heavy.

NTU pass us. We are in second place.

Queens pass us. We are in third place.

Driver change.

Tennant Creek. We are 33 minutes behind Queens and 12 minutes behind NTU. SunShark is 18 minutes behind us.

Despite the weather predictions, the cloud is clearing. We increase speed so that we will be out of the Davenport Ranges by the end of the day.

We pass NTU, and are back in second place. Queens is 8km ahead.

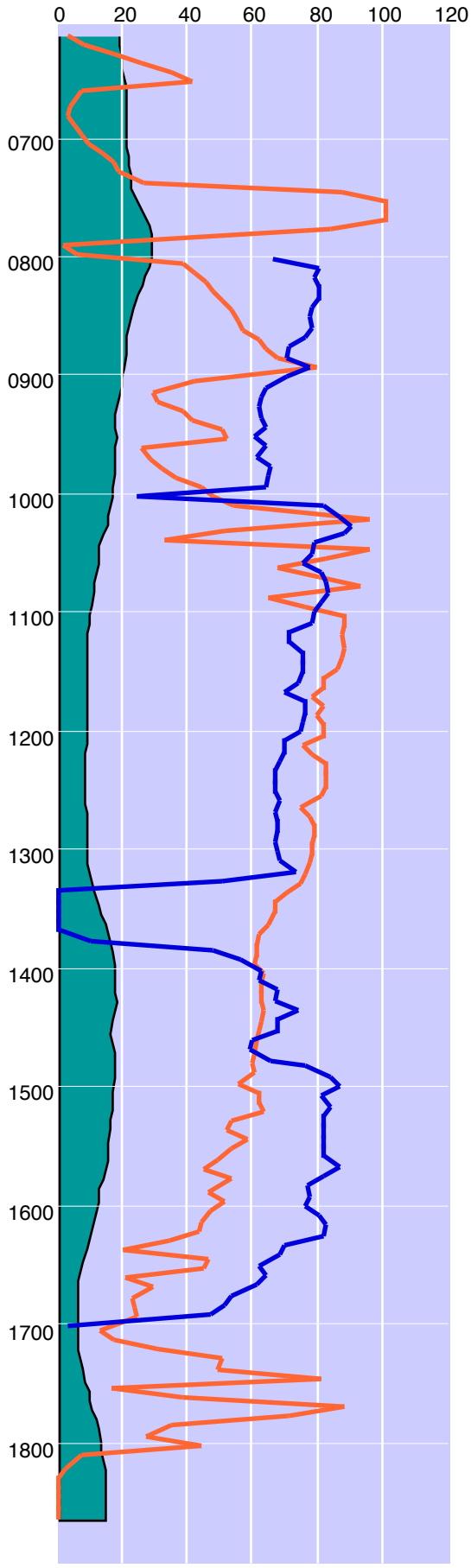

Once again, the sun is behind clouds for much of the morning charge session.

We overtake Queens. We are in first place, but heading back into cloud.

Driver change. The entire team is suffering from small bladders.

Power drops on three of the array sections. We slow down to compensate for the reduced power.

We are overtaken by Queens, and are back into second place.

Alice Springs. We are 7 minutes behind Queens, and 26 minutes ahead of SunShark.

Power is down on all but one of the array sections, but comes back up again as the car cools.

We stop13km south of Erldunda. Queens are 23km ahead; SunShark are 2km behind us.

After many telephone calls we find the problem with the array—the trackers shed power when they reach 80˚C. We build a ventilaton system for the trackers and fit a temperature sensor.

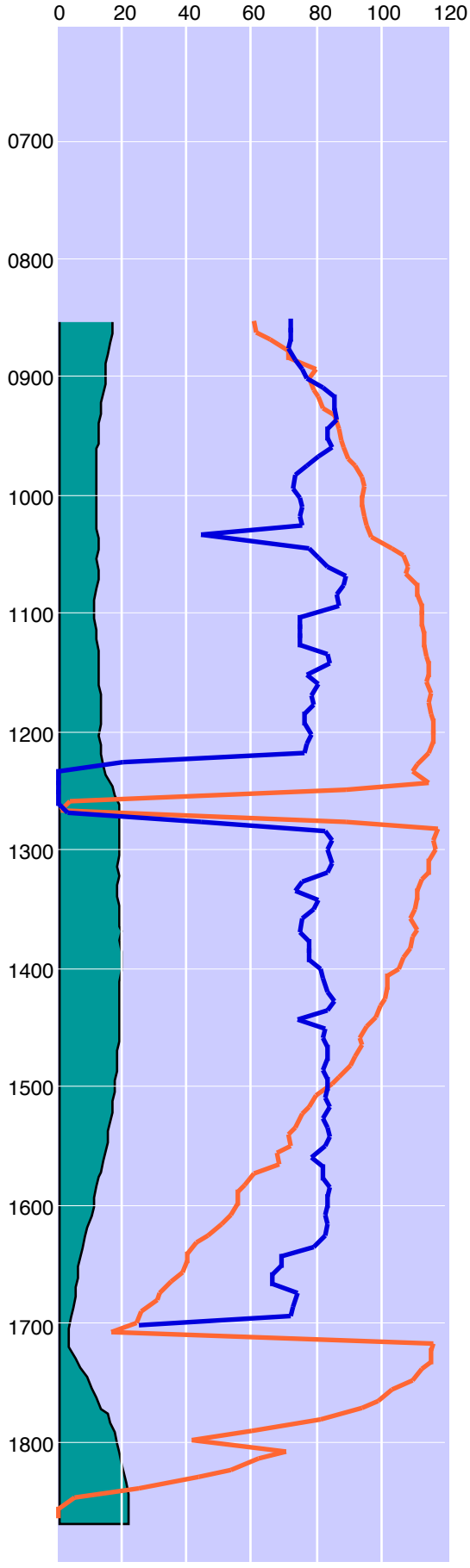

Telemetry is not working. We prepare to drive using only the ampere-hour meter in the car. And today is the day we want to flatten our battery.

The sky is cloudy for all but the last 15 minutes of the morning charge session.

SunShark pass us. We are back to third place.

Telemetry starts working. We are not sure why.

The trackers are at 80˚C, and array power is levelling out at 900W. We stop and remove the cover from the trackers. Temperature drops by 10˚C, and power increases by 100W.

Cadney. We are 10 minutes behind Queens, and 8 minutes behind SunShark.

The trackers turn off during the stop when the battery voltage exceeds 200V. Immediately before the evening charge session we will remove some cells from the battery so that it will not happen again.

We pass SunShark. We can see Queens in the distance.

We pass Queens. We are in front again. We stop 177km south of Coober Pedy.

Today was almost perfect. The sky was clear, we maintained a constant 80km/h for nearly the entire day, and we finished without abusing our battery. Queens and SunShark both stopped early to recharge.

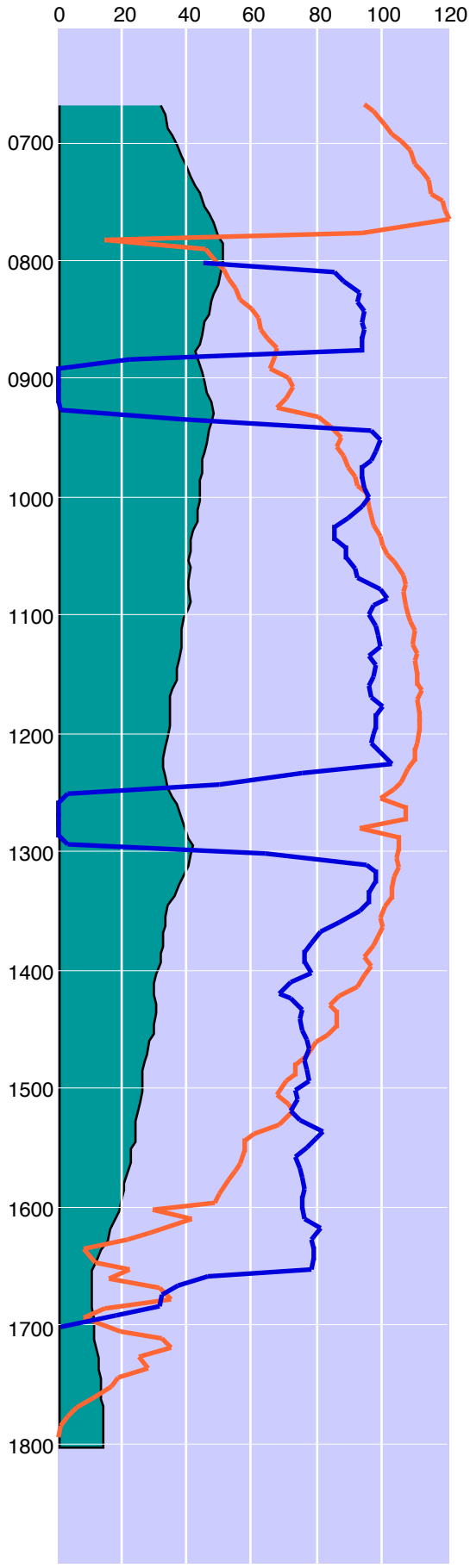

The telemetry system does not like these cold mornings.

For the first time the morning sky is clear. We finish the charge session with our battery half full.

Glendambo. So far today we have averaged 83km/h. Queens arrive 12 minutes behind us, having averaged 74km/h. SunShark are 29 minutes behind us, averaging 73km/h.

We have good sun and a tail wind, so are able to increase our speed to almost 100km/h.

Port Augusta. Our average speed over the last leg was 92km/h. We leave the stop before any other team arrives. We are 33 minutes ahead of Queens, 43 minutes ahead of NTU, and 47 minutes ahead of SunShark.

The tail wind changes to a head wind, so we slow down.

Clouds are predicted for Adelaide.

Adelaide is clouding over from the south. We will make the timing finish, but may not be able to get to Victoria Park by 1700.

We pass the timing finish at 1636. There is no way we can reach Victoria Park in heavy traffic by 1700. We slow down to 30km/h so that we will still be north of Gepps Cross at 1700. Unless we break down, no other team may overtake us. We stop at Capt'n Snooze.

The next morning we drive through peak traffic and rain to the finish line.

18.7 Summary

In practice, a constant speed strategy is a simple and effective driving strategy. The main difficulty is calculating the speed that will balance the energy collected with the energy used. To do this you need to predict irradiation four or five days in advance. We have developed a practical scheme based on predicting daily irradiation at locations along the route. Shorter term predictions are unnecessary provided you have adequate energy in your battery to get you through short-term variations in brightness without varying the speed of the car too much. By driving to match the predicted battery charge profile you can ensure that you will not empty the battery too soon.

19 Beyond solar cars

Whenever we have the car on display, the two most frequently asked questions are ‘does it get hot in there?’ and ‘how fast does it go?’

The third question is ‘when will we all be driving one?’ The answer is probably never. Solar racing cars are experimental vehicles, designed to push the limits of technology and to excite the imagination. They have been spectacularly sucessful; the motors, solar cells, batteries, control systems, tyres and bodies designed and built for solar cars are among the most efficient ever, and public awareness of the cars and their capabilities is high.

But there are many features of the current generation of solar cars that make them impractical:

- solar cells require a large, flat area facing the sky, making the cars both wider and longer than conventional cars and wider and longer than is aerodynamically efficient;
- the cost of high-efficiency solar cells is prohibitive;
- the rare-earth magnets in high-efficiency motors are expensive;
- batteries have a very low energy content compared to fossil fuels, and battery life is short when the batteries are repeatedly fully discharged;
- the interior space is small, and it takes several people to get a driver into or out of the car;
- the driver does not have a good, all-round view of the road; and
- the cars are too low to be seen by other road users.

In January 2000 Aurora drove the Aurora 101 from Sydney to Melbourne in a day, a distance of 870 km. A commuter car does not need anywhere near this range. What it does need is:

- two comfortable seats, luggage space, easy entry and exit, and good all-round vision;
- a small, lightweight, aerodynamic body and energy-efficient tyres and brakes;
- a non-polluting, renewable energy source;
- an energy storage system that can be 'recharged' quickly and conveniently, either by swapping energy storage packs or, even better, by recharging the car from an external energy storage system; and
- inexpensive components, such as switched-reluctance motors and commercial solar cells.

Whatever comes next, in cars and in general power supply, efficient energy management will play an increasingly important role as we move away from fossil fuels.

Bibliography

Aguira, R. J., Collares-Pereira, M. & Conde, J. P. 1988, 'Simple procedure for generating sequences of daily radiation values using a library of Markov transition matrices', *Solar Energy*, vol. 40, no. 3, pp. 269–279, Pergamon Press.

Allen G. & Allen, G. 1991, *Solar and Electric Vehicles*, New South Wales Department of Minerals and Energy.

Arnold, V. I. 1978, *Mathematical Methods of Classical Mechanics*, Graduate Texts in Mathematics, trans. K. Vogtmann & A. Weinstein, Springer-Verlag.

Arrowsmith, D. K. & Place, C. M. 1982, *Ordinary Differential Equations*, Chapman and Hall.

Arrowsmith, D. K. & Place, C. M. 1990, *An Introduction to Dynamical Systems*, Cambridge University Press.

Atkinson, K. E. 1978, *An Introduction to Numerical Analysis*, John Wiley & Sons.

Baddeley, V., Humphris, C. & Pudney, P. 1994, 'The Aurora Q1 solar-powered racing car', *Proceedings of the 1994 ANZAAS Congress, Geelong, Australia*.

Bard A. J. & Faulkner, L. R. 1980, *Electrochemical Methods: Fundamentals and Applications*, John Wiley & Sons.

Bellman, R. E. & Dreyfus, S. E. 1962, *Applied Dynamic Programming*, Princeton University Press.

Boland, J. 1995, 'Time series analysis of climatic variables', *Solar Energy*, vol. 55, no. 5, pp. 377–388, Pergamon Press.

Boland, J., Gaitsgory, V., Howlett, P. & Pudney, P. 1998, 'Efficient frontiers and solar cars', *Solar '98, Proceedings of the Annual Conference of ANZSES*, Christchurch, New Zealand, 25-27 November 1998, pp. 438–445.

Boyce, W. E. & DiPrima, R. C. 1977, *Elementary Differential Equations*, Third Edition, John Wiley & Sons.

Cesari, L. 1983, *Optimisation—Theory and Applications*, Springer-Verlag.

Conte, S. D. & de Boor, C. 1980, *Elementary Numerical Analysis: An Algorithmic Approach*, 3rd edition, McGraw-Hill Kogakusha.

Daniel, J. W. & Moore, R. E. 1970, *Computation and Theory in Ordinary Differential Equations*, Freeman.

Davis, M. H. A. & Vinter, R. B. 1985, *Stochastic Modelling and Control*, Monographs on Statistics and Applied Probability, Chapman and Hall.

Duffie, J. A. & Beckman, W. A. 1980, *Solar Engineering of Thermal Processes*, John Wiley & Sons.

Flemming, W. H. 1993, *Controlled Markov Processes and Viscosity Solutions*, Springer-Verlag.

Frick, R. A., Walsh, P. J., Rice, S. P. & Leadbeater, M. 1988, *Australian Solar Radiation Data Handbook*, Techsearch.

Gates, D. J. & Westcott, M. 1996, 'Solar cars and variational problems equivalent to shortest paths', *SIAM Journal of Control and Optimisation*, vol. 34, no. 2, pp. 428–436.

Goldstine, H. H. 1980, *A History of the Calculus of Variations*, Springer-Verlag.

Gordon, J. M. & Reddy, T. A. 1988, 'Time series analysis of daily horizontal solar radiation', *Solar Energy*, vol. 41, no. 3, pp. 215–226, Pergamon Press.

Hestenes, M. R. 1966, *Calculus of Variations and Optimal Control Theory*, John Wiley & Sons.

Hibbert, D.B. 1993, *Introduction to Electrochemistry*, MacMillan Physical Science Series, MacMillan Press.

Hokoi, S., Matsumoto, M. & Ihara, T. 1990/91, 'Statistical Time Series Models of Solar Radiation and Outdoor Temperature—Identification of Seasonal Models by Kalman Filter', *Energy and Buildings*, vol. 15–16, pp. 373–383.

Houghton, E. L. & Carpenter, P. W. 1993, *Aerodynamics for Engineering Students*, Fourth Edition, Edward Arnold.

Howlett, P. G. & Pudney, P. J. 1995, *Energy-Efficient Train Control*, Advances in Industrial Control, Springer.

Howlett, P. G. & Pudney, P. J. 1998, 'An optimal driving strategy for a solar powered car on an undulating road', *Dynamics of Continuous, Discrete and Impusive Systems*, vol. 4, pp. 553–567.

Howlett, P., Pudney, P., Tarnopolskaya, T. & Gates, D. 1997, 'Optimal driving strategy for a solar car on a level road', *IMA Journal of Mathematics Applied in Business & Industry*, vol. 8, pp. 59–81.

Ingraham, R. L. 1992, *A Survey of Nonlinear Dynamics: "Chaos Theory"*, World Scientific.

Jasinksi, R. 1967, *High Energy Batteries*, Plenum Press.

Kirk, D. E. 1970, *Optimal Control Theory: An Introduction*. Prentice-Hall.

Kirk-Othmer Encyclopedia of Chemical Technology 1991, Fourth Edition, vol. 3, Wiley.

Kordesch, K. (ed) 1977, *Batteries: Volume 2, Lead-Acid Batteries and Electric Vehicles*, Marcel Dekker.

Kyle, C. R. 1991, *Racing with the Sun*, Society of Automotive Engineers.

Lasnier, F. & Ang, T. G. 1990, *Photovoltaic Engineering Handbook*, Adam Hilger.

Lee, E. B. & Markus, L. 1967, *Foundations of Optimal Control Theory*, John Wiley & Sons.

Lovins, A. B., Barnett, J. W. & Lovins, L. H. 1993, 'Hypercars: The Coming Light-Vehicle Revolution', *<http://www.rmi.org/hypercars/hypercars_intro.html>*.

Lovins, A. B., Brylawski, M. M., Cramer, D. R. & Moore, T. C. 1996, 'Hypercars: materials, manufacturing, and policy implications', *<http://www.rmi.org/hypercars/JESTOC.html>*.

Lovins, A. B. & Lovins, L. H. 1995, 'Reinventing the wheels', *<http://www.rmi.org/hypercars/Reinventing_the_Wheels.html>*.

Manwell, J. F. & McGowan, J. G. 1993, 'Lead acid battery storage model for hybrid energy systems', *Solar Energy*, vol. 50, no. 5, pp. 399–405, Pergamon Press.

Marr, W. W., Walsh, W. J. & Symons, P. C. 1992, 'Modelling battery performance in electric vehicle applications', *Energy Conversion and Management*, vol. 33, no. 9, pp. 843–847, Pergamon Press.

Mohler, R. R. 1991, *Nonlinear Systems: Volume 1, Dynamics and Control*, Prentice Hall.

Nasar, S. A., Boldea, I. & Unnewehr, L. E. 1993, *Permanent Magnet, Reluctance and Self-Synchronous Motors*, CRC Press.

Phillips, W. F. 1983, 'Harmonic Analysis of Climatic Data', *Solar Energy*, vol. 32, no. 3, pp. 319–328.

Pillai, S. K. 1989, *A First Course on Electrical Drives*, 2nd edition, John Wiley & Sons

Plaat, O. 1971, *Ordinary Differential Equations*, Holden Day.

Pontryagin, L. S. 1962, *The Mathematical Theory of Optimal Processes*, trans. K. N. Trirogoff, Interscience Publishers.

Protogeropoulos, C., Marshall, R. H. & Brinkworth, B. J. 1994, 'Battery state of voltage modelling and an algorithm describing dynamic conditions for long-term storage simulation in a renewable system', *Solar Energy*, vol. 53, no. 6, pp. 517–527, Pergamon Press.

Roche, D. M., Schinckel, A. E. T., Storey, J. W., Humphris, C. P. & Guelden, M. R. 1997, *Speed of Light: The 1996 World Solar Challenge*, Photovoltaics Special Research Centre, University of New South Wales.

Shapiro, A. H. 1961, *Shape and Flow: The Fluid Dynamics of Drag*, Anchor Books.

Shepherd, C. M. 1965, 'Design of primary and secondary cells', *Journal of the Electrochemical Society*, vol. 112, no. 7, pp. 657–664.

Smith, G. 1971, *Storage Batteries*, 2nd edition, Pitman Publishing.

Stengel, R. F. 1986, *Stochastic Optimal Control*. John Wiley & Sons.

Stone, R. 1989, *Motor Vehicle Fuel Economy*, Macmillan.

Storey, J. W. V., Schinckel, A. E. T. & Kyle, C. R. 1994, *Solar Racing Cars: 1993 World Solar Challenge*, Australian Government Publishing Service.

Tolle, H. 1975, *Optimization Methods*, Springer Verlag.

Tuckey, B. 1989, *Sunraycer*, Chevron Publishing Group.

Vergara-Dominguez, L., Garcia-Gomez, R., Figueiras-Vidal, A. R., Casar-Corredera, J. R. & Casajus-Quiros, F. J. 1985, 'Automatic Modelling and Simulations of Daily Global Solar Radiation Series', *Solar Energy*, vol. 35, no. 6, pp. 483–489.

Vinal, G. 1955, *Storage Batteries*, 4th edition, John Wiley & Sons.

Vincent, C. A. 1984, *Modern Batteries*, Edward Arnold.

Watkins, S., Liu, B. & Humphris, C. 1998, 'The aerodynamics of the Aurora solar-powered vehicle', *13th Australasian Fluid Mechanics Conference*, Monash University, Melbourne, Australia, 13-18 December 1998.

West, J. G. W. 1994, 'DC, induction, reluctance and PM motors for electric vehicles', *Power Engineering Journal*, April 1994, pp. 77–88.

Whitt, F. R. & Wilson, D. G. 1982, *Bicycling Science*, 2nd edition, MIT Press.

Yoshida, H. & Terai, T. 1990/91, 'An ARMA Type Weather Model for Air-Conditioning, Heating and Cooling Load Calculation', *Energy and Buildings*, vol. 15–16, pp. 625–634.

Yosida, K. 1978, *Functional Analysis*. 5th edition, Springer-Verlag.

Zwillinger, D. 1989, *Handbook of Differential Equations*, 2nd edition, Academic Press.